이학박사학위논문

Applications of Designed Nucleases in Various Organisms

2020년 2월

서울대학교 대학원

화학부 생화학 전공

이 충 일

Abstract

Applications of Designed Nucleases in Various Organisms

CHOONGIL LEE

Department of Chemistry

The Graduate School

Seoul National University

According to a development of life technology for industry and medical science, it became clear that genome editing tools will be arisen in the future. Moreover, it is necessary for understanding and finding a way of application in designed nucleases. In agreement with its need, we can improve living resources and healthy life by utilizing designed nucleases.

I have been studying genome editing for an application of various organisms using designed nucleases such as ZFN, TALEN and CRISPR. At the first study, I had modified *CMAH* gene in pig genome and using its knockout(KO) cells for SCNT. The *CMAH* gene is related to immune rejection in xenotransplantation. We had aimed to produce null *CMAH* organ donor pigs using by ZFN and SCNT. We improved efficiency of *CMAH* gene KO cells by aid of MACS and FACS surrogate reporter systems. Finally we could generate *CMAH* KO pig blastocysts. In the second

study, we utilized TALEN for pig genome editing. In this study we had generated *CMAH* and *GGTA1* gene KO cell lines in immortalized pig fibroblast. We could confirm a development of blastocyst using immortalized *CMAH* KO cell by SCNT. In the third study, we observed *NR* gene mutation by delivering Cas9 RNP into the protoplast of *petunia*. This results could suggest a possibility for gene editing in *petunia* by Cas9 RNP. At the last study, we showed overcoming premature termination codons (PTCs) which causes genetic defeat in a human genetic diseases. We named this method as for CRISPR-pass and proved its possibility in *XPC* gene patient-derived fibroblast.

In a summary we tried to do gene editing in a various organisms with ZFN, TALEN and CRISPR. At the same time we also tried to help for understanding of designed nuclease and suggested a way of its applications.

Keywords: Zinc Finger Nuclease, TAL-Effector Nuclease, Xenotransplantation, CRISPR-Cas9, Adenine Base Editor, Pre-mature termination codon, CRISPR-pass.

Student Number: 2012-20286

Table of Contents

Abstract.....i

Table of Contents..... iii

List of Figures.....vii

List of Tables ix

PART 1. Applications of designed nucleases: Zinc Finger Nuclease (ZFN), TAL Effector Nuclease (TALEN) and Clustered Regularly Interspaced Short Palindromic Repeats (CRISPR)-Cas9

Ⅰ. Introduction 2

Ⅱ. Materials and Methods.....8

1. Production of Mutated Porcine Embryos Using Zinc Finger Nucleases and a Reporter-based Cell Enrichment System.....8

a. ZFNs and surrogate reporters 8

b. Preparation of cells and culture conditions.....8

c. Plasmid DNAs transfection 8

d. Analysis of mutations 9

e. Production and culture of cloned porcine embryos 9

f. Statistical analysis.....10

2. Production of *CMAH* Knockout Preimplantation Embryos Derived From Immortalized Porcine Cells Via TALE Nucleases 11

a. Chemicals.....11

b. Primary cell culture and maintenance. 11

c. Immortalization 11
d. Doubling time 12
e. Cell size 12
f. PCR 12
g. Sequencing 12
h. Karyotyping 13
i. Single cell colony formation 13
j. Gene expression 14
k. Telomerase activity test 14
l. Nuclear transfer 14
m. *CMAH* knockout using TALEN and magnetic separation 15
n. T7E1 assay 15
o. Fluorescent PCR 15
p. Fluorescence-activated cell sorting 16
q. Statistical analysis 16
3. Site-directed mutagenesis in *Petunia* × *hybrida* protoplast system using direct delivery of purified recombinant Cas9 ribonucleoproteins 16
a. *Petunia* protoplast preparation 16
b. Recombinant Cas9 Protein and Guide RNA design 17
c. Transfection 17
d. Genomic DNA extraction and T7 endonuclease 1 (T7E1) assay 18
e. Targeted deep sequencing 18
Ⅲ. Results 20
1. Production of Mutated Porcine Embryos Using Zinc Finger Nucleases

and a Reporter-based Cell Enrichment System 18
a. Enrichment system for cells containing ZFN-mediated mutations ... 18
b. Mutations in cloned blastocysts derived from ZFN-treated cells 24
2. Production of *CMAH* Knockout Preimplantation Embryos Derived From Immortalized Porcine Cells Via TALE Nucleases 27
a. Generation of porcine immortalized cell and analysis of immortalized cell's properties. 27
b. Preimplantation development of cloned embryos derived from immortalized cells. 32
c. *CMAH* knockout and SCNT. 32
d. *GGTA1* knockout. 43
3. Site-directed mutagenesis in *Petunia* × *hybrida* protoplast system using direct delivery of purified recombinant Cas9 ribonucleoproteins..... 51
a. Efficient protoplast system enhances Cas9 transfection in P. hybrida. 51
b. Targeted mutagenesis of *NR* gene in *Petunia* protoplast system using direct delivery of RGEN RNPs. 52
c. Detection and estimation of Cas9/sgRNA mediated *Petunia NR* gene mutations. 60
Ⅳ. Discussion 68

PART 2. Application of designed nuclease: Adenine base editor (ABE)

Ⅰ. Introduction 70

Ⅱ. Materials and Methods 72

1. General Methods and Cloning 72
2. ClinVar Database Analysis 72
3. Cell Culture and Transfection 73
4. EGFP-PTC-KI Cell Lines 74
5. Flow Cytometry 74
6. Targeted Deep Sequencing 74
7. Treatment with Ataluren and Gentamicin 75
8. Western Blotting 75
9. Functional Assessment 75
10. Statistics 76
11. Data Availability 76

Ⅲ. Results 77

1. *In Silico* Investigation of Applicable Targets for CRISPR-Pass in the ClinVar Database 77
2. Construction of Six KI HeLa Cell Lines Carrying Various Types of PTCs in *EGFP* Gene 79
3. CRISPR-Pass Rescues the Function of the *EGFP* Gene in Six KI HeLa Cell Lines 81
4. CRISPR-Pass Rescues the Function of the *XPC* Gene in Patient-Derived Fibroblasts 91

Ⅳ. Discussion 104

References 106

Abstract in Korean 119

List of Figures

Figure 1. Enrichment system for cells containing ZFN-mediated mutations.....22

Figure 2. Somatic cell nuclear transfer with ZFN-treated donor cells 23

Figure 3. Mutations in cloned blastocysts derived from ZFN-treated cells 25

Figure 4. Cellular analysis of porcine immortalized cells.....28

Figure 5. Gene expression in immortalized cells and embryonic development.....30

Figure 6. Sequencing results from genomic DNA from immortalized cell lines....35

Figure 7. Generating *CMAH* knockout cells and its analysis.....36

Figure 8. T7E1 assay results from *CMAH* KO single cell colonies 37

Figure 9. Fluorescent PCR results from *CMAH* KO single cell colonies.....38

Figure 10. Inserted 282bp sequences in #24 colony.....39

Figure 11. Relative telomerase activity (RTA) 40

Figure 12. SCNT with *CMAH* KO donor cells.....42

Figure 13. Illustration of TALEN binding sites and results of *GGTA1*-TALEN KO 44

Figure 14. T7E1 assay results from 1st *GGTA1* KO single cell colonies 45

Figure 15. Fluorescent PCR results from 1st *GGTA1* KO single cell colonie 46

Figure 16. T7E1 assay results from 2nd GGTA1 KO single cell colonies. 47

Figure 17. Fluorescent PCR results from 2nd GGTA1 KO single cell colonies.....48

Figure 18. Design of gRNAs to target six specific sites of *P. Hybrida Nitrate reductase* (*NR*) gene locus and schematic description of *Petunia NR* locus.....54

Figure 19. The nucleotide sequences of *Petunia NR* gene locus and regions of RNA-guided Cas9 at NR (1-6)-RGEN target sites 55

Figure 20. Scheme for Cas9/sgRNA-mediated mutagenesis of Nitrate reductase gene in *Petunia* protoplast system..... 56

Figure 21. Expression of GFP in *Petunia* protoplasts 57

Figure 22. Cas9/sgRNA-mediated mutagenesis of *Nitrate reductase* (*NR*) gene in *Petunia* using direct delivery of RGEN RNPs 59

Figure 23. CRISPR-Pass for Restoring Abbreviated Gene Expression 78

Figure 24. Coding or noncoding targeting depends on the EGFP sequence and the PTC position 80

Figure 25. Rescued EGFP expression after treatment with ABEs 82

Figure 26. FACS results 84

Figure 27. Restoring the Function of EGFP Gene Expression in Six KI HeLa Cell Lines Carrying Various Types of PTCs 87

Figure 28. CRISPR-pass for *XPC* patient-derived fibroblasts 92

Figure 29. Restoring Abbreviated XPC Gene Expression in Patient-Derived Fibroblasts 94

Figure 30. Prolonged expression of the XPC protein after ABE treatment 95

Figure 31. Off-target analysis for CRISPR-pass targeting XPC 97

List of Tables

Table 1. *In vitro* culture of cloned embryos derived from ZFN-treated donor cells 26

Table 2. List of primers 49

Table 3. List of real-time PCR primers 50

Table 4. Estimation of mutation rate in NR gene sequences in wild type non-transfected and NR-RGEN transfected protoplasts by targeted deep sequencing using direct delivery of RGEN RNP's 62

Table 5. List of sgRNA's determined to target *Petunia NR* gene locus in this study 65

Table 6. List of templates used for in vitro transcription of sg-RNAs 66

Table 7. List of primers used in nested PCR for T7E1 and Deep target sequencing assay 67

Table 8. FACS results. The percentages of EGFP (+) cells in populations of ABE-treated EGFP-PTC-KI cells 89

Table 9. NGS results. The percentages of A to G substitutions in populations of ABE-treated EGFP-PTC-KI cells 90

Table 10. A-to-G substitution rates (%) in potential ABE off-target sites 98

Table 11. List of oligomers encoding sgRNAs 99

Table 12. PCR primers used in this study 100

Table 13. List of off-target sites 103

PART 1. Applications of designed nucleases: Zinc Finger Nuclease (ZFN), TAL Effector Nuclease (TALEN) and Clustered Regularly Interspaced Short Palindromic Repeats (CRISPR)-Cas9

Ⅰ. Introduction

In a development of life technology, genome editing tools, such as designed nucleases have been also improved. The first designed nuclease was Zinc Finger Nuclease (ZFN) (Bibikova et al., 2003; Maeder et al., 2008; Urnov et al., 2005). The second designed nuclease was Transcription Activator-Like Effector Nuclease (TALEN) (Boch et al., 2009; Cermak et al., 2011; Gaj et al., 2013; Kim et al., 2013b; Miller et al., 2011; Moscou and Bogdanove, 2009). The third designed nuclease was Clutstered Regularly Interspaced Short Palindromic Repeats (CRISPR) (Cho et al., 2013; Cong et al., 2013; Hwang et al., 2013b; Jiang et al., 2013a; Jinek et al., 2012; Mali et al., 2013). At last, there were modified-form of CRISPRs for nucleotides base editing, such as Adenine base editor (ABE) (Gaudelli et al., 2017) and Cytidine Base editor (CBE) (Komor et al., 2016). Moreover recently developed "prime editing" system allows all kind of nucleotides changes in a genome (Anzalone et al., 2019). By using designed nucleases, I have been studying about genome editing in various organisms, for example genome of porcine, *petunia* and patient derived-fibroblast.

In the first study, I had tried to genome editing in porcine. Pigs are a useful experimental animal for biomedical research because of their anatomical and physiological similarities with humans (Smith and Swindle, 2006) and relatively high production efficiency (Koo et al., 2012). For these reasons, various transgenic pigs have been generated since the middle of the 1980s (Whyte and Prather, 2011). However, production of knockout or gene targeted pigs was extremely rare until very recently because of very low efficiency of homologous recombination in somatic cells and a lack of appropriate technologies, such as embryonic stem cells, in this species. A pioneering work using zinc finger nucleases (ZFNs) to produce knockout rats (Geurts et al., 2009) enabled us to perform a new approach for producing knockout mammals without homologous recombination or embryonic stem cells. ZFNs are engineered proteins composed of the FokI endonuclease domain linked to a DNA-binding zinc finger protein domain. Pairs of the ZFNs efficiently generate sequence-specific DNA double-strand breaks on a chromosome; consequently, targeted mutations can be introduced into cells of interest (Kim et al., 2009; Kim et al., 2011b; Watanabe et al., 2010). Since first showed that the ZFN system can be used in

porcine cells, several knockout pigs have been generated using ZFNs and somatic cell nuclear transfer (SCNT) techniques.

However, the protocols developed in the former studies cannot be used as a general application for producing knockout pigs with ZFNs. Most of the previous reports screened for the presence of ZFN-mediated mutations in donor cells by detecting loss of a specific surface molecule (Hauschild et al., 2011; Li et al., 2013b; Lutz et al., 2013) or ectopic marker gene expression (Whyte et al., 2011) affected by the mutation. For example, a specific surface molecule, alpha 1,3-galactose, is only available to detect mutations of alpha 1,3 galactosyltransferase and related genes. Also, ectopic marker gene expression, such as eGFP or luciferase, is necessary to generate the cell lines which have the gene sequences prior to gene targeting. Unfortunately, most of the other mutant cells generated by ZFN or other engineered nucleases, especially endogenous gene-modified cells, are somewhat phenotypically indistinguishable. Therefore, alternative protocols for screening or enriching mutated cells are needed.

To overcome the hurdle, we developed a new protocol for generating mutated porcine embryos using a transiently transfected episomal reporter-based enrichment system for cells with ZFN-induced mutations (Kim et al., 2013a; Kim et al., 2011a). With the enrichment system, mutation frequencies of 8.7% to 47% (11- to 17-fold higher than frequencies in non-enriched cell populations) can be achieved. Moreover, gene-modified cells enriched with this system are alive and suitable for subsequent experiments. Hence, we assumed that this enrichment system, in combination with the SCNT technique, could provide a new generalized platform for producing mutated embryos. In the first study, we assessed the enrichment system in porcine cells and analyzed mutations in cloned pig embryos derived from the enriched ZFN-treated cells.

In a second study. Like as first study, pigs are considered to be good biomedical models for researches such as xenotransplantation because of their many physiological similarities with humans (Aigner et al., 2010; Kwon et al., 2013; Lai et al., 2002; Matsunari and Nagashima, 2009). Somatic cell nuclear transfer (SCNT) with genetically modified somatic cells has been used to generate pig models via transgenesis (Wolf et al., 2001). Typical gene modifications are ectopic expression or knockout of target genes (Liu et al., 2013; Lutz et al., 2013). While many

cloned piglets have been produced using ectopic expression, only three kinds of knockout piglets (α-galactosidase, cystic fibrosis, and interleukin-2 receptor) using homologous recombination have been born (Lai et al., 2002; Rogers et al., 2008a; Rogers et al., 2008b). Developing knockout pig models has been hampered to date because fibroblasts generally have a limited life span during in vitro culture and because of the low efficiency of the homologous recombination process (Kwon et al., 2013). To overcome these two issues, immortalization of fibroblasts and more efficient knockout protocols are needed. For immortalization, several genes such as *BMI*, *SV40LT*, and human telomerase reverse transcriptase (*hTERT*) can be transfected into cells. In previous studies, *SV40LT* and *hTERT* were used to immortalize porcine cells (Meng et al., 2010; Oh et al., 2007; Sagong et al., 2012; Saito et al., 2005). TALEN is an emerging high-end technology used to create targeted double-stranded breaks in DNA (Hwang et al., 2013a). TALEN has employed for genome editing, resulting in target gene deletion or insertion in human, mouse, and rat cells (Ding et al., 2013; Kim et al., 2011a; Panda et al., 2013; Tong et al., 2012; Zhu et al., 2013). Application of TALEN to cells of large animals like pigs could more efficiently generate knockout cell lines and thus help to elucidate the underlying molecular processes (Carlson et al., 2012). After establishing knockout cell lines, the cell nuclei could potentially be reprogrammed in enucleated oocytes and produce knockout cloned offspring.

In this study, to prove TALEN-mediated knockout, we elected to delete the *CMAH* gene, which is another important cell surface glycoprotein with α-galactosidase, for xenotransplantation pig models, and then, gene knockout cells were used for feasibility of embryonic development via SCNT. Here, we hypothesized that using immortalization and TALEN approaches together in porcine cells could serve as practical in vitro models of genome editing.

In a third study, targeted gene modification using artificial nuclease enzyme such as CRISPR-CRISPR associated nuclease 9 (Cas9) system has announced as an emerging genome editing tool for plant breeding to improve plant varieties with novel traits (Feng et al., 2013; Svitashev et al., 2015; Wang et al., 2014a). Besides the CRISPR/Cas9 system, other nucleases such as ZFNs (Beerli and Barbas, 2002) and TALENs (Chen and Gao, 2013; Li et al., 2012), have also been used to modify target gene loci. All these nuclease enzymes usually create double

strand breaks (DSBs) in the target DNA sequences in a sequence-specific manner through sequence-specific DNA-binding domain (Gaj et al., 2013). Common cellular DNA repair mechanisms such as homology-directed repair (HDR) and error-prone non-homologous end joining (NHEJ) are processed to repair these DSBs (Wyman and Kanaar, 2006). They will cause insertion, deletion, or exchange of nucleotides, leading to gene modification at the target sites. DSB by typical ZFNs and TALENs requires dimerization of FokI monomer to increase site-specific cleavage of DNA, indicating an active form of nuclease (Bitinaite et al., 1998). However, in some instances, formation of FokI homodimers can decrease site-specific cleavage and cause unwanted off-target effects (Gaj et al., 2013; Miller et al., 2007). CRISPR/Cas9 system, unlike other nuclease systems, requires only a common protein Cas9 with each single guide RNA (sgRNA) to help create DSBs precisely in target gene loci. Compared to other nucleases such as ZFNs or TALENS, CRISPR/Cas9 could be more efficient and simpler for genome editing (Kim et al., 2014).

Type-II CRISPR/Cas9 system is originally derived from bacteria and archaea. It mainly acts as a defense system against invading foreign DNAs using RNA-guided endonuclease (RGEN) activity (Jinek et al., 2012). The general structure of CRISPR locus usually consists of a Cas9 nuclease, a precursor CRISPR RNA (pre-crRNA) containing an array of 20 nucleotide nuclease guide sequences partially from pathogen invaders, and a trans-activating crRNA (tracrRNA). Pre-crRNAs are transcribed and processed into mature crRNA that can eventually form complex with pre-crRNA and Cas9 nuclease to produce crRNA–tracrRNA–Cas9. Nuclease guide sequences in crRNA will guide this crRNA–tracrRNA–Cas9 complex to cleave complementary foreign DNA sequences accompanied by protospacer adjacent motifs (PAM) such as 5′NGG3′ (Jinek et al., 2012) Cas9 system from Streptococcus pyogenes (SpCas9). The CRISPR/Cas9 system has been successfully employed to create mutations in both animal (Cho et al., 2013; DiCarlo et al., 2013; Hsu et al., 2014; Hwang et al., 2013b) and plant genomes (Feng et al., 2013; Hyun et al., 2015; Jiang et al., 2014; Li et al., 2013a; Miao et al., 2013; Nekrasov et al., 2013; Shan et al., 2013; Xie and Yang, 2013).

In 2014, cloning free CRISPR/Cas system has been established in human (Kim and Kim, 2014) and animal systems (Aida et al., 2015) using direct delivery of RGEN ribonucleoproteins (RNPs), purified Cas9 protein, and target-specific in vitro transcribed sgRNA. Using this same approach, purified TALEN proteins have been reported to be able to induce mutations in plant system (Luo et al., 2015). These DNA-free genome editing tools have gained more attention than the older plasmid mediated delivery method that requires tissue-specific delivery tools. In addition, the older plasmid mediated delivery method has to be optimized for promoter for each organism, which sometimes can induce unwanted DNA fragment insertion at target sites of host cells (Kim et al., 2014). In addition, genome editing via DNA-free proteins delivery (Luo et al., 2015; Woo et al., 2015) might be excluded from genetically modified organism (GMO) regulations in plants because no foreign DNA is introduced (Kanchiswamy et al., 2015).

The efficiency of genome editing is mainly based on transfection of nuclease proteins with appropriate delivery methods. In most animal experiments, the usual delivery method of Cas9 protein is by using lipofection transfection reagent or through electroporation (Sander and Joung, 2014). In plants, tissue culture dependent transient expression such as callus culture, protoplast transfection, and agro bacterium mediated agro infiltration are used (Jiang et al., 2013b; Li et al., 2013a; Nekrasov et al., 2013; Shan et al., 2013; Xie and Yang, 2013). Some studies have reported that engineered CRISPR/Cas is active in creating mutations during protoplasts transfection. In addition, mutated genes are stably expressed in regenerated plants such as Arabidopsis and rice (Feng et al., 2013; Woo et al., 2015). These attributes make the protoplast strategy versatile for delivering Cas9 proteins to achieve target gene editing in plants. *Petunia* × *hybrid*, also known as garden *Petunia*, belongs to Solanaceae family. It is cultivated around the world as a flower with agronomic and ornamental value.

Petunia has been utilized to study and understand floral development (Vandenbussche et al., 2004), transposable element systems (van Houwelingen et al., 1999), and insertion mutagenesis (Meyer, 2001). Moreover, due to its ease for genetic transfection (Conner AJ et al., 2009) along with a wide range of aforementioned research backgrounds, *Petunia* has been suggested as a good system for studying genetics of phenotypic traits (Gerats and Vandenbussche,

2005; Gübitz et al., 2009). Based on these facts, the present study was carried out with Cas9 mediated mutagenesis for nitrate reductase gene in *Petunia* × *hybrida* protoplast system. Since *NR* genes can facilitate nitrogen uptake and nitrate metabolism, any changes in their expression by transgenic approach will cause deficiency in nitrate assimilation, which eventually triggers phenotypic changes (Zhao et al., 2013). Therefore, *NR* genes are excellent targets to study changes in gene sequence or gene expression by Cas9-based system.

In this study, we described RGEN RNPs technology in *Petunia* × *hybrida* to establish a site-directed mutagenesis system. We successfully delivered purified Cas9 protein preassembled with in vitro transcribed sgRNA into *Petunia* protoplasts in the presence of polyethylene glycol (PEG). Our results revealed that targeted gene mutation such as insertion and deletion could be created in four out of six specific sites of a *NR* gene in the genome of *Petunia*. The mutation efficiency of RGEN RNPs at target sites was assessed by targeted deep sequencing. Our results further suggests that direct delivery of Cas9-sgRNA system could be used for site-directed mutagenesis in *Petunia*. This site-directed mutagenesis system can be exploited for gene targeting in other related species.

Ⅱ. Materials and Methods

1. Production of Mutated Porcine Embryos Using Zinc Finger Nucleases and a Reporter-based Cell Enrichment System

a. ZFNs and surrogate reporters

Plasmids encoding ZFNs that target exon 6 of the pig CMP-N-acetylneuraminic acid hydroxylase (*CMAH*) gene were previously described (Kim et al., 2009). Enrichment system with reporters, eGFP or H-2K^k as selection markers for fluorescence activated cell sorting (FACS) and magnetic activated cell sorting (MACS), respectively were constructed as previously described (Kim et al., 2013a; Kim et al., 2011a).

b. Preparation of cells and culture conditions

A primary culture of pig fetal fibroblast cells that has been established as described by Cho et al. (2011) was used. Briefly, fetal tissues were minced and dissociated in TrypLE Express (Gibco, CA, USA) for 10 min at 37°C. Cells were cultured in Dulbecco's modified Eagle's/Nutrient Mixture F-12 medium (DMEM/F12, Gibco) supplemented with 10% (v/v) fetal bovine serum, 1 mM Glutamax I (Gibco), 25 mM $NaHCO_3$, 1% (v/v) minimal essential medium, nonessential amino acid solution (Gibco) and 1% (v/v) Anti-Anti (Gibco) at 39°C in a humidified atmosphere of 5% CO_2 and 95% air.

c. Plasmid DNAs transfection

Fibroblasts were cultured to 80% to 90% confluence, then washed twice with D-PBS(−) (Gibco) and treated with 0.05% trypsin-EDTA (Gibco) to isolate and collect. Fibroblasts (2×10^6 cells) were electroporated using a 100μL Nucleocuvette, CA137 program code, in an Amaxa 4D-Nucleofector (Lonza, P3 Primary Cell 4D-Nucleofector X Kit L) with a total of 45 μg plasmid DNA at a 2:2:1 weight ratio (plasmid encoding a left ZFN: plasmid encoding a right ZFN: eGFP reporter or H-2Kkreporter). Mutant cells were enriched using a flow cytometer (FACSAria

III, BD Biosciences, USA) or MACSelect K^k System (Miltenyi Biotec, Bergisch Gladbach, Germany) as described (Kim et al., 2013a; Kim et al., 2011a). The sorted cells were cultured for 2 additional days after sorting prior to SCNT or mutation analysis for proliferation and removing the dead cells.

d. Analysis of mutations

For detection of ZFN-induced mutations at the pig CMAH locus, the ZFN target locus was amplified from genomic DNA isolated from fibroblasts or cloned blastocysts (DNeasy kit, Qiagen) by nested PCR and subjected to the T7E1 assay (Kim et al., 2009). Primers used for the amplifications of the CMAH locus were as follows: 1st PCR/5′-tgtggacgtgccagactat-3′ and 5′-aaggcaatcaggctccttag-3′, 2nd PCR/5′-tctacggaaatgctcctgct-3′ and 5′-tctacggaaatgctcctgct-3′.

For sequence analysis, PCR amplicons that included ZFN-target sites were purified using the Gel Extraction Kit (MACHERRY-ALGEN) and cloned into the T-Blunt vector using the T-Blunt PCR Cloning Kit (SolGent). Cloned plasmids were sequenced using the primers used for PCR amplification.

e. Production and culture of cloned porcine embryos

In vitro maturation of porcine oocytes, SCNT, and in vitro culture of the cloned embryos were performed as described elsewhere (Park et al., 2012) with slight modification. Briefly, ovaries were collected at a local abattoir and transported to the laboratory in sterile physical saline at 30°C to 35°C. Cumulus-oocyte complexes (COCs) were aspirated from antral follicles (3 to 6 mm) with 18-gauge needle attached to a 10 mL disposable syringe. COCs with several layers of cumulus cells and uniform cytoplasm were chosen and cultured in tissue culture medium 199 (Gibco) supplemented with 10 ng/mL EGF, 0.57 mM cysteine, 0.91 mM sodium pyruvate, 5 μg/mL insulin, 1% (v/v) Pen-Strep (Gibco) and 10% porcine follicular fluid at 39°C in a humidified atmosphere of 5% CO_2. For first 22 h of culture, 0.5 μg/mL follicle stimulating hormone and 0.5 μg/mL luteinizing hormone were added to the culture medium and then removed for a further 22 h. After a total of 44 h maturation culture, oocytes were denuded by pipetting with

0.1% hyaluronidase in TALP medium supplemented with 0.1% polyvinyl alcohol. Denuded oocytes with evenly-granulated and homogeneous cytoplasm were selected and then utilized for SCNT. A cumulus-free oocyte was held with a holding micropipette and the zona pellucida was partially dissected with a fine glass needle to make a slit near the adjacent cytoplasm, presumably containing the metaphase-II chromosomes, were extruded by aspiration with the same needle. Enucleation was confirmed by staining the cytoplasm with 0.5 μg/mL bisbenzimide during manipulation. ZFN-treated and sorted cells were trypsinized and observed under a microscope (Nikon). Cells with impaired membrane were excluded as morphological changes in cell membrane like irregular cell surface indicate cell death (Buja et al., 1993; Van Cruchten and Van Den Broeck, 2002). The cells expressed both RFP and eGFP (Figure 2a, circled) were manually selected using a micromanipulator (Nikon-Narishige, Japan) and fused with enucleated porcine oocytes (Figure 2b) with an electro cell fusion generator (LF101, Nepagene, Ichikawa, Japan) by applying a single direct current pulse (200 V/mm, 20 μs) and a pre- and post-pulse alterating current field of 5 V, 1 MHz, for 5 s, respectively. After 0.5 to 1.5 h oocytes were activated with a single DC pulse of 1.5 kV/cm for 60 μs utilizing BTX electro-cell Manipulator 2001 (BTX, Inc., San Diego, USA). Reconstructed embryos were cultured in porcine zygote medium-5 (Funakoshi, IFP0410P, Tokyo, Japan) was maintained under a humidified atmosphere of 5% CO2, 5% O2, and 90% N2 at 38.5°C for 7 days; cleavage and blastocyst rates were recorded at day 2 and 7, respectively.

f. Statistical analysis

One way ANOVA analysis was performed to compare cleavages and blastocysts rates between each group after SCNT using Prism software (Version 6, GraphPad).

2. Production of *CMAH* Knockout Preimplantation Embryos Derived From Immortalized Porcine Cells Via TALE Nucleases

a. Chemicals

All chemicals were obtained from Sigma-Aldrich (St. Louis, MO) unless otherwise stated.

b. Primary cell culture and maintenance

Male fetal fibroblasts from one miniature pig fetus, which were used as control cells, were isolated and cultured. Euthanized fetus was dissected into three parts: head, body, and tail. Just the body parts of fetuses were washed three times in phosphate-buffered saline and then chopped into small pieces in a 60 mm dish with trypsin. Trypsinized tissues were then incubated for 30 minutes at 37 °C. Well-dissociated tissues were centrifuged at 1,500 rpm for 2 minutes. The supernatant was discarded, and the pellet was resuspended with phosphate-buffered saline and then centrifuged at 1,500 rpm for 2 minutes. These procedures were repeated two times. Finally, the supernatant was discarded, and the pellet was resuspended in Dulbecco's Modified Eagle's Medium (DMEM; Gibco, Carlsbad, CA) supplemented with 15% fetal bovine serum (Gibco), 1% Penicillin/Streptomycin (P/S; Gibco), 1% nonessential amino acid (NEAA; Gibco), and 100 mmol/l β-mercaptoethanol (β-ME) by inverting the tube several times. The cells resuspended in this medium were held at room temperature (~25 °C) for 5 minutes, and then, the suspension was transferred into a cell culture dish for ~10 days with culture medium changed every 2–3 days. These primary cells were cultured, expanded, and frozen at −196 °C for further use. The cell cultures were maintained in DMEM with 15% fetal bovine serum, 1% P/S, 1% NEAA, and 100 mmol/l β-ME.

c. Immortalization

For immortalization, *hTERT* (from Addgene, http://www.addgene.org/, Plasmid #12245)

were amplified by PCR. Purified *hTERT* fragments were inserted in pCMV-IRES-DsRed vectors, which were purchased from Clontech (Seoul, Korea.). *pCMV-hTERT-IRES-DsRed* plasmids were transfected into male fetal fibroblasts which was same cells as control cells using FugeneHD (Figure 1a). Two days after transfection, 1,000 μg/ml neomycin (G418; Gibco) were treated for 7 days to isolate the transfected cells and then growing cells to neomycin resistance were subcultured (Figure 1).

d. Doubling time

Controls and immortalized cells were plated in 12-well plates at 4×10^4 cells/well. Every 24 hours, cells in four of the wells were trypsinized, and cell numbers were calculated manually under a hemocytometer. Then, the doubling time was calculated using the doubling time online calculator (http://www.doubling-time.com/compute.php) 33 every 3 passages up to passage 21, and passage 33 was evaluated as well.

e. Cell size

Images from trypsinized cells on the hemocytometer were taken under a microscope (×200). Sizes of 100 cells were measured by ImageJ (http://rsbweb.nih.gov/ij/) 34 every 3 passages up to passage 21, and passage 33 was evaluated as well.

f. PCR

Genomic DNA was extracted with the G-spin Genomic DNA Extraction Kit (iNtRON Biotechnology, Gyeonggi-do, Korea) according to the manufacturer's protocol. Amplification of target genes was achieved using Maxime PCR PreMix (i-StarTaq, iNtRON). Primer sets, conditions, and expected sizes are annotated in Table 2.

g. Sequencing

Target DNA samples were delivered to a sequencing company (Macrogen, Seoul, Korea). Briefly, sequencing reactions were performed in the DNA Engine Tetrad 2 Peltier Thermal Cycler

(BIO-RAD, Seoul, Korea) using the ABI BigDye (R) Terminator v3.1 Cycle Sequencing Kit (Applied Biosystems, Seoul, Korea), following the protocols supplied by the manufacturer. Single-pass sequencing was performed on each template using a selected primer (primer sequences: AACGTTCCGCAGAGAAAAGA). The fluorescent-labeled fragments were purified by the method recommended by Applied Biosystems because it removes unincorporated terminators and dNTPs (dNTP indicates the mixture of dATP, dCTP, dGTP and dTTP). The samples were subjected to electrophoresis in an ABI 3730xl DNA Analyzer (Applied Biosystems).

h. Karyotyping

To perform karyotyping, cultured cells were treated as follows. First, 200 μl of colcemid (Gibco) stock solution was added to the culture. Then, the culture was returned to the incubator (37 °C, 5% CO2) for 4 hours. After incubation, cells were collected in 15 ml tubes and then centrifuged at 1,000 rpm for 10 minutes. The medium was carefully aspirated, and then, 5 ml of hypotonic solution (0.075 mol/l KCl) was added and allowed to stand at 37 °C for 10 minutes. Then, 500 μl of Carnoy's fixative (methanol:acetic acid 3:1) was added and mixed by inverting the tube, followed by centrifugation at 1,000 rpm for 10 minutes. The hypotonic solution was aspirated carefully, and 3 ml of Carnoy's fixative was added and mixed well. After more than 20 minutes, the mixture was centrifuged at 1,000 rpm for 10 minutes. The supernatant fixative solution was carefully aspirated till leaving about two times of volume to pellets. The pellet was spread on a prepared glass slide which was then baked at 60 °C for 30 minutes. The slide was treated with 50% H2O2 for 3 minutes, then baked again at 60 °C for 30 minutes. Finally, the slide was stained with the Giemsa stain-GTG banding method. Chromosome imaging were accomplished with the ChIPS-Karyo (Chromosome Image Processing System; GenDix, Seoul, Korea).

i. Single cell colony formation

Trypsinized cells were placed on the lid of Falcon dish (Catalog number #351006; Falcon, Franklin Lakes, NJ) in drops of 20 μl of DMEM containing 15% fetal bovine serum, 1%

P/S, 1% NEAA, and 100 mmol/l β-ME. To evaluate single cell colony-forming competence, one cell was picked up in a micropipette attached to a micromanipulator. The cell was transferred into a 4 μl drop of DMEM containing 15% fetal bovine serum, 1% P/S, 1% NEAA, and 100 mmol/l β-ME that was covered with mineral oil. After 7 days, growing cell colonies were collected and sequentially subcultured into 96-, 24- and 6-well plates. Then, cells from the 6-well plates were moved sequentially to 60 and 100 mm dishes.

j. Gene expression

Total RNAs were extracted to analyze gene expression in the immortalized cells by using the easy-spin Total RNA Extraction Kit (iNtRON). Then, complementary DNAs (cDNAs) were synthesized using Maxime RT Premix (iNtRON) according to the manufacturer's protocol. Information on primers is listed in Table 3. Gene expression for *p53, p16, Bax, Bcl-xl, DNMT1, DNMT3a, DNMT3b, GLUT1,* and *LDHA* was measured with a RT-PCR machine (7300 Real-Time PCR System; Applied Biosystems).

k. Telomerase activity test

Quantification and characterization of telomerase activity was done by the telomeric repeat amplification protocol. For this test, TeloTAGGG Telomerase PCR ELISAPLUS (Roche, Basel, Switzerland) kit was used with manufacturer's indications.35 RTA within different samples in an experiment were obtained using the following formula: RTA = [(AS-AS0)/AS,IS]/[(ATS8-ATS8,0)/ATS3,IS] × 100 (AS; absorbance of sample, AS,0; absorbance of heat-treated sample, AS,IS; absorbance of internal standard (IS) of the sample, ATS8; absorbance of control template, ATS8,0; absorbance of lysis buffer, ATS8,IS; absorbance of IS of the control template).

l. Nuclear transfer

Donor cells were subjected to nuclear transfer, which was done following the protocol previously established in our studies (Koo et al., 2009). Briefly, immature oocytes were obtained from pig ovaries and cultured for 40 hours to support maturation. The *in vitro* matured oocytes

were enucleated using an aspiration pipette, then microinjected with a control or transfected donor cell, fused by electrical stimulation, and activated using an electrical protocol. The resulting activated embryos were cultured for 7 days. Cleavage and blastocyst stages were observed on days 2 and 7 of culture, respectively.

m. *CMAH* knockout using TALEN and magnetic separation

All TALEN plasmids were obtained from ToolGen (ToolGen, Seoul, Korea). 37 1 x 10^6 immortalized cells were transfected using 30 μl of Turbofect (Fermentas, Glen Burnie, MD) and 10 μg of plasmid DNA at a weight ratio of 45:45:10 (plasmid encoding a TALEN:plasmid encoding the other TALEN:magnetic reporter) according to the manufacturer's protocol (Kim et al., 2013a; Kim et al., 2011a). The transfected cells were cultured for 2 days at 37 °C and subjected to magnetic separation. Trypsinized cell suspensions were mixed with magnetic bead-conjugated antibody against H-2K^k (MACSelect K^k microbeads; Miltenyi Biotech, Cologne, Germany) and incubated for 15 minutes at 4 °C. Labeled cells were separated using a column (MACS LS column; Miltenyi Biotech, Germany) according to the manufacturer's protocol.

n. T7E1 assay

Genomic DNA was extracted using the G-DEX IIc Genomic DNA Extraction Kit (iNtRON) after 3 days of transfection. TALEN target sites were PCR amplified using primer pairs listed in Table 2. The T7E1 analysis was done as described previously (Kim et al., 2013a; Kim et al., 2009). The amplicons were denatured by heating and annealed to form heteroduplex DNA, which was treated with 5 units of T7 endonuclease 1 (New England Biolabs, Ipswich, MA) for 20 minutes at 37 °C and then analyzed by 2.5% agarose gel electrophoresis.

o. Fluorescent PCR

Carboxyfluorescein was labeled on 5′ end of the forward primer by an oligo synthesis company (Bioneer, Daejon, South Korea). PCR products were processed for fragment separation by capillary electrophoresis on an ABI 3730xl using POP-7 polymer. The GeneScan Rox500 size

standard (Life Technologies, Grand Island, NY) was run as an internal size marker. Samples were denatured at 95 °C for 5 minutes and run on the genetic analyzer. Data were analyzed for allele sizes and peak heights using the pick scanner software v1.0 (Life Technologies).

p. Fluorescence-activated cell sorting

CMAH biallelic knockout cells were trypsinized and resuspended in staining buffer (0.1% bovine serum albumin in phosphate-buffered saline) to reach a final concentration of 5×10^5 to 1×10^6 cells/ml. The cells were incubated for 20 minutes on ice with the antibody anti-Neu5Gc (Sialix, Waban, MA). After incubation, the cells were washed twice with staining buffer and resuspended, then the stained cells were analyzed by fluorescence-activated cell sorting.

q. Statistical analysis

All data were analyzed by one-way ANOVA followed by Tukey's multiple comparison test or paired t-test using GraphPad Prism version 5.01 (http://www.graphpad.com/scientific-software/prism/) to determine differences among experimental groups. Statistical significance was determined when the P value was less than 0.05.

3. Site-directed mutagenesis in *Petunia* × *hybrida* protoplast system using direct delivery of purified recombinant Cas9 ribonucleoproteins

a. *Petunia* protoplast preparation

Protoplasts were isolated from 20-day-old in vitro grown seedlings of *Petunia* × *hybrida* cv. 'Madness' (PanAmerican Seed, IL) after germination in Murashige and Skoog (MS) medium. Young leaves (about 10–15) were pre-plasmolysed with 13 M cell protoplast washing (CPW) solution [KH_2PO_4 (27.2 mg L^{-1}), KNO_3 (101 mg L^{-1}), $MgSO_4$. $7H_2O$ (243 mg L^{-1}), KI (0.16 mg L^{-1}), $CuSO_4.5H_20$ (0.025 mg L^{-1}), $CaCl_2$ (1480 mg L^{-1}), Mannitol

(13 %)] (Cocking EC, 1974) solution followed by enzyme digestion with 20 mL of solution containing different concentrations of Cellulase R-10 + Macerozyme R-10 (1 + 0.05, 1.50 + 0.10, and 2 + 0.25 %, enzymes were dissolved in 8 mM $CaCl_2$, 1 M Manitol, 0.1 M MES, and 0.1 % BSA, Yakult, Japan). The digestion was performed at 25 °C in a rotary shaker at 40 rpm for 4 h. After digestion, protoplasts were filtered through a Nylon mesh (75 µm) and harvested by centrifugation at 600 rpm for 5 min. Collected protoplasts were incubated at 4 °C in CPW salts with Mannitol 9 % solution for 1 h. After centrifugation at 600 rpm for 5 min, the CPW solution was discarded. *Petunia* protoplast pellets were resuspended in 300 µL of MaMg solution (100 mM MES, 1 M Mannitol, 1 $MgCl_2$) and mixed with 300 µL of 40 % Poly ethylene glycol-6000 (PEG). A 50 µg of plasmid construct carrying green fluorescence protein (GFP) marker gene was further added to determine the efficiency of *Petunia* protoplast transfection.

b. Recombinant Cas9 Protein and Guide RNA design

Ready-to-use recombinant Cas9 protein (160 KD) was purchased from ToolGen, Inc. (Seoul, Korea). gRNAs were designed for six target-specific sites with high out-of-frame scores (Bae et al., 2014) for high complete knock out efficiency in the coding regions of *NR* gene locus (Figure 4, Table 5) using CRISPR RGEN Tools website (http://rgenome.net/) (Bae et al., 2014) (Park et al., 2015). A complete coding sequences of *NR* gene locus was amplified and sequenced from *Petunia* × *hybrida* cv. Madness' according to available sequence information of *nitrate reductase* in GenBank (L13691.1). Amplified *NR* gene locus was then used to guide RNA design. sgRNAs were in vitro transcribed and synthesized according to published method (Kim et al., 2014) using specific pairs of DNA oligonucleotides for the target site (Table 6). Purified recombinant Cas9 protein and sgRNA were used in a molar ratio of 1:3 during *Petunia* protoplast transfection.

c. Transfection

To create double standard breaks in *Petunia Nitrate reductase* (NR) gene loci, resuspended protoplasts were transfected with Cas9 protein (90 µg) and sgRNA (50 µg). A 25 µL

of transfection reaction mixture containing 2.5 μL Cas9 protein buffer (50 mM Tris–HCl, 10 mM $MgCl_2$, 100 mM NaCl, 1 mM DTT and pH 7.5), Cas9 protein, sgRNA, resuspended protoplasts along with PEG, and adequate volume of nuclease free water were incubated at room temperature for 30 min. To remove PEG, transfected protoplasts were washed twice with 5 mL of CPW and centrifuged at 600 rpm for 5 min. Pelletized protoplasts were resuspended in 2 mL of MS salt medium (2 % Sucrose and 4 % myo-inositol) to reach a final concentration of 1.0×10^5 mL^{-1}. Protoplasts were resuspended in MS medium and transferred to 6 mL petri dishes followed by incubation in the dark at 25 °C for 24 h.

d. Genomic DNA extraction and T7 endonuclease 1 (T7E1) assay

Genomic DNA was extracted from transfected protoplasts using i-genomic plant DNA extraction kit (Intronbio, Seoul, Korea) according to the manufacturer's instructions. To identify mutations at targeted genomic loci, T7 endonuclease 1 (T7E1) assay was carried out using published method (Kim et al. 2009, 2014). The genomic region of *NR* target site was amplified using nested PCR primers (Table 7). Amplified PCR products were hybridized with mutant and wild-type DNA fragments to form heteroduplex after denaturation and re-annealing using the following program: 95 °C for 120 s, 85 °C for 20 s, 75 °C for 20 s, 65 °C for 20 s, 55 °C for 20 s, 45 °C for 20 s, 35 °C for 20 s, and 25 °C for 20 s, with a 0.1 °Cs−1 decrease rate between steps. Re-annealed PCR products were digested with T7E1 endonuclease (New England Biolabs) at 37 °C for 20 min. Digested PCR products were subjected to agarose gel electrophoresis and gel purification. Purified PCR bands were cloned into pGEM-T vector and sequenced using M13 universal primer.

e. Targeted deep sequencing

Target sites in the *NR* gene loci were amplified by PCR and sequenced according to published methods (Cho et al., 2014). Corresponding target sites were PCR amplified using primers listed in Table 7. Amplifications were performed using Phusion polymerase (New England Biolabs, Ipswich, MA). Amplified PCR products were sequenced using Illumina MiSeq

platform. Mutations induced by RGENs were calculated based on the presence of insertions or deletions around the RGEN cleavage site (3 bp upstream of PAM).

Ⅲ. Results

1. Production of Mutated Porcine Embryos Using Zinc Finger Nucleases and a Reporter-based Cell Enrichment System

a. Enrichment system for cells containing ZFN-mediated mutations

Unlike in rodents, it is technically and economically difficult to obtain in vivo fertilized porcine embryos for genetic manipulation. Moreover, the high incidence of polyspermy (Gil et al., 2010) and low cryo-survival of boar sperm (Rodriguez-Martinez and Wallgren, 2010) also create problems for the production of in vitro fertilized embryos in this species. Therefore, microinjection of ZFNs into fertilized embryos, a technique used for producing knockout rodents, cannot easily be translated to pigs in most laboratories. On that account, we modified our SCNT protocols to produce mutated pig embryos. In first, mutated cells were prepared by transfection of ZFNs into porcine fibroblasts, coupled with reporter-based enrichment systems utilizing two different cell sorting methods, FACS and MACS, described previously (Kim et al., 2013a; Kim et al., 2011a). The enriched mutated cells were used as donor cells for SCNT. During the SCNT procedure, we re-confirmed the expression of reporter genes under microscope and only the cells with double positive for RFP and eGFP expressions (Figure 2a, circled) were used to produce cloned embryos.

To test the feasibility of using these knockout cell enrichment approaches for pig fibroblast cells, we used ZFNs targeting CMAH exon 6 (Figure 1a) and surrogate reporters containing either the eGFP gene alone (eGFP reporter) or eGFP and a truncated H-2Kk surface marker (MACS reporter), whose expression in cells can be recovered by a ZFN-induced frameshift mutation in *CMAH*. Indeed, the use of both surrogate reporter systems together with appropriate sorting methods (FACS or MACS) successfully supported enrichment of fibroblasts containing ZFN-induced mutations in *CMAH* (Figure 1c and d). When these mutant-enriched cell populations were subjected to SCNT, the competence of reconstructed embryos derived from the MACS-separated and FACS-separated cell populations was comparable. Importantly, whereas the cloned embryos from the MACS-separated cell population showed a similar rate of blastocyst

development as compared to the control, the blastocyst development of the cloned embryos from the FACS-separated cell population was significantly impaired (Table 1; 13.1±2.5% vs 24.3± 0.8%). This difference might be caused by various stresses — including hydraulic pressure, shear force, vibrations, and high voltages — that cells experience during flow cytometry (Wolff et al., 2003). Consistent with this idea, large numbers of membrane-damaged cells were observed after FACS-mediated cell separation.

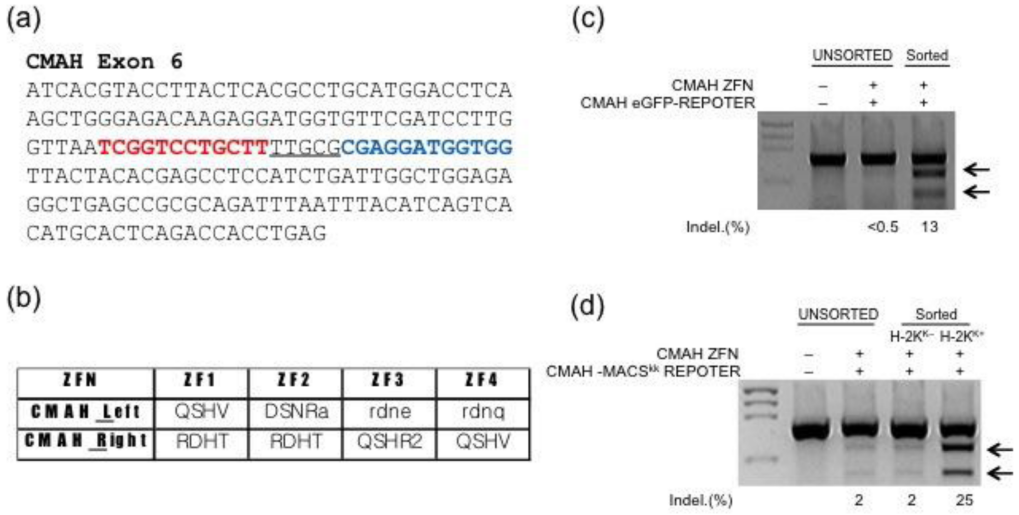

Figure 1. Enrichment system for cells containing ZFN-mediated mutations. (a) Sequences of the ZFN binding sites in the *CMAH* gene. The binding site of the right (red letters) and left (blue letters) ZFNs and the spacer sequence (underlined) are indicated. (b) The zinc finger module composition of CMAH ZFNs. (c and d) ZFN-driven *CMAH* mutations detected by the T7E1 assay in cell populations isolated by FACS (c) and MACS (d) using a ZFN surrogate reporter. H-2K^k, a truncated mouse MHC class I, is used a selection marker for MACS. Arrows indicate the expected positions of DNA bands from specific cleavage of a mutated site by the mismatch-sensitive T7E1 enzyme. The numbers at the bottom of the gel indicate mutation percentages calculated by band intensities.

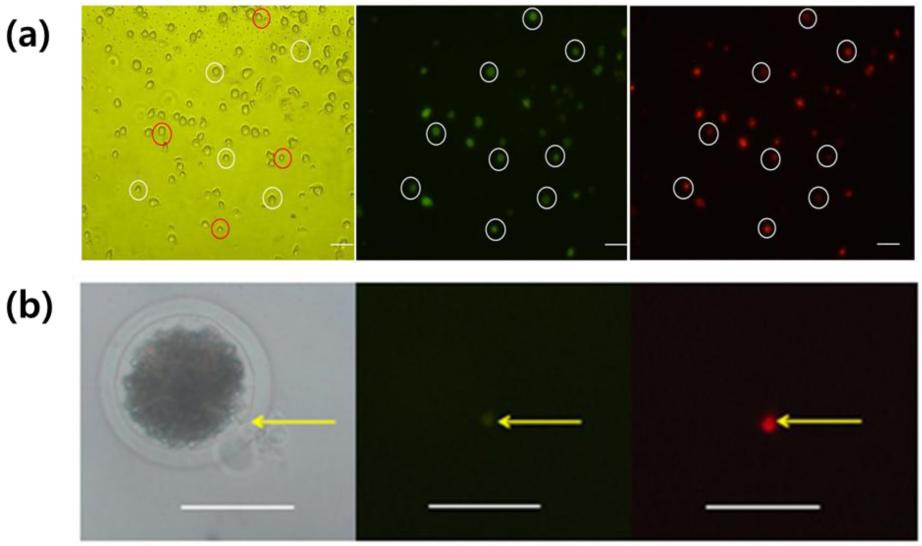

(by Sol Ji Park in College of Veterinary medicine, Seoul National University)

Figure 2. Somatic cell nuclear transfer with ZFN-treated donor cells. (a) Cells with intact membrane (circled in red) expressing both eGFP and RFP simultaneously (circled in white) were selected as donor cells (scale bar = 200 μm). (b) A manually-selected donor cell (arrow) was fused with a porcine oocyte matured in vitro(scale bar = 100 μm).

b. Mutations in cloned blastocysts derived from ZFN-treated cells

We also analyzed the ZFN target sites in the cloned blastocysts. The T7E1 assay results revealed that ZFN-induced mutations at the target site in embryos from both the FACS and MACS groups (Figure 3a). Mutated sequences, including insertions, deletions, and substitutions at the target site, as well as the wild-type sequence, were found in the assessed blastocysts (Figure 3b). Therefore, the mutations established in the study might not be biallelic. Interestingly, three different types of sequences were detected in the FACS group. This result revealed that the ZFN-initiated double-strand breaks and repair by the non-homologous end joining pathways might be still ongoing after the one-cell embryo stage. This phenomenon has been commonly observed in various species of animals derived from ZFN-treated embryos, such as zebrafish (Doyon et al., 2008), mouse (Carbery et al., 2010), rabbit (Flisikowska et al., 2011), and rat (Geurts et al., 2009). Recently, mutant mice with biallelic deletions of the target site were obtained by injection of TALENs, another type of artificial restriction enzyme, into 1-cell embryos (Sung et al., 2013). Thus, the use of TALENs instead of ZFNs might facilitate the establishment of homozygous mutations in pig embryos. Our reporter based enrichment system also can be used with TALENs, therefore, it can be recommended to modify the current method for using TALENs instead of ZFNs to produce biallelic mutated pigs.

Recent reports showed that knockout pigs could be produced by co-transfection of nucleases (ZFNs or TALENs) with an antibiotic-selection marker followed by clonal selection (Carlson et al., 2012; Yang et al., 2011). These previous reports suggested a novel approach for generating knockout pigs. However, clonal selection from a single primary cell requires a lengthy period of time and sophisticated techniques. Use of the reporter-based enrichment system represents an alternative to the antibiotic-based selection method for reducing the time and effort needed to produce knockout pigs.

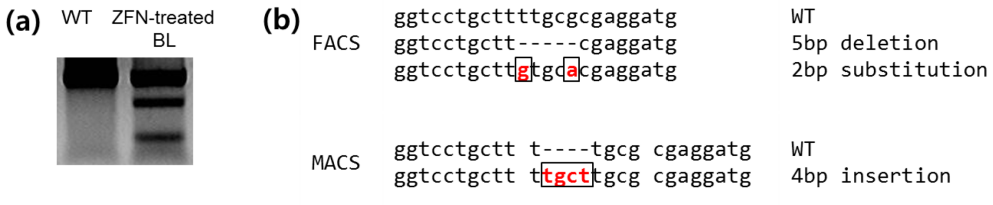

Figure 3. Mutations in cloned blastocysts derived from ZFN-treated cells. (a) The T7e1 assay showed ZFN-mediated mutations in cloned blastocysts. (b) Genomic DNA sequences from the cloned blastocyst.

Table1. *In vitro* culture of cloned embryos derived from ZFN-treated donor cells.

	n	Cleavage (%)	Blastocyst (%)
Control	105	82 (77.7±4.5)	20 (24.3±0.8)a
FACS	157	116 (61.11±6.5)	16 (13.1±2.5)b
MACS	119	83 (65.0±1.9)	14 (16.7±1.6)ab

(by Sol Ji Park in College of Veterinary medicine, Seoul National University)

[a,b]Values with different superscript letters in the same column indicate significant differences.

2. Production of *CMAH* Knockout Preimplantation Embryos Derived From Immortalized Porcine Cells Via TALE Nucleases

a. Generation of porcine immortalized cell and analysis of immortalized cell's properties

Differences between controls and immortalized cells in morphology, doubling times, and cell size. After transfection, outgrowing colonized fibroblasts were cultured. Along with immortalization of the cells, their size was reduced (Figure 1d). Mean doubling time of control and immortalized cells were 46.4 ± 1.1 and 26.9 ± 0.6 hours, respectively, and these values were significantly different ($P < 0.05$; Figure 4b). Mean cell size of the immortalized cells was 17.9 ± 0.2 μm and always less than 20 μm, while mean cell size of control cells was progressively increasing until these cells enter into replicative senescence. Significant differences in cell size between control and immortalized cells were observed from passage 12 (Figure 4c). PCR, RT-PCR, and sequencing. Integration and expression of the hTERT gene was observed by genomic DNA PCR and RT-PCR in 3 and 18 passages of control and immortalized cells, respectively. PCR and RT-PCR data indicated that the *hTERT* gene was integrated into immortalized cells (Figure 5a,b). Also, sequencing results from both PCR amplificons were exactly the same as those inserted sequences from the vector (see Supplementary Figure 6). Karyotyping. A total of 20 cells in each analysis were subjected on karyotyping. Karyotyping of immortalized cells, prior to passage number 15, revealed normal chromosomes, while subsequently abnormal chromosomes were detected in one cell (Figure 4e). Similar observations were made in control cells, indicating that eight cells showed abnormalities (trisomy in chromosome #17) (Figure 4e).

Single cell colony formation Immortalized cells could be populated from a single cell in a 100 mm dish. This ability was replicated three times more using single cells. However, control cells did not have the ability to be expanded from a single cell in a 100 mm dish.

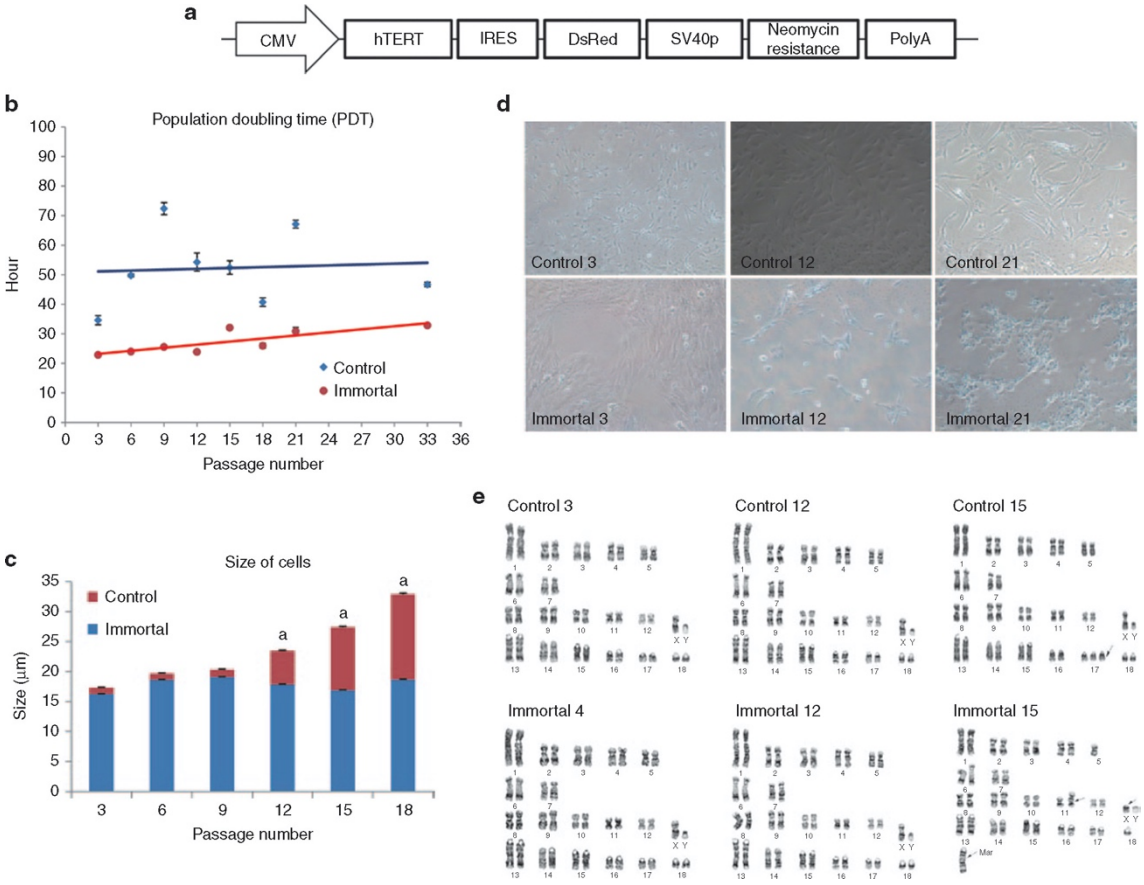

(by JoonHo Moon in College of Veterinary medicine, Seoul National University)

Figure 4. Cellular analysis of porcine immortalized cells. (a) Illustration of pCMV-hTERT-IRES-DsRed, (b) Population doubling time, significant differences in doubling time between control and immortalized cell were investigated, and those were 46.4 ± 1.1 and 26.9 ± 0.6, respectively. (c) Size differences between control cells and immortalized cells, mean cell size of the immortalized cells were 17.9 ± 0.2 which was constantly under the 20 μm while that of control cells were sequentially increasing in mean cell size until these cells enter into senescence or crisis. Significant differences in cell size between control and immortalized cells were observed from passage number 12. (d) Morphologies of control cells and immortalized cells, numbers represent passages. (e) Results of karyotyping, both control and immortalized cells, showed abnormalities from passage number 15. Arrows indicate the abnormal site in chromosomes.

Gene expression Gene expression in immortalized cells and control cells are summarized in Figure 5d. In this analysis, tumor suppressor gene (p53) expression level was not significantly changed during increasing passage number in immortalized or control cells except passage numbers 6 and 15. Cyclin-dependent kinase inhibitor 2A (p16) expression was significantly downregulated during increasing passages (from passage 6) in immortalized cells. Also, Bax, which is a well-known proapoptotic gene, was significantly downregulated during increasing passage numbers (from passage 6) in immortalized cells. However, Bcl-xl, an antiapoptotic gene, was significantly changed in passage numbers 6 and 18. In the analysis of metabolic genes, expression of glucose transporter 1 (GLUT1) and lactate dehydrogenase A (LDHA) were significantly upregulated in late passage of immortalized and control cells, respectively. Expression of methylation relation genes (DNA methyltransferase (DNMT)1, DNMT3a, and DNMT3b) was not changed.

Telomerase activity test: Relative telomerase activity (RTA) of control and immortalized cells were 0.41 ± 0.16 and 5.37 ± 0.09, respectively. Telomerase activity was significantly increased in immortalized cells compared with control cells (Figure 11).

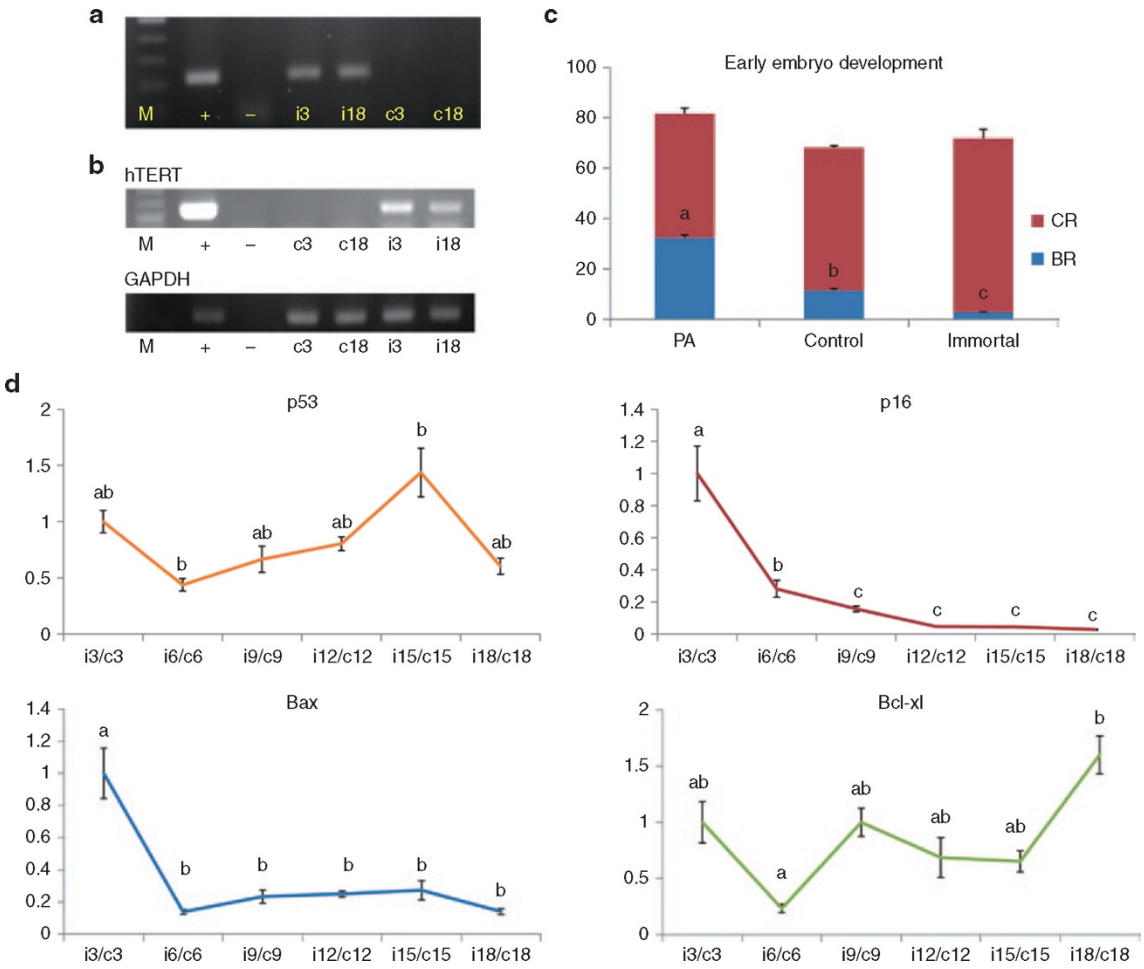

(by JoonHo Moon in College of Veterinary medicine, Seoul National University)

Figure 5. Gene expression in immortalized cells and embryonic development. (a) Detection of hTERT (M, marker; +, positive control vector; −, negative control vector; c, control cells; i, immortalized cells; and numbers referred to passages). (b) Expression of hTERT (M, marker; +, positive control vector; −, negative control vector; c, control cells; i, immortalized cells; and numbers referred to passages). (c) Early embryonic development: changes among early embryonic development when cell properties were changed into immortal states. PA referred parthenogenetic activation. Those control and immortal indicated SCNT results when the donor cell were control and immortalized cells, respectively. Cleavage rates (CRs) were not changed among groups, but blastocyst formation (BR) rates were serially significantly decreased among three groups. (d) Gene expression: tumor suppressor gene (p53) expression level was not significantly changed during the increasing of passage number in immortalized cells/control cells. Cyclin-dependent kinase inhibitor 2A (p16) expression were significantly downregulated during

the increasing of passage numbers in immortalized cells/control cells. Also Bax, which is well known for proapoptotic gene, were significantly downregulated during the increasing of passage numbers in immortalized cells/control cells. However, Bcl-xl, antiapoptotic gene, was significantly upregulated during the increasing of passage numbers in immortalized cells/control cells. *hTERT*, human telomerase reverse transcriptase; SCNT, somatic cell nuclear transfer.

b. Preimplantation development of cloned embryos derived from immortalized cells

Development rates were evaluated in three groups: parthenogenetically activated embryos (total numbers of oocytes: 211), SCNT-derived embryos using control somatic cells as nuclear donors (total numbers of oocytes: 112), and SCNT-derived embryos using immortalized cells as nuclear donors (total numbers of oocytes: 107). Three replicates were done in all three groups. Two days after activation, cleavage rates evaluated under a microscope were 81.6 ± 2.2, 68.1 ± 0.8, and $71.8 \pm 3.6\%$, respectively. No significant differences were observed in cleavage rate among the three groups. However, significant differences were observed in blastocyst formation rates, which were 32.3 ± 1.2, 11.5 ± 0.7, and $2.9 \pm 0.2\%$, respectively (Figure 5c).

c. *CMAH* knockout and SCNT

After transfecting TALEN DNAs, 500 reporter gene–positive cells were cultured in a 100 mm dish and grown into colonies; 116 single cell–derived colonies were selected. In a T7E1 mutation assay, we found 45 colonies to be mutated (see Figure 13). These 45 colonies were subjected to fluorescent PCR for determination of biallelic mutated colonies (see Figure 14). Three biallelic mutation colonies with morphologically good cells were finally selected (Figure 7d) and sequenced for confirmation of biallelic mutation. In #13, a 1 bp insertion and 1 bp deletion were found; in # 24, a 282 bp insertion (sequence of 282 bp was noted in Figure 15) and in #26, 2 and 8 bp deletions were observed (Figure 7c). In addition, as shown by fluorescence-activated cell sorting, CMAH expression was removed in all three cell lines (Figure 6e). Furthermore, 36 cloned embryos derived from *CMAH* knockout cells were reprogrammed after insertion into enucleated oocytes, cleaved (91.7%), and developed into a blastocyst (2.8%) (see Figure 17).

It is well established in humans and in mice that cell lines are necessary to understand or evaluate the molecular process (Graham et al., 1977; Scherer et al., 1953; Todaro and Green, 1963). However, in pigs, such research has been limited to date. In this study, we developed immortalized cells, and furthermore, those cells were used for TALEN to knockout the interesting

genes. For inducing immortalization, genes such as *SV40LT*, *BMI*, and *hTERT* were used in previous studies (Garcia-Escudero et al., 2010). Among these genes, *hTERT* has especially been used to immortalize cells because of reduced chromosome damage (Gaudelli et al., 2017; Ray et al., 1990). In this study, *hTERT* successfully induced pig fetal fibroblasts into immortalization. In addition, our immortalized cells can be cultured for single cell colony formation at least three times. Therefore, single immortalized cell was cultured and propagated to unlimited numbers, indicating that single mutated cells can be isolated and used for many assays requiring cells, DNAs, RNAs, and proteins. For investigating properties of the immortalized cells, expression of proliferative, apoptotic, metabolic, and methylation-related genes were analyzed. Even though significant change of p53 expression at specific passage was observed during long-term culture, p16 was dramatically downregulated (Figure 5) from passage 6. The fact that loss of p16 function after transfection with hTERT is much related to immortalization is in line with our results (Kim et al., 2002). As expected, antiapoptotic gene (*Bax*) was increased but proapoptotic gene (*Bcl-xl*) was decreased. In metabolic gene expression, *GLUT1* was significantly increased because immortalized cell utilize more glucose for unlimited cell proliferative competence like cancer cells (Macheda et al., 2005). Moreover, expression of *LDHA*, which is soluble cytosolic enzyme resulting from apoptosis or necrosis, was increased in late-passage control cells (Chan et al., 2013). One point is about methylation gene expression. In contrast to our results, a previous study reported increase of DNMT1 expression in human fibroblast after hTERT transfection (Young et al., 2003). However, in our case, the DNMTs expression levels were not changed after immortalization. In this study, we found that downregulation (p16 and Bax) and upregulation (GLUT1 and telomerase activity) plays an important role in maintaining the unlimited cell propagation (Figures 5d and 4).

Additionally, it has raised a scientific interest on SCNT embryo production using immortalized cells with long-term culture properties. With respect to early embryonic development, no significant differences were observed in cleavage rates among PA embryos, SCNT embryos derived with control cells, and SCNT embryos derived with immortalized cells. However, significant differences were observed in blastocyst formation rates among these three groups. In particular, blastocyst formation rates were significantly decreased in the immortalized

cell SCNT group. The very low embryonic development using immortalized cells is similar to that reported in a previous study, in which immortalized bovine epithelial cells used in SCNT could not support embryo development into blastocysts (Zakhartchenko et al., 1999). However, with ovine immortalized fibroblasts using hTERT as in this study, there was no significant difference between control and immortalized groups in their ability to support SCNT early embryo development (Cui et al., 2003). In two previous studies (Cui et al., 2003; Zakhartchenko et al., 1999), it was concluded that transformed cells with abnormal cellular responses (like serum starvation) failed to support embryonic development into blastocysts. Therefore, we assume that morphological and proliferative changes in our cells immortalized using hTERT affected normal cellular gene expression profiles including p16 and resulted in very low embryonic development. Because of short cell doubling time, it is hard to get exact G0/G1 cells from immortalized cells. This is another possible reason why SCNT embryos using immortalized cells could not well developed to blastocysts. TALEN, an emerging genome editing tool, can be applied to generate mutant pigs. To knockout a gene using TALEN, several pairs on a specific coding domain region should be designed and evaluated for choosing the most effective pairs. Thus, effective TALEN DNA pairs deleted the DNA with an efficiency of 3.9–43% to date (Hwang et al., 2013a). However, validation systems to determine effective pairs in different species could provide different genome editing efficiencies (Yang et al., 2011). In fibroblasts, before homogeneous knockout cell lines were achieved, single isolated mutated cells became senescent and thus could not be subjected to further analysis and application. Therefore, we strongly suggest that in porcine genome editing, these immortalized cells could be used as appropriate in vitro test cell lines to select effective pairs of TALEN.

(by JoonHo Moon in College of Veterinary medicine, Seoul National University)

Figure 6. Sequencing results from genomic DNA from immortalized cell lines.

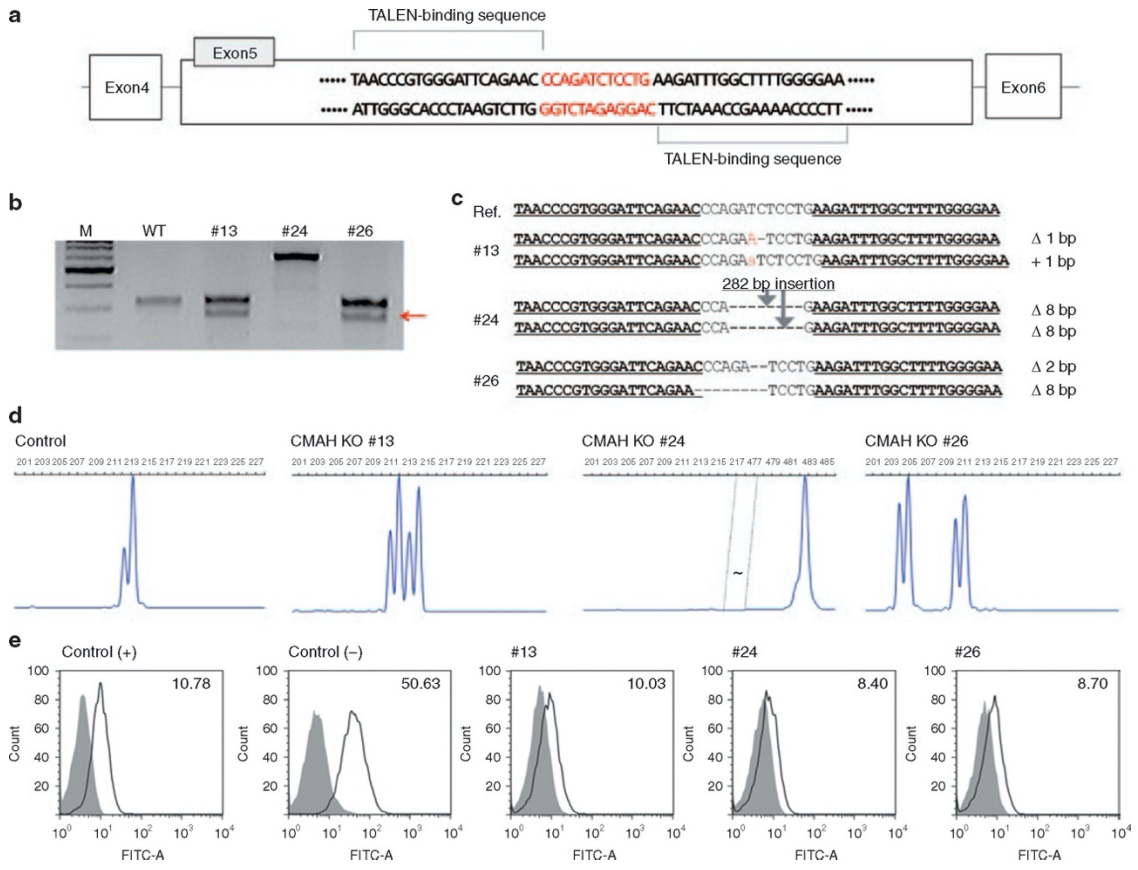

Figure 7. Generating *CMAH* knockout cells and its analysis. (a) DNA-binding sequences and the spacer region for CMAH-TALEN. (b) T7 endonuclease I (T7E1) assays: T7E1 assays were conducted using genomic DNA from three CMAH knockout clones. The arrow indicates the size (~170 bp) of T7E1-digested DNA fragments. (c) DNA sequences of the CMAH locus from each *CMAH* knockout clone. "−" denotes deleted nucleotides. Red colored upper case letter and lower case letter sequences represent nucleotide substitutions and insertion, respectively. (d) Fluorescent PCR (fPCR) assay of the *CMAH* knockout clones. (e) FACS analysis of *CMAH* knockout clones. The expression level of N-glycolylneuraminic acid (Neu5Gc) is detected by anti-Neu5Gc antibody on the *CMAH* knockout cell membrane. The expression levels of Neu5Gc on each *CMAH* knockout clone are comparable with control (+). Control (+), human embryonic kidney cell line; control (−), nontransfected porcine fibroblasts; FACS, fluorescence-activated cell sorting; TALEN, transcription activator-like effector nuclease.

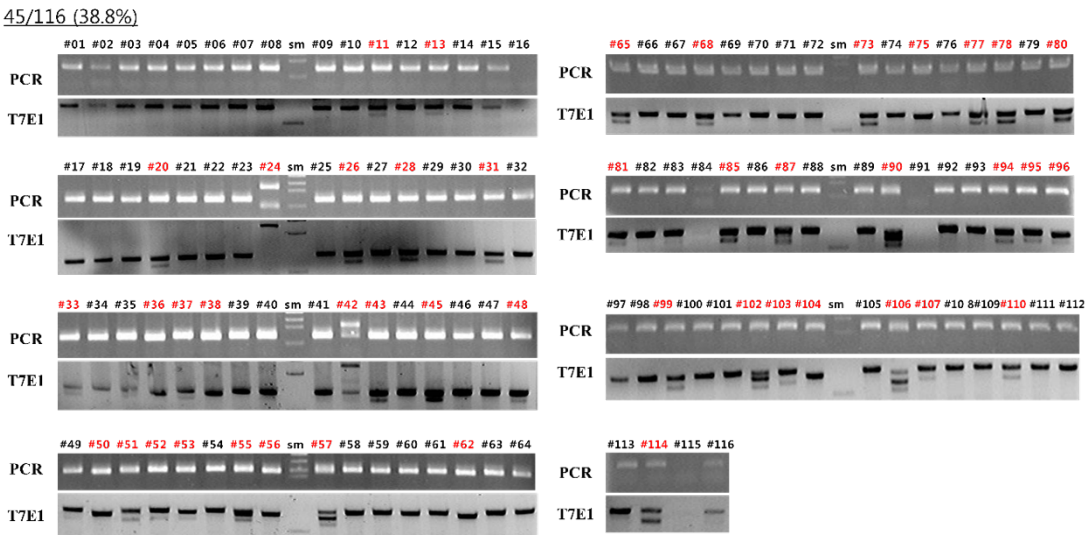

Figure 8. T7E1 assay results from *CMAH* KO single cell colonies. *CMAH* KO single cell colonies were subjected on T7E1 assay for confirming knocked out colonies. Among 116 colonies, 45 colonies were knocked out, which efficiency rate was 38.8% .

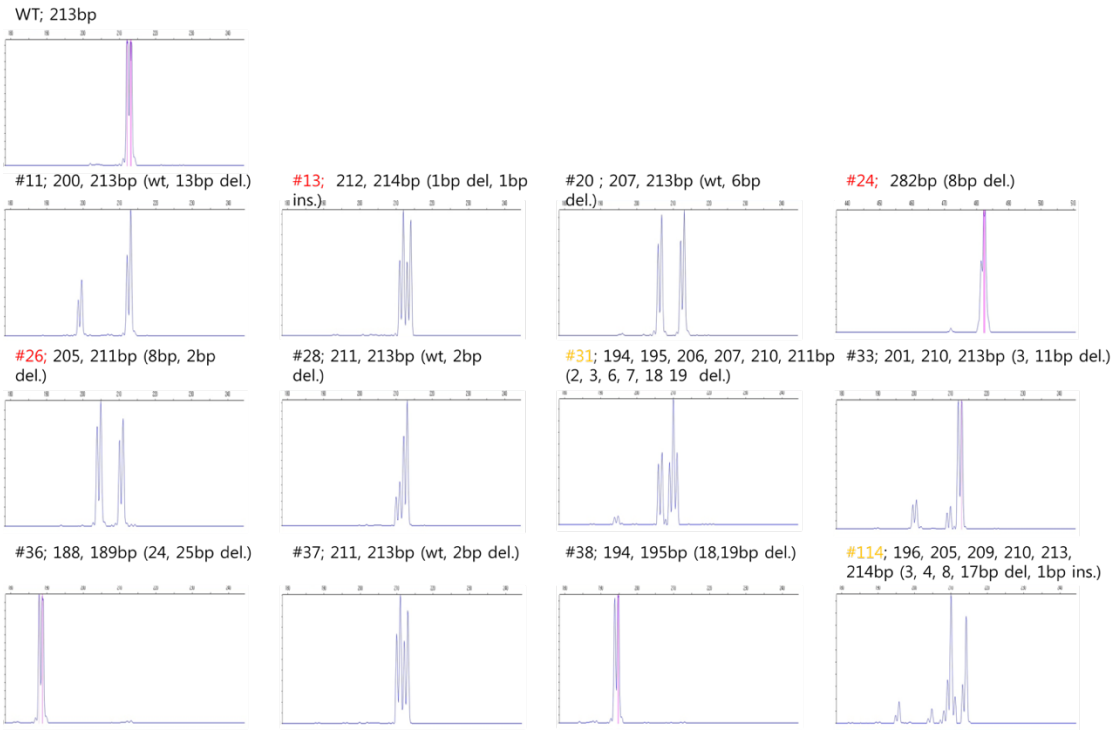

Figure 9. Fluorescent PCR results from *CMAH* KO single cell colonies. Among them 3 colonies were confirmed that biallelic knock-out colonies those were #13, #24 and #26.

AGTTCTAGCCACTAGACCACCAGGGAACTCCCTATTCTAAATTCTTGAG

CACATTATTTAGGAACCTCAGGAACTTGGCAAGGATTACAAGGAAATAT

ATCTAGATTTAAAAAAAAATCTTTTAACAGAGGTCCCAAAGGAGAGTCA

TGCACAGCTATGGGAGGAAGTTCAGAAACTGCCCTTGCTACCAGATCA

CTGTCAGATAAAATGGCCAGCTACATGTTTCTGCACATTGCCCTAAGAT

CTTTACAAACTTTTCTGTGCATTTTTCCACTTTTAAAA

Figure 10. Inserted 282bp sequences in #24 colony.

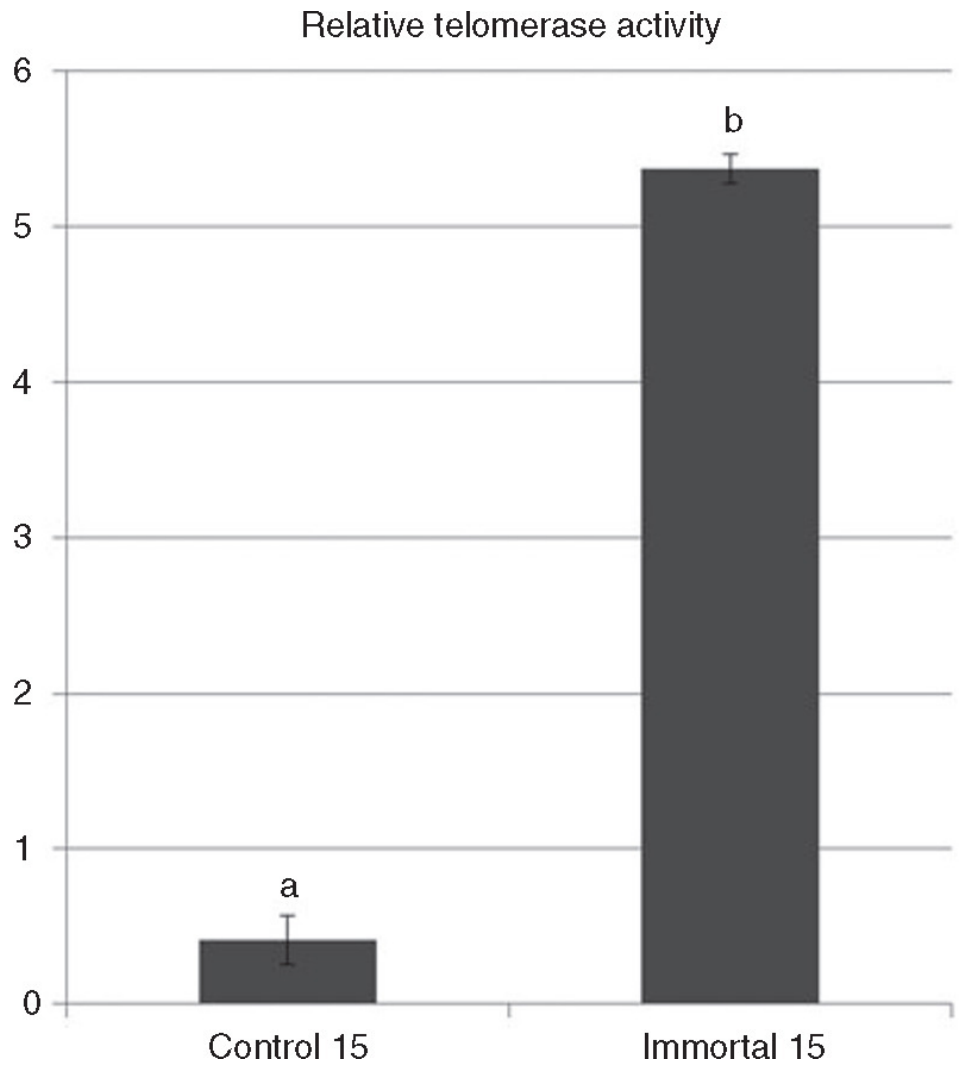

(by JoonHo Moon in College of Veterinary medicine, Seoul National University)

Figure 11. Relative telomerase activity (RTA). RTA of control and immortalized cells were 0.41 ± 0.16 and 5.37 ± 0.09, respectively. Telomerase activity was significantly increased in immortalized cells compared with control cells.

Because immortalized cell line can be grown up from a single cell to billions of cells, we randomly chose 100 single cells and cultured them into colonies of homogeneous s cells. Using single cell colony formation competence as a selection criterion, we can more easily generate knockout cell lines. Indeed, in this study, single cell colonies grew well, and these were used to analyze each colony to evaluate mutation characteristics. As a result, TALEN activity showed 38.8% efficiency, and many cell lines were isolated (see Figure 13). From the finally chosen cells, three biallelic mutated cell lines developed that did not express the cell surface carbohydrate chain, N-glycolylneuraminic acid (Neu5Gc). From one of these three mutated cell lines, colony number 24, cells were used as nuclear donor cells for SCNT. Although the blastocyst formation rate was low, we observed that immortalized cells with *CMAH* knockout can be reprogrammed in porcine enucleated oocytes and develop to the blastocyst stage.

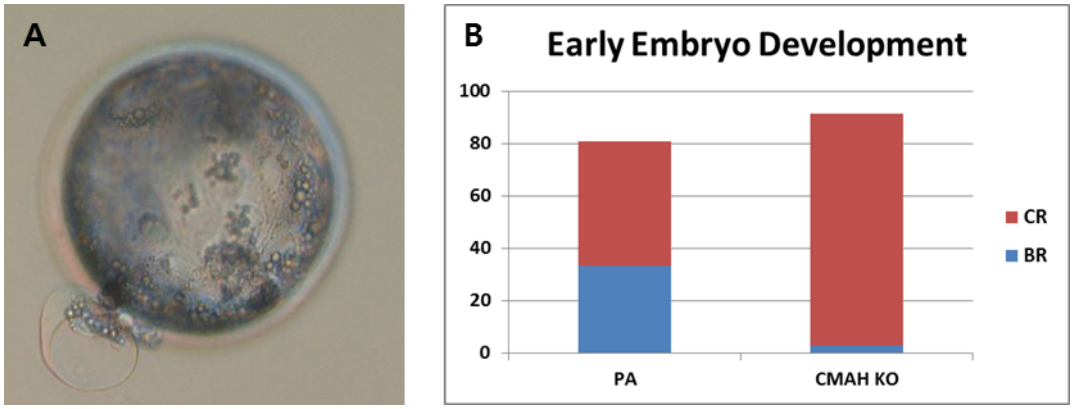

(by JoonHo Moon in College of Veterinary medicine, Seoul National University)

Figure 12. SCNT with *CMAH* KO donor cells. (A) One blastocyst derived from SCNT with *CMAH* KO donor cell. (B) Development rates were evaluated in two groups: parthenogenetically-activated embryos (total numbers of oocytes: 69) and SCNT-derived embryos using *CMAH* KO cells as nuclear donors (total numbers of oocytes: 36). CR: Cleavage Rate, BR: Blastocyst Rate

d. *GGTA1* knockout

Additionally, the other gene, *GGTA1*, which is responsible for hyperacute rejection in xenotransplantation, was also knocked out in this cell line using exactly the same methods with high efficiency (see Figures 13–17) (Kwon et al., 2013).

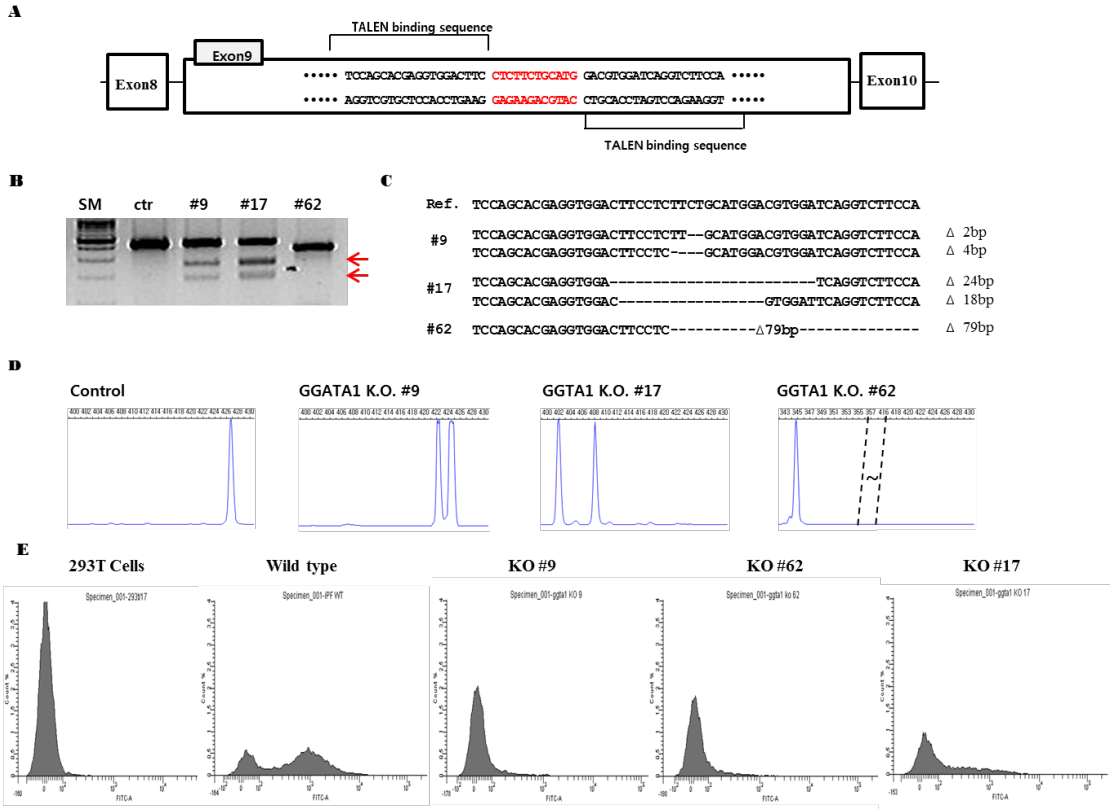

Figure 13. Illustration of TALEN binding sites and results of GGTA1-TALEN KO. (A) DNA-binding sequences and the spacer region for GGTA1-TALEN. (B) T7 endonuclease I (T7E1) assays. (C) DNA sequences of the GGTA1 locus from each GGTA KO clones. (D) Fluorescent PCR (fPCR) assay of the *GGTA1* KO clones. (E) FACS analysis of *GGTA1* KO clones.

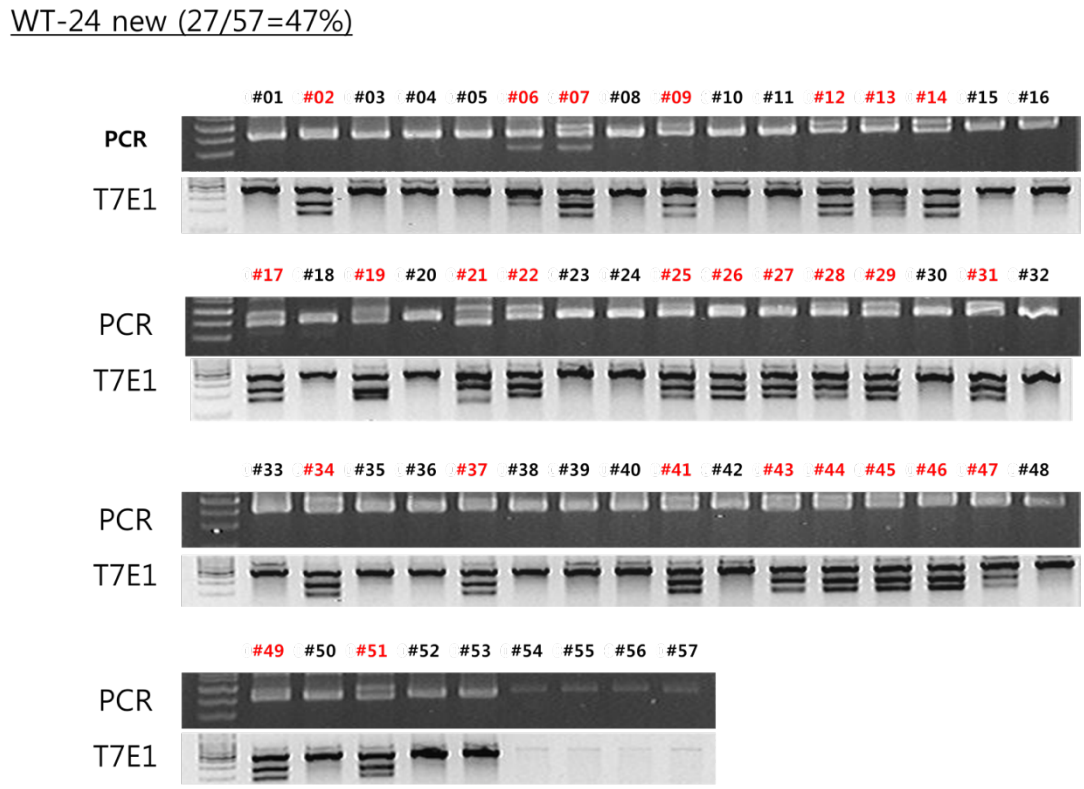

Figure 14. T7E1 assay results from 1st *GGTA1* KO single cell colonies. *GGTA1* KO single cell colonies were subjected on T7E1 assay for confirming knocked out colonies. Among 57 colonies, 27 colonies were knocked out, which efficiency rate was 47%.

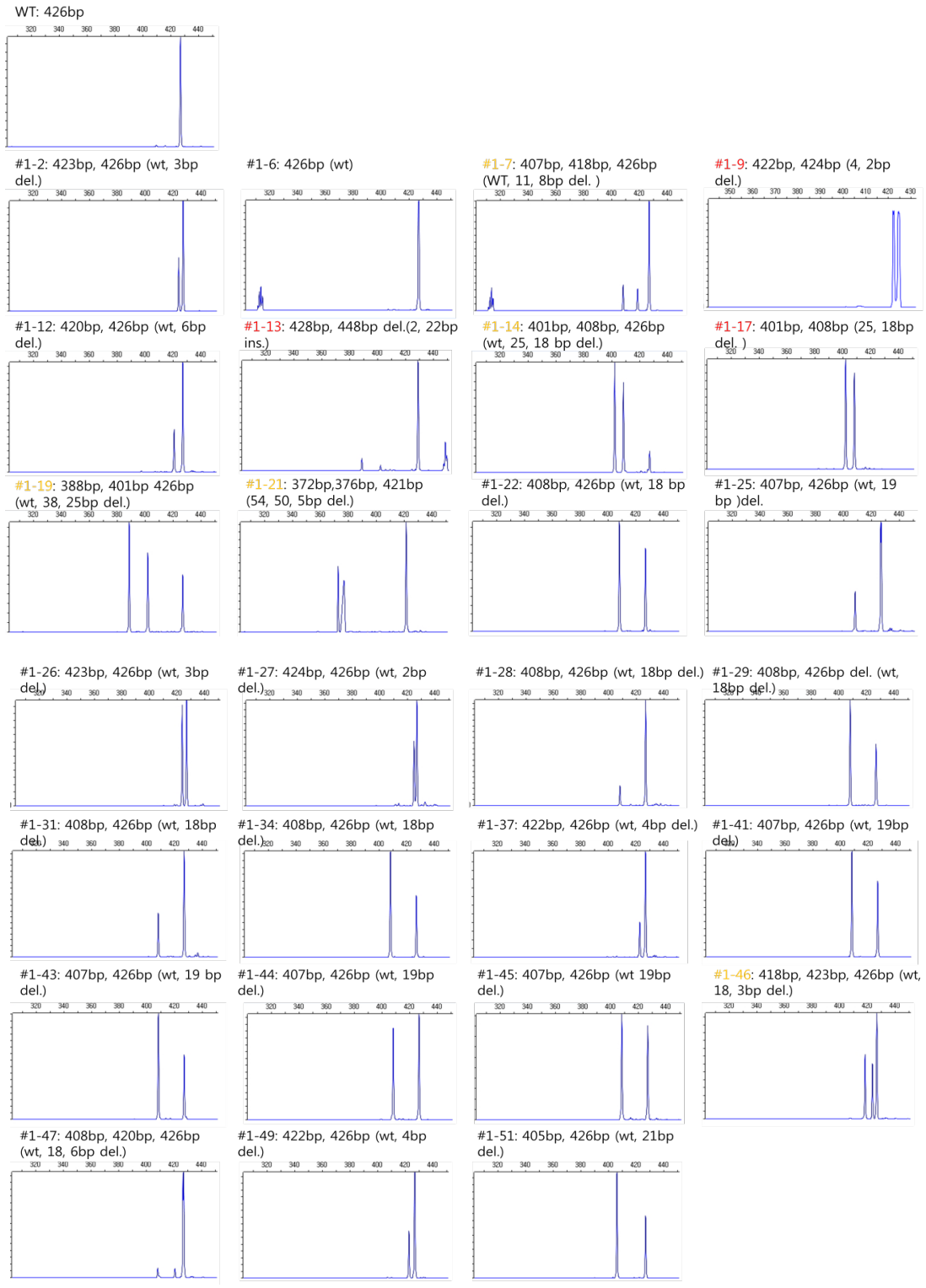

Figure 15. Fluorescent PCR results from 1st *GGTA1* KO single cell colonies.

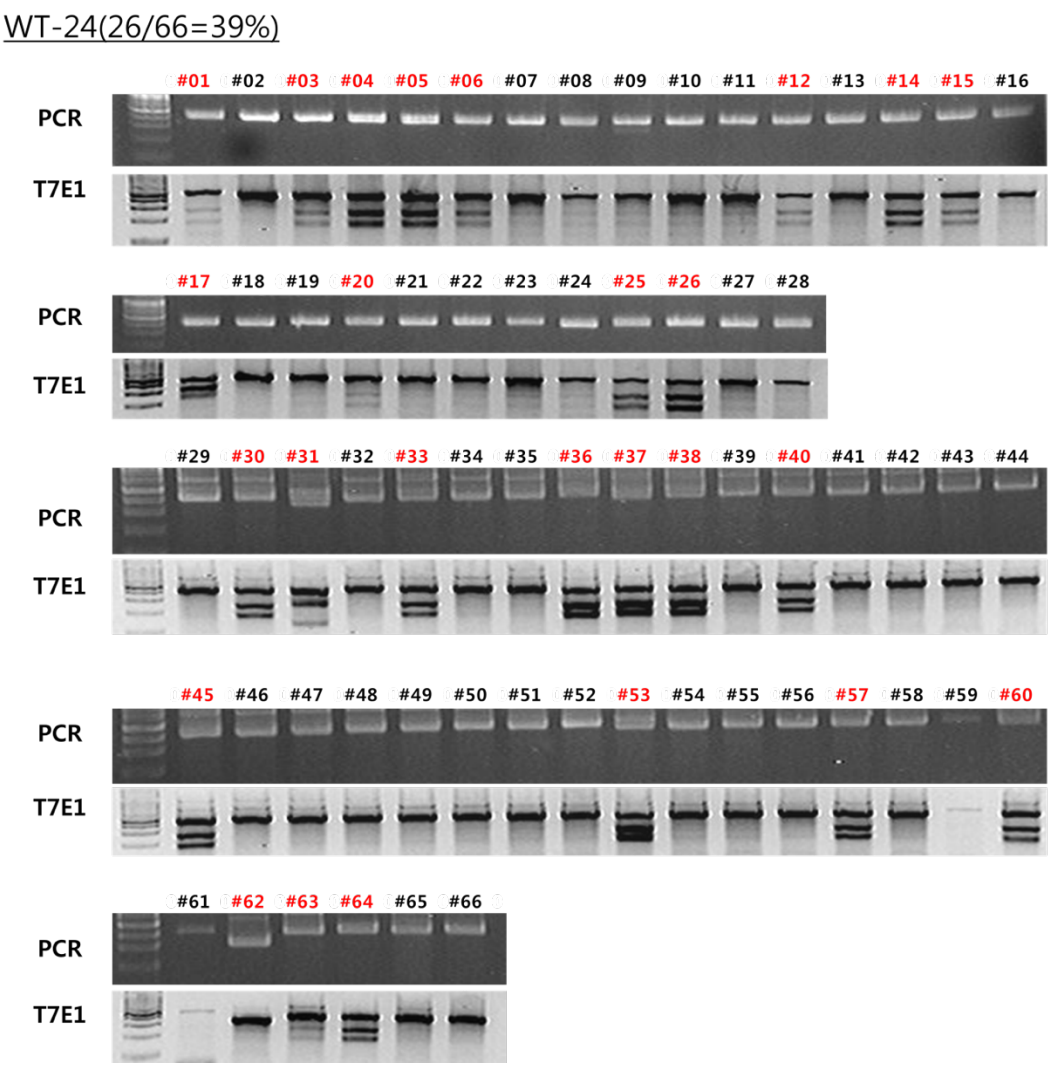

Figure 16. T7E1 assay results from 2nd *GGTA1* KO single cell colonies. *GGTA1* KO single cell colonies were subjected on T7E1 assay for confirming knocked out colonies. Among 66 colonies, 26 colonies were knocked out, which efficiency rate was 39% .

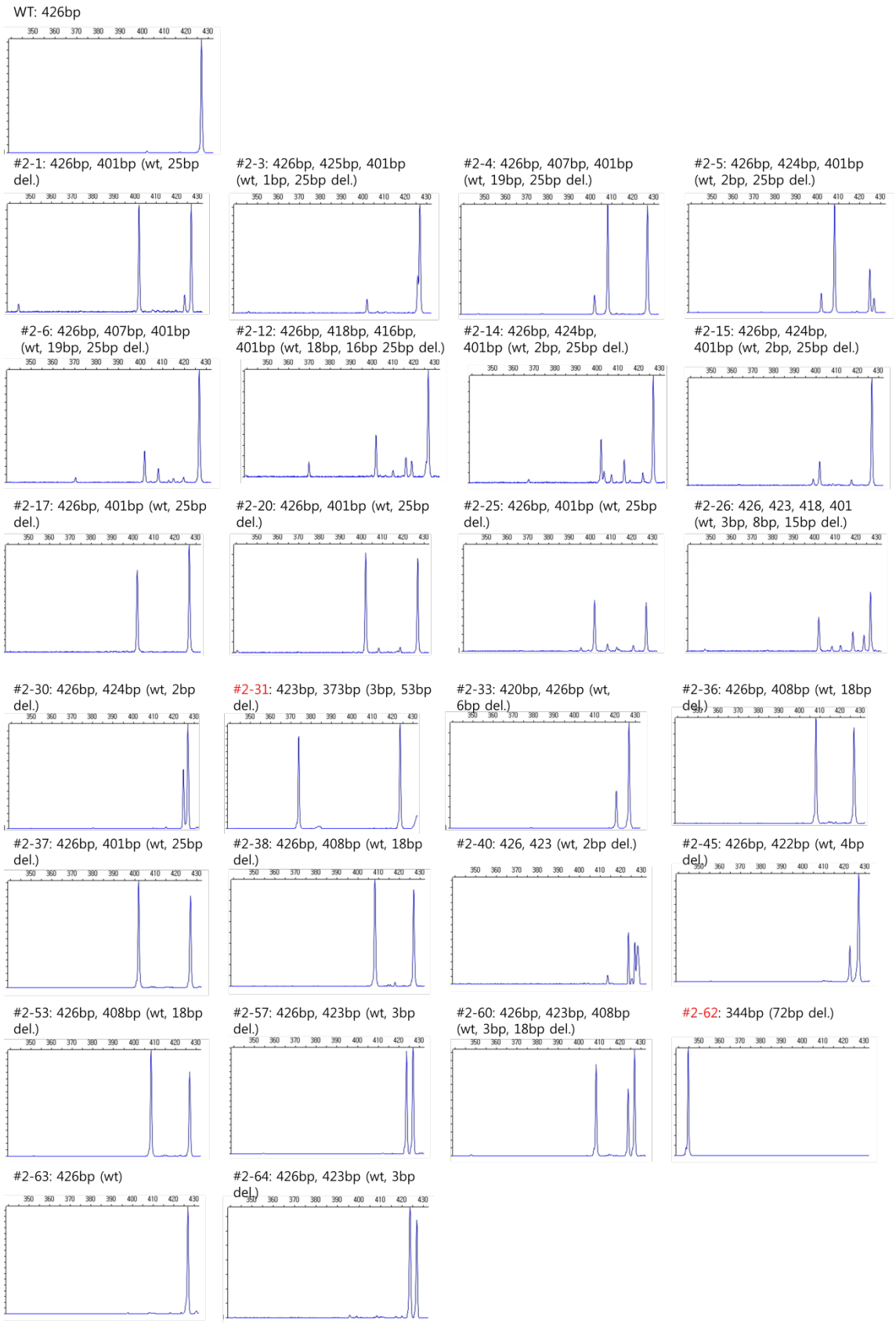

Figure 17. Fluorescent PCR results from 2nd *GGTA1* KO single cell colonies.

Table 2. List of primers.

Gene	Primer sequences (5'-3')		Size of PCR product (bp)	GenBank accession no.
	Forward	Reverse		
hTERT	GTGGTGAACTTCCCTGTAGAAGAC	GAAACAGGCTGTGACACTTCAG	250	NC_000005.9
GAPDH	ACCTGCCGTCTGGAGAAACC	GACCATGAGGTCCACCACCCTG	252	AF017079
1st CMAH	TTGGTCTTCAGCCCTCATCT	CTGGTAGCAAGGGCAGTTTC	743	NM_001113015.1
2nd CMAH	TTGGTCTTCAGCCCTCATCT	ATTTAACATTTCCTTACCTGCAC	307	NM_001113015.1
fPCR CMAH	TTGAGCCATGCATTTCTGTC	ATTTAACATTTCCTTACCTGCAC	213	NM_001113015.1

(with JoonHo Moon in College of Veterinary medicine, Seoul National University)

Table 3. List of real-time PCR primers.

Gene	Primer sequences (5'-3')		Size of PCR product (bp)	GenBank accession no.
	Forward	Reverse		
Bcl-xl	TGGTGGTTGACTTTCTCTCC	ATTGATGGCACTAGGGGTTT	134	AF216205
BAX	GCCGAAATGTTTGCTGACGG	CGAAGGAAGTCCAGCGTCCA	146	AJ606301
p53				NM_213824
p16	CCTCACCATCATCACACTGG	GGCTTCTTCTTTTGCACTGG	213	AJ316067
DNMT 1	CTGGACACTTTGGTGGTCCT	GCGGGATCTTCTCCAGAGTT	185	DQ060156.1
	TCGAACCAAAACGGCAGTAG	CGGTCAGTTTGTGTTGGAGA	215	NM_001097437.1
DNMT 3a	CTGAGAAGCCCAAGGTCAAG	CAGCAGATGGTGCAGTAGGA	238	
DNMT 3b	AGTGTGTGAGGAGTCCATTGCTGT	GCTTCCGCCAATCACCAAGTCAAA	133	NM_001162404.1
	GCTTCCAGTATGTGGAGCAACT	AAGCAATCTCATCGAAGGTCC	132	X17058.1
GLUT1	ATCTTGACCTATGTGGCTTGGA	TCTTCAGGGAGACACCAGCAA	214	NM_001172363.1
LDHA				
GAPDH	TCTCTGCTCCCTCCCCGTTC	TGGCAATGCACGGAACACAC	51	AF017079

(by JoonHo Moon in College of Veterinary medicine, Seoul National University)

3. Site-directed mutagenesis in *Petunia* × *hybrida* protoplast system using direct delivery of purified recombinant Cas9 ribonucleoproteins

a. Efficient protoplast system enhances Cas9 transfection in *P. hybrida*

The protoplast transient expression system has been proved to be a versatile method for CRISPR/Cas9 mediated genome editing in plants. One of the greatest advantage of using protoplast system is that it could provide high level of transgene expression (Shan et al., 2013; Xie and Yang, 2013). CRISPR-Cas9 mediated genome editing using transient transfection system has been successfully applied to many plants, resulting in functional characterization of some potential genes as well as genetic improvement of several agricultural crops. Protoplast transfection has been used as a transfection platform to target genes such as Flagellin Sensitive2 and Receptor for activated C kinase 1 (Arabidopsis) (Li et al., 2013a), Betaine aldehyde dehydrogenase 2 (rice) (Shan et al., 2013), Mildew resistance locus (Wheat) (Wang et al., 2014b), Inositol phosphate kinase (Maize) (Liang et al., 2014), and Phytoene desaturase (Nicotiana Tabaccum) (Gao et al., 2015). In the present study, we isolated protoplasts from leaf mesophyll tissues and standardized a protocol for *Petunia* protoplast transient expression system to test RGEN RNPs (Figure 20). A successful isolation of protoplasts depends on various factors, including different combinations of enzyme concentrations and incubation period (Oh. MH, 1994). They often vary from one plant to another plant. In this study, we used various concentrations for enzymatic digestion to isolate protoplasts from *Petunia* leaves. The yield of protoplasts ranged from 0.3×10^6 to 1.6×10^6 protoplasts for 4–7 h of incubation with 1–2 % cellulase and 0.05–0.25 % macerozyme, depending on the incubation time and enzyme concentrations. A maximum yield of 1.8×10^6 protoplasts was obtained when 0.25 % of macerozyme and 1.5 % of cellulase were used with an incubation time of 4 h. However, during the transfection, the concentration of protoplasts was decreased to 1.0 × 105 mL−1. The yields of protoplasts in this study were similar to those previously reported in *Petunia* genotypes (Meyer. L et al., 2009), indicating that *Petunia* × *hybrida* could be used as a well-established protoplast system for transient gene expression.

The efficiency of *Petunia* protoplast transfection was validated with GFP marker gene. To isolated protoplasts, 50 µg of plasmid vector (PBI221::GFP) containing GFP was used for transfection using the PEG mediated delivery method. Since PEG is considered as an important factor in chemical mediated transfection in plants (Negrutiu et al., 1987), we used three different concentrations of PEG (30, 40, and 50 %). After 24 h of transfection, fluorescence microscopic analyses revealed that approximately 50 and 90 % of transfected protoplasts had GFP expression after 24 and 72 h of incubation, respectively (Figure 21), when 40 % of PEG-6000 was used. These observations were similar to the results of a previous report in rice protoplast system (Xie and Yang, 2013), in which 90 % of GFP expression was noted after 72 h of incubation when 40 % PEG was used. Taken together, these results suggested that the established protoplast system in *Petunia* is well suited for pursuing transfection of recombinant Cas9 protein.

b. Targeted mutagenesis of *NR* gene in *Petunia* protoplast system using direct delivery of RGEN RNPs

To demonstrate RGEN RNPs mediated genome editing in *Petunia*, *PhNR* gene encoding enzyme Petunia nitrate reductase (Salanoubat and Bui Dang Ha, 1993) was selected as a target gene for site-directed mutagenesis using the CRISPR/Cas9 system. Nitrate reductase (NR) catalyzes the first enzymatic step of nitrogen metabolism in higher plants. Many previous studies have reported that changes in expression of *NR* gene via transgenic approach can give a lot of beneficial effects to plants, such as generating interesting phenotypic variations including reduced nitrate levels in leaves, abundant seed protein content, and conferred chlorate herbicide resistance (Zhao et al., 2013) (Dubois et al., 2005) (Vaucheret. H et al., 1997; Wilkinson and Crawford, 1993). Therefore, targeted site mutation of *NR* gene will allow us to test their functional effect on P. *hybrida*.

To induce site-directed mutations in *NR* gene locus, we designed six different sgRNAs based on their corresponding target sites in the *Petunia NR* gene locus, namely NR1, NR2, NR3 NR4, NR5 and NR6 (Figure 18). All these sgRNAs were designed to pair with their corresponding 20 nucleotides at target sites (Table 5) in *NR* gene locus and to help Cas9 system to create site-

specific DSBs at 3 bp upstream of the PAM motifs. To disturb endogenous *NR* genes in *Petunia* protoplasts, we used a RNP complex consisting of purified recombinant Cas9 protein and in vitro synthesized target site-specific sgRNA that contained both crRNA and tracrRNA as described in a previous study (Kim et al., 2014). In cultured human cells, direct delivery of Cas9 proteins has been found to be effective in creating mutations and reducing off-target mutations (Kim et al., 2014). Without any plasmid mediated expression of RGENs usually used in animal and plant systems, the present study demonstrated a direct delivery of RNP complex (Cas9 protein + sgRNA) to *Petunia* protoplasts. Following transfection and 24 h of incubation, RGEN mediated insertion or deletion ("indel") frequency in *NR* gene locus was detected and measured.

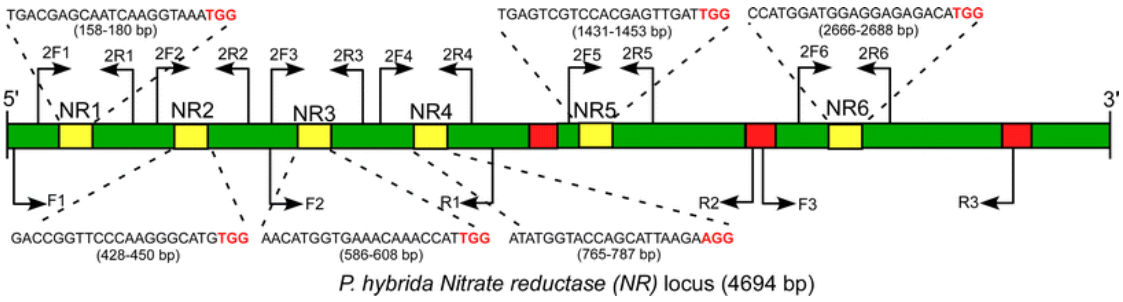

(by Saminathan Subburaj in Chungnam National University)

Figure 18. Design of gRNAs to target six specific sites of P. *Hybrida* Nitrate reductase (*NR*) gene locus and schematic description of *Petunia NR* locus. The green and red rectangles represent exons and introns, respectively. The targeted sites by engineered gRNA are shown as NR1, NR2, NR3, NR4, NR5, and, NR6. The nucleotide sequences of corresponding gRNAs are shown with PAM. The protospacer adjacent motif is shown in red. F1 + R1 to F3 + R3, and 2F1 + 2R1 to 2F6 + 2R6 indicate the position of different kinds of nested PCR primers used to amplify genomic fragment encompassing Cas9 target sites.

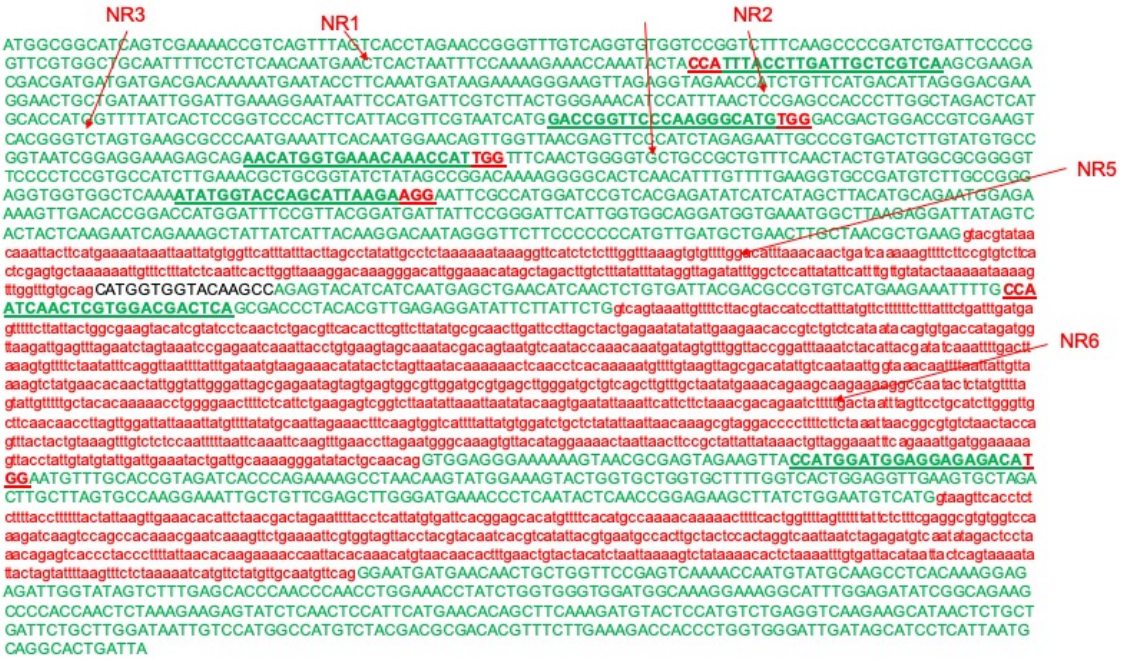

(by Sung Jin Chung in Chungnam National University)

Figure 19. The nucleotide sequences of *Petunia NR* gene locus and regions of RNA-guided Cas9 at NR (1-6)-RGEN target sites. Nucleotides in red and green indicates introns and exons, respectively. Red arrows indicates the positions of NR (1-6)-RGENs. The nuclease target sequences are underlined and shown in bold. Three bp PAM motifs are shown in red.

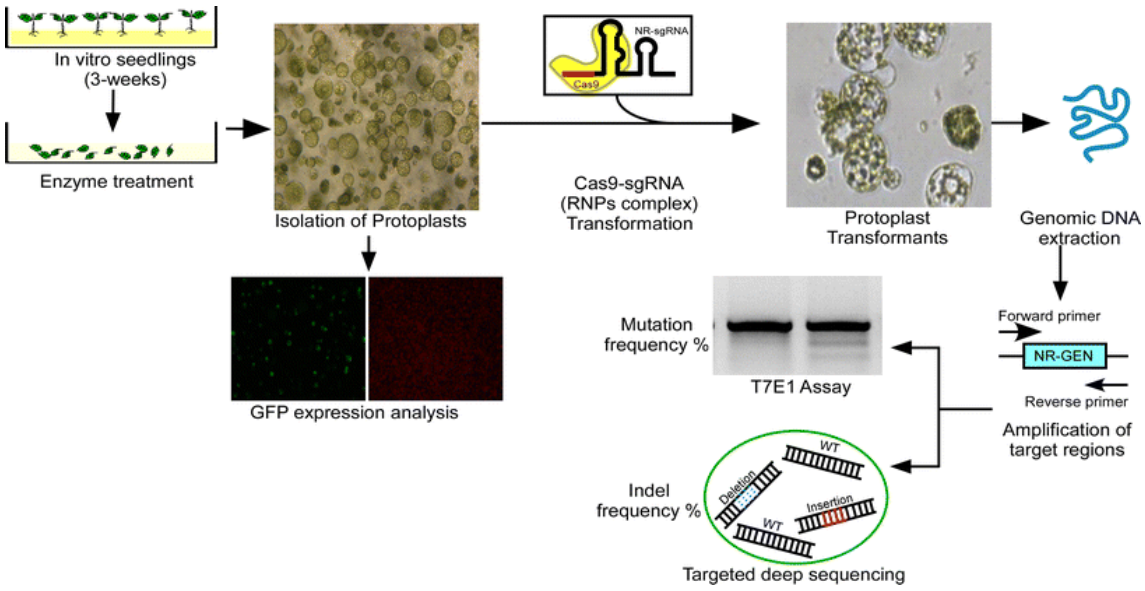

(by Saminathan Subburaj in Chungnam National University)

Figure 20. Scheme for Cas9/sgRNA-mediated mutagenesis of Nitrate reductase gene in *Petunia* protoplast system. Protoplast isolation, production of RNP complex, transfection, identification of target site DNA mutagenesis, and evaluation of mutations were performed for transfected protoplasts.

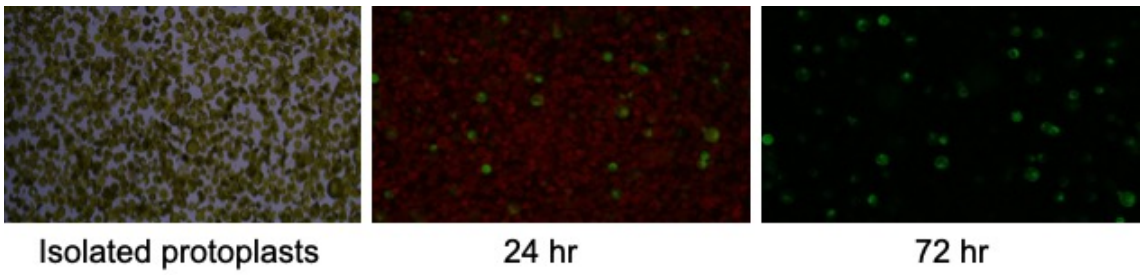

Figure 21. Expression of GFP in *Petunia* protoplasts. *Petunia* protoplasts were transformed with a plasmid carrying PBI221::GFP and observed with a fluorescence microscope at 24 and 72 hours after transformation. The transformed protoplasts were green, and un-transformed protoplasts were red.

We employed a common mutation detection assay called T7E1 enzyme digestion to detect whether there were polymorphisms in *NR* genes induced by the endonuclease activity of designed RGENs. T7E1 has the ability to cleave at mismatched sites due to DNA repair mechanisms of NHEJ (Kim et al., 2009; Morton et al., 2006) during the endonuclease action of ZFNs, TALENs, and Cas9 endonucleases on targeted gene sites. Total genomic DNA were extracted from transfected protoplasts. RGEN target sites in the *NR* gene locus were amplified using site-specific primers (Figure 18; Table 7). PCR amplified products were denatured and reannealed to form heteroduplexes by hybridization with mutated and wild-type (WT) sequences. The resulting DNA sequences might have indel mutations near the DSB site that could be specifically recognized by T7E1 enzyme during digestion. As shown in Figure 22a–d, T7E1 digested DNA products were successfully detected from four (NR1, NR2, NR4 and NR6) of six RGEN transfected protoplasts samples. No product was detected in WT or Cas9 protein only as negative controls. In addition, we detected the expected uncleaved and cleaved band sizes for NR-1, 2, 4, and 6 (Figure 22a–d; Table 7), confirming that the presence of RGEN-induced mutant sectors at target sites within the *NR* genomic locus.

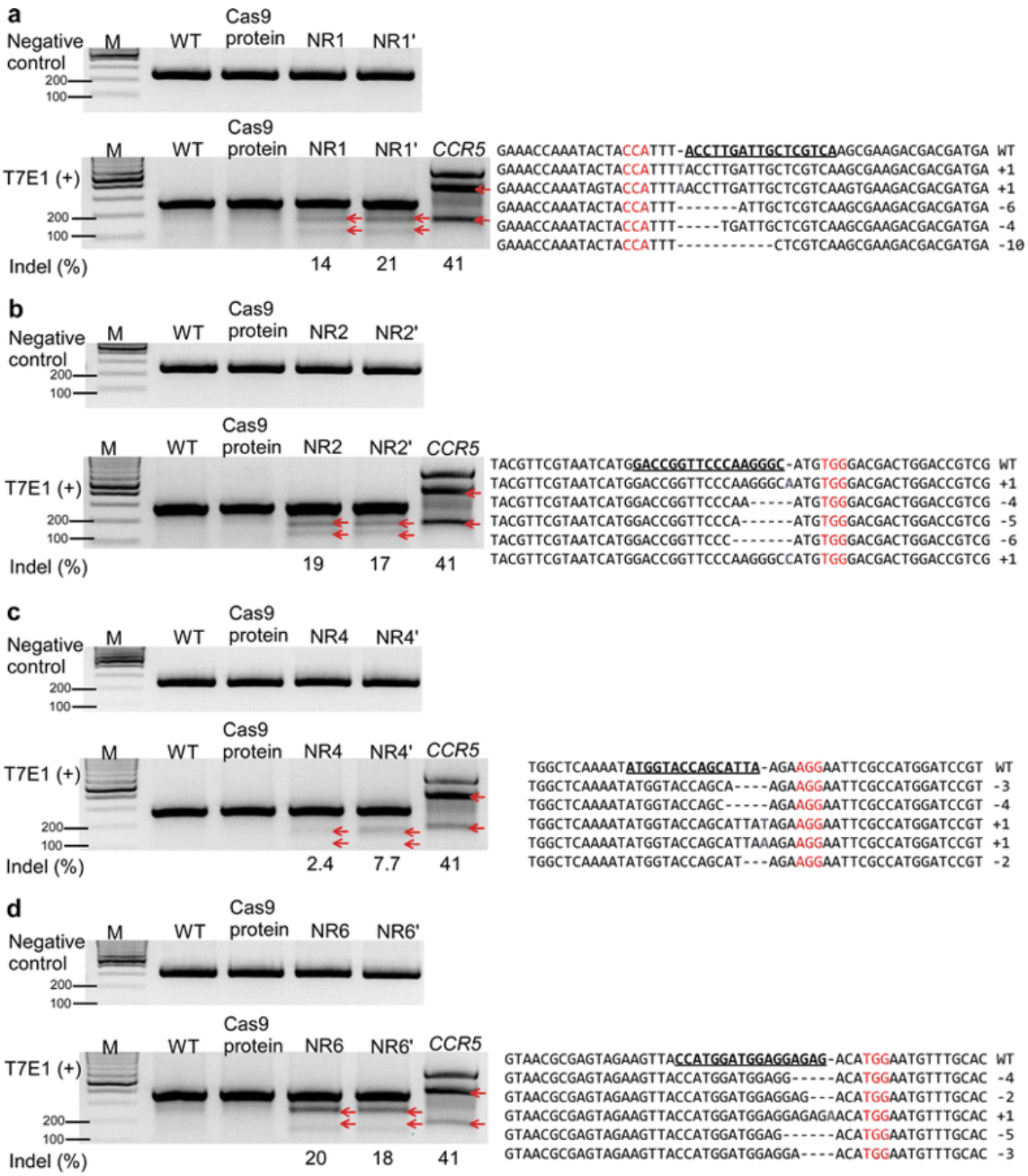

(by Seok-Min Ryu in Seoul National University)

Figure 22. Cas9/sgRNA-mediated mutagenesis of Nitrate reductase (*NR*) gene in *Petunia* using direct delivery of RGEN RNPs. a–d Mutations at NR target sites detected and measured by T7E1 assay. Upper panel gel images showing PCR band before T7E1 assay as negative control. T7E1-mediated cleaved products are marked with red arrows in the lower panel. Two replicates (NR, NR′) of independent experiments are shown here. A *CCR5* gene PCR was used as a positive control in the T7E1 assay. On the right panel, representative mutant DNA sequences at the NR locus obtained from targeted deep sequencing are shown. Nuclease target sequences are underlined and shown in bold. Three bp PAM motifs are shown in red. Insertion mutation is shown in blue.

c. Detection and estimation of Cas9/sgRNA mediated *Petunia NR* gene mutations

We calculated mutation frequencies (%) in NR samples by measuring the band size according to standard procedures (Perez et al. 2008; Kim et al. 2014). In order to determine the ratio of T7E1-undigested (uncleaved) to T7E1-digested (cleaved) DNA products, a standard 569 bp fragment of the *CCR5* gene encompassing a mismatch mutation (at position 390th nt) was also run as positive control along with NR samples and their corresponding replicates (NR′) (Figure 22a–d). The delivered RGENs as RNPs induced mutations in *PhNR* at frequencies ranging from 2.4 to 21 % (Figure 22a–d). The mutation frequency in each NR sample was almost equal to their replicates NR′ except for NR1 and NR4 which showed variations in mutation frequency compared to their replicates NR1′ and NR4′. The mutation frequencies of indels were 14, 19, 2.4, and 20 % in NR1, NR2, NR4, and NR6, respectively. The mutation frequencies of indels in replicates were 21, 17, 7.7 and 18 % for NR1′, NR2′, NR4′, and NR6′, respectively (Figure 22a–d). The average mutation frequency at four different sites (NR1, NR2, NR4, and NR6) in *phNR* gene locus was 14.9 ± 2.2 %.

In rice and maize protoplast systems, Cas9 and gRNA complex-mediated genome editing via plasmid vector induced targeted mutation frequencies of 21 and 13 % with 72 and 48 h of transfection time, respectively (Shan et al. 2013; Liang et al. 2014). Almost similar mutation frequencies (21 and 20 % in NR1′ and NR6, respectively) were induced in *Petunia* protoplast system within 24 h of transfection time in this study, indicating that RGEN RNPs direct delivery is more efficient than the vector based system. Using direct delivery of recombinant Cas9 proteins, mutation frequencies of 16–72 % have been reported in animal cell lines (Kim et al., 2014). Discrepancies in mutation frequencies might be due to variations in experimental assays and methods between plant system and animal system. Recently, Woo et al. (2015) have reported that the direct delivery approach of recombinant Cas9 proteins can induce targeted mutations in tobacco, Arabidopsis, and rice protoplasts with efficiencies ranging from 17 to 23 %, similar to the results of this study in *Petunia* Protoplasts (21 % in NR1′).

To further confirm targeted mutations and investigate mutated patterns at different sites in the *NR* gene (Figure 18; Table 7), we carried out targeted deep sequencing for bulk genomic DNAs obtained from individual targeted cells except for NR3 because it gave non-specific products during PCR amplification. Sequencing data were deposited at National Center for Biotechnology Information (NCBI) Sequence Read Archive (SRA) (http://www.ncbi.nlm.nih.gov/sra/) under the accession number of PRJNA305984. Targeted deep sequencing results showed that there were various numbers of mutated sequences in PCR amplicon sequencing of each target site. Based on the number of total sequences and the number of mutated indel sequences published by Cho et al. 2014, we calculated the indel (mutation) rate frequency (%) of each NR-RGEN samples (Table 4). Our results showed that the four different targeted distinct sites had mutagenic rates of 5.30–17.83 %. The average mutation rate obtained at the five different sites in the *NR* gene locus was 11.5 ± 2 % (Table 4).

Table 4. Estimation of mutation rate in *NR* gene sequences in wild type non-transfected and NR-RGEN transfected protoplasts by targeted deep sequencing using direct delivery of RGEN RNP's.

Protoplast samples	Wild type -transfectants			Cas9 protein -transfectants			NR-RGEN -transfectants				
	Total	Indel	Indel frequency (%)	Total	Indel	Indel frequency (%)	Total	Indel	Indel frequency (%)	Ins[a]	Del[b]
NR1	45,168	3	0.01	35,735	9	0.03	53,898	2854	5.30	1506	1348
NR2	52,699	20	0.04	52,773	24	0.05	71,103	8688	12.22	4128	4560
NR3[c]	–	–	–	–	–	–	–	–	–	–	–
NR4	29,653	4	0.01	36,003	9	0.03	40,670	4392	10.80	1537	2855
NR5[d]	34,842	4572	13.12	22,547	6118	27.13	23,754	8241	34.69	2025	6216
NR6	34,024	131	0.39	28,372	39	0.14	35,095	6256	17.83	1107	5149
Average[e]			0.11 ± 0.1			0.06 ± 0.02			11.5 ± 2	2069.5 ± 536.9	3478 ± 666.6

(by Seok-Min Ryu in Seoul National University)

[a]Numbers of insertions were analyzed in the case of NR-RGEN transfectants.

[b]Numbers of deletions were analyzed for NR-RGEN transfectants.

[c]Protoplast sample 'NR3' was excluded from targeted deep sequencing analysis due to non-specific products during PCR amplification.

[d]Values for protoplast sample 'NR5' was ignored during estimation because of high Indel rate (>10 %) in both WT and Cas9 transfectants resulting from the presence of heterogeneous sequences adjacent to target locus.

[e]Values of average and standard deviation error were calculated for NR1, NR2, NR4, and NR6 only.

As shown in Figure 22, various mutation patterns including insertions and deletions were found at cleavage sites of NR1, NR2, NR4, and NR6 due to obvious DSBs and NHEJ repair systems based on targeted deep sequencing results. For each target site, representative polymorphic sequences were chosen (Figure 22) and the numbers of insertions and deletions were analyzed for NR-RGEN transfectants (Table 4). The estimated average ratio of deletion to insertion produced in the five NR-RGEN target sites of *NR* gene locus was about 63:37 (Table 4). The observed sizes of representative mutagenic deletion and insertion were 1–12 and 0–1 bp, respectively (Figure 22a–d). These observed mutagenic patterns were found to be similar to those of earlier mutagenic studies using different endonuclease enzymes such as ZFNs, TALENs, and RGENs (Kim and Kim, 2014; Kim et al., 2013c; Shan et al., 2013; Woo et al., 2015; Xie and Yang, 2013) . Taken together, these results showed that the direct delivery of RGEN RNPs successfully entered *Petunia* protoplast cells and cleaved the targeted distinct sites of endogenous *NR* genes, leading to gene mutations such as indels via DSBs.

Using *Petunia* as an example, we demonstrated that direct delivery of recombinant Cas9 protein could be guided by sgRNA for precise genome editing. Editing genomes with CRISPR/Cas system has been considered as a simpler and more cost effective system than ZFNs or TALENs (Hsu et al., 2014; Kim et al., 2014). However, when plasmid vectors are used, all endonucleases have been reported to cause off-target effects (Shan et al., 2013; Xie and Yang, 2013) and unwanted genome integration due to the persistence of plasmids (Gaj et al., 2013). To overcome these problems, recent studies have been demonstrated that direct delivery of purified recombinant nuclease proteins such as Cas9 (Kim et al., 2014; Woo et al., 2015) and TALENs (Luo et al., 2015) combined with guide RNA can be used in plant and animal systems to cleave target DNA sequences. One of the greatest advantage of using direct delivery of Cas9 protein is that it can create mutations quickly in a precise manner (Kim et al., 2014; Woo et al., 2015). In addition, it is capable of reducing off-target effects since it is degraded soon after its introduction. Furthermore, RGEN RNPs mediated organisms might be excluded from GMO regulations because no foreign DNA is introduced (Kanchiswamy et al., 2015). In the present study, we did not investigate the occurrence of off-target sites due to limited genome information available for *Petunia*. Recent studies have reported that off-target mutations induced by RGEN RNPs are

rarely found or limited when Cas9 is used at 2–10 fold molar excess of gRNA (Kim et al., 2014; Woo et al., 2015) . The present study used only a low ratio of sgRNA to Cas9 protein (3:1) which was within the ratios used in previous studies, suggesting that its off-target effects might be low. Comprehensive *Petunia* genome-wide approaches are needed to completely identify off-target effects of the delivery system using Cas9 proteins with sgRNA.

Table 5. List of sgRNA's determined to target *Petunia NR* gene locus in this study. Nucleotides in bold indicates the PAM motif in sgRNA sequences.

Target	sgRNA	Sequence (5'-3')	Strand Direction	Position (bp)
NR1	NR1-RGEN	TGACGAGCAATCAAGGTAAA**TGG**	-	158–180
NR2	NR2- RGEN	GACCGGTTCCCAAGGGCATG**TGG**	+	428–450
NR3	NR3- RGEN	AACATGGTGAAACAAACCAT**TGG**	+	586–608
NR4	NR4- RGEN	ATATGGTACCAGCATTAAGA**AGG**	+	765–787
NR5	NR5- RGEN	TGAGTCGTCCACGAGTTGAT**TGG**	-	1431–1453
NR6	NR6- RGEN	CCATGGATGGAGGAGAGACA**TGG**	+	2666–2688

(by Seok-Min Ryu in Seoul National University)

Table 6. List of templates used for in vitro transcription of sg-RNAs.

Target	Primer	Sequence (5'-3')
NR1	sg-RNA Forward	GAAATTAATACGACTCACTATAGGTGACGAGCAATCAAGGTAA AGTTTTAGAGCTAGAAATAGCAAGTTAAAATAAGGCTAGTCCG
NR2	sg-RNA Forward	GAAATTAATACGACTCACTATAGGGACCGGTTCCCAAGGGCAT GGTTTTAGAGCTAGAAATAGCAAGTTAAAATAAGGCTAGTCCG
NR3	sg-RNA Forward	GAAATTAATACGACTCACTATAGGAACATGGTGAAACAAACCA TGTTTTAGAGCTAGAAATAGCAAGTTAAAATAAGGCTAGTCCG
NR4	sg-RNA Forward	GAAATTAATACGACTCACTATAGGATATGGTACCAGCATTAAG AGTTTTAGAGCTAGAAATAGCAAGTTAAAATAAGGCTAGTCCG
NR5	sg-RNA Forward	GAAATTAATACGACTCACTATAGGTGAGTCGTCCACGAGTTGA TGTTTTAGAGCTAGAAATAGCAAGTTAAAATAAGGCTAGTCCG
NR6	sg-RNA Forward	GAAATTAATACGACTCACTATAGGCCATGGATGGAGGAGAGAC AGTTTTAGAGCTAGAAATAGCAAGTTAAAATAAGGCTAGTCCG

(by Seok-Min Ryu in Seoul National University)

Table 7. List of primers used in nested PCR for T7E1 and Deep target sequencing assay.

Target site	1st PCR		2nd PCR		Approximate Product size (bp)
	Primer Sequence (5'-3')	Annealing Regions (bp)	Primer Sequence (5'-3')	Annealing Regions (bp)	
NR1	F1: GTGTGGTCCGGTCTTTCAAG	56-75	2F1: ACACTCTTTCCCTACACGACGCTCTTCCGATCTcgtggctgcaattttcctct	97-117	262
	R1: ATCTCGTGACGGATCCATGG	795-813	2R1: GTGACTGGAGTTCAGACGTGTGCTCTTCCGATCTcagcagttccttcgtcccta	273-292	
NR2	F1: GTGTGGTCCGGTCTTTCAAG	56-75	2F2: ACACTCTTTCCCTACACGACGCTCTTCCGATCTttggctagactcatgcacca	364-383	264
	R1: ATCTCGTGACGGATCCATGG	795-813	2R2: GTGACTGGAGTTCAGACGTGTGCTCTTCCGATCTcggcacatacaagagtcacg	546-608	
NR3	F2: CGTGACTCTTGTATGTGCCG	546-565	2F3: ACACTCTTTCCCTACACGACGCTCTTCCGATCTgtctagtgaagcgcccaatg	476-495	212
	R2: TGTCGTATTTGCTACTTCACAGG	1746-1769	2R3:GTGACTGGAGTTCAGACGTGTGCTCTTCCGATCTtaccgcagcgtttcaagatg	669-688	
NR4	F2: CGTGACTCTTGTATGTGCCG	546-565	2F4: ACACTCTTTCCCTACACGACGCTCTTCCGATCTcatcttgaaacgctgcggta	669-688	261
	R2: TGTCGTATTTGCTACTTCACAGG	1746-1769	2R4: GTGACTGGAGTTCAGACGTGTGCTCTTCCGATCTaatccatggtccggtgtcaa	847-866	
NR5	F2: CGTGACTCTTGTATGTGCCG	546-565	2F5: ACACTCTTTCCCTACACGACGCTCTTCCGATCTttgtgcagcatggtggtac	1339-1358	274
	R2: TGTCGTATTTGCTACTTCACAGG	1746-1769	2R5: GTGACTGGAGTTCAGACGTGTGCTCTTCCGATCTcgaagtgtgaacgtcagagt	1594-1613	
NR6	F3: AGTTCCTGCATCTTGGGTTG	2261-2280	2F6: ACACTCTTTCCCTACACGACGCTCTTCCGATCTatggaaaaagttacctattgt	2484-2503	350
	R3: TTCGTTTGTGGCTGGACTTG	3036-3055	2R6: GTGACTGGAGTTCAGACGTGTGCTCTTCCGATCTggtgcttttggtcactggag	2750-2767	

(by Seok-Min Ryu in Seoul National University)

Ⅳ. Discussion

In the first study, our results show that porcine transgenesis can be accomplished using ZFNs together with an enrichment reporter system. We described two types of transient reporter enrichment systems that can enrich cells with nuclease-induced mutation using FACS or MACS. The cloned embryos derived from cells enriched using MACS showed better developmental competence than did those derived from cells enriched by FACS. The desired mutated sequence was found in both systems. Therefore, the current procedure could provide a new generalized platform for producing mutated porcine embryos.

In second the study, the *hTERT* gene prolonged the usual life span of porcine fibroblasts into immortalized status. Immortalized cells with single cell survival properties were treated with TALEN to delete *CMAH*. Then, knocked out cells were employed to generate preimplantation embryos. These immortalized cells must become useful tools as an in vitro model to select the most effective TALEN pairs and knockout-specific genes to support development of biomedically useful pig models.

In the third study, we demonstrated an efficient targeted mutagenesis in *NR* gene of *Petunia* using direct delivery of engineered RGEN RNPs. Results of mutation frequencies and mutation patterns analyses in this study suggested that engineered RGEN RNPs were powerful in creating site-directed mutagenesis in endogenous *NR* genes in *Petunia* protoplasts. However, further studies are required to examine their potential off-target effects and the response of these regenerated plantlets induced by the CRISPR/Cas system in *Petunia*. Nonetheless, our results suggest that direct delivery of engineered RGEN RNPs is an effective breeding tool for *Petunia* and possibly many other crops if not all.

PART 2. Application of designed nuclease: Adenine base editor (ABE)

Ⅰ. Introduction

Nonsense mutations, in which premature termination codons (PTCs) are formed by base-pair substitution, truncate protein synthesis during translation. Such gene dysfunction is a source of severe pathological phenotypes in genetic diseases. Hence, compelling ribosomal read through of the full coding sequence is a reasonable strategy for treating such genetic disorders. To address this issue, previous studies showed to induce the skipping of exons containing PTCs by using antisense oligonucleotides (AONs) (Alter et al., 2006), (Aartsma-Rus and van Ommen, 2007). In other ways, a few small-molecule drugs such as ataluren (Roy et al., 2016; Siddiqui and Sonenberg, 2016), and aminoglycosides (Kuschal et al., 2013) (e.g., gentamicin) have been utilized to bypass nonsense mutations by introducing near-cognate tRNAs at the site of the PTC (Pichavant et al., 2011; Singh et al., 1979). However, those approaches act transiently and have nonspecific effects for the drugs. Alternatively, CRISPR-mediated homology-directed repair (HDR) can be used for gene correction but is limited by low correction efficiency, especially in differentiated nonreplicating cells from higher eukaryotes including humans (Kim, 2018; Komor et al., 2018; Nami et al., 2018).

It was reported that CRISPR-mediated base editing technologies enable highly efficient direct conversion of DNA bases without producing double-strand breaks (DSBs). Cytidine deaminase-based base editors (CBEs) produce C-to-T or G-to-A substitutions between the fourth and eighth bases in the nonbinding strand of single-guide RNA (sgRNA) at protospacer DNA (Komor et al., 2016; Nishida et al., 2016) . On the other hand, A-to-G or T-to-C transitions in the same DNA positions can be achieved by adenine base editors (ABEs) (Gaudelli et al., 2017). In addition to the initial versions of CBEs and ABEs, including ABE7.10, Koblan et al. (Koblan et al., 2018) improved the base-editing activities by expression optimization and ancestral reconstruction, which were named BEmax and ABEmax, respectively. Moreover, Hu et al. (Hu et al., 2018) and Nishimasu et al. (Nishimasu et al., 2018) independently developed new Cas9 variants, named xCas9 and SpCas9-NG, that recognize 5′-NG-3′ and 5′-NAR-3′ sequences, expanding the targetable sites. By combining xCas9 3.7 with ABE7.10 (called xABE here),

Hu et al. (Hu et al., 2018) further demonstrated how to expand the targetable sites for adenine base editing. To date, a few groups have reported to successfully correct target genes by restoring the open reading frame in PTCs by using the ABEs, such as a TAG-PTC of EGFP gene in rice (Li et al., 2018) and both TAA-PTC of the Tyr gene and TAG-PTC of the *DMD* gene in mice. (Ryu et al., 2018) However, although a few meaningful examples were shown, the systematic gene rescue for all possible cases is not demonstrated yet. It is expected that by targeting the coding strand with ABEs, the three possible PTCs, 5′-TAA-3′, 5′-TAG-3′, and 5′-TGA-3′, can be converted to 5′-TGG-3′, which will be translated to tryptophan (Trp). Alternatively, by targeting the noncoding strand, the three PTCs can be converted to 5′-CAA-3′ (translated to glutamine; Gln), 5′-CAG-3′ (Gln), or 5′-CGA-3′ (arginine; Arg), respectively (Figure 23A). In this study, we established an ABE-mediated read-through method, named CRISPR-pass, to bypass PTCs by converting adenine to guanine or thymine to cytosine. We constructed all type of PTCs knockin (KI) cell lines and then showed the read through for all cases. Ultimately, we showed gene rescue at a patient-derived fibroblast containing PTC.

Ⅱ. Materials and Methods

1. General Methods and Cloning

All ABEs were purchased from Addgene (pCMV-ABE7.10, #102919; xCas9(3.7)-ABE(7.10), #108382; pCMV-ABEmax, #112095). The pXY-ECFP-AAVS1-NHEJ-KI donor vector plasmid (Backliwal et al., 2008) (Nguyen et al., 2015) provided by professor J.S. Woo at Korea University, South Korea, and modified by J.Y.) was digested with SacI and BsrGI, and Gibson assembly was then used to generate plasmids containing mutated versions of EGFP. The linearized vector was incubated with amplified EGFP DNA sequences, respectively containing each PTC at the appropriate location, with 20 nucleotides of overhanging homologous sequence at either end (5′-GGTCTATATAAGCAGAGCTC-3′ and 5′-TGTGCGGCTCACTTGTACAG-3′), in a solution containing 2× Gibson master mixture at 50°C for 1 h. 38 After then, pXY-EGFP-AAVS1-NHEJ-KI vector was digested again with SacI. The linearized vector was incubated with additional amplified DNA sequences (5′-ggtctatataagcagagctctcgtcgacgagctcgtttagtgaaccgtcagatcgtttaaacaagttggtcgtgaggcactgggcaggtaag tatcaaggttacaagacaggtttaaggagaccaatagaaactgggcttgtcgagacagagaagactcttgcgtttctgataggcacctattg gtcttactgacatccactttgcctttctctccacaggtgtccagggtaccgagctcgccgccatggtgag-3′) and 2× Gibson master mixture in 50°C. Each sequence of oligos encoding sgRNA was purchased from Macrogen (South Korea). Oligos were heated and cooled down by a thermocycler for complementary annealing. Double-strand oligos were ligated into linearized pRG2 plasmid linearized by BsaI restriction enzyme (Addgene, #104274). List of oligomers for sgRNAs and primer sequences for cloning are in Tables 11 and 12.

2. ClinVar Database Analysis

Bioinformatic analysis of the ClinVar database of human disease-associated mutations was conducted using Python. The ClinVar database (Common_and_clinical_20170905) was used for this analysis. The Python script used to analyze mutation patterns in human diseases and to identify mutations that could be CRISPR-pass targets can be accessed at https://github.com/Gue-ho/CRISPR-pass. In brief, the steps of the analysis were as follows.

1. Among entries in the ClinVar database, we identified mutation patterns in the following categories: indels (insertions or deletions), silent mutations, nonsense mutations, and missense mutations.

a. For precise analysis, entries in each mutation pattern category were subdivided depending on their nucleotide sequence using information about the surrounding genomic sequence and coding sequence (CDS). CDSs were extracted from the SNP database at NCBI. If no CDS was found in NCBI, than data were taken from GRCh38 and hg19.

2. Among the sorted entries from the ClinVar database, the number of nonsense mutations that were potential CRISPR-pass targets were counted. The targetable Cas9 sites were grouped by their associated PAM sequences, such as GG, AG, GA, GC, GT, GAN, and AA.

a. Each Cas9-targetable site was filtered depending on the ABE target range (positions 4 to 8 in the protospacer from the end distal to the PAM) it contained.

b. To prevent counting sequences more than once, in the case of SpCas9, a sequence was counted when at least either GG or AG was possible; the number was counted as a targetable PAM for xABE when at least one of the PAM was possible.

3. Cell Culture and Transfection

HeLa (ATCC, CCL-2) cells were grown in DMEM with 10% fetal bovine serum (FBS) and a penicillin/streptomycin mix (100 units/mL and 100 mg/mL, respectively). 2.5×10^5 HeLa cells were transfected with each ABE (ABE, xABE, or ABEmax)-encoding plasmid (0.7 μg) and each sgRNA expression plasmid (0.3 μg) using Lipofectamine 2000 (Invitrogen) according to the manufacturer's protocol. Cells were collected 5 days after transfection, and the cell's genomic DNA was prepared using NucleoSpin Tissue (MACHEREY-NAGEL & Co.).

GM14867 (*XPC* mutant fibroblasts) were purchased from Coriell Institute and maintained in Eagle's minimum essential medium (EMEM) with 15% FBS and a penicillin/streptomycin mix. BJ-5ta cells (cat. no. CRL-4001, ATCC) were maintained in a 4:1 mixture of DMEM and medium 199 with 10 μg/mL hygromycin B and 10% FBS. ARPE-19 cells (cat. no. CRL-2302, ATCC) were maintained in DMEM:F12 with 10% FBS and a penicillin/streptomycin mix. For plasmid-mediated expression of ABEs and sgRNAs, 6 ×

10^5 fibroblasts were co-transfected with 14 μg of ABE-encoding plasmid and 6 μg of sgRNA-expressing plasmid. Fibroblasts were transfected with the Amaxa P3 primary cell 4D-nucleofector kit using program DS-137, according to the manufacturer's protocol. A-to-G substitutions were analyzed 5 days after transfection.

4. EGFP-PTC-KI Cell Lines

2.5×10^5 HeLa cells were transfected with Cas9-encoding plasmid (0.35 μg), AAVS1-sgRNA-encoding plasmid (0.15 μg), and EGFP-PTC encoding plasmid (0.5 μg) using the Neon transfection system (Invitrogen) with the following parameters: pulse voltage, 1,005; pulse width, 35 ms; pulse number, 2. Seven days after transfection, the culture medium was changed to 150 μg/mL hygromycin B (Thermo Fisher Scientific, cat. no. 10687010)-containing HeLa cell culture medium. Seven days after hygromycin B treatment, single cells were selected and cultured. Single cell-derived clones were analyzed and used for further experiments.

5. Flow Cytometry

Five days after transfection, ABE-treated cells were trypsinized and resuspended in PBS. Single-cell suspensions were analyzed using a FACSCanto II (BD Biosciences) installed at Hanyang LINC+ Equipment Center (Seoul, South Korea).

6. Targeted Deep Sequencing

Genomic DNA segments that encompass the nuclease target sites were amplified using Phusion polymerase (New England Biolabs). Equal amounts of the PCR amplicons were subjected to paired-end read sequencing using Illumina MiSeq at Bio-Medical Science (South Korea). Rare sequence reads that constituted less than 0.005% of the total reads were excluded. Off-targets were selected by Cas-OFFinder (http://www.rgenome.net/cas-offinder/) (Bae et al., 2014), and base substitutions were analyzed by BE-Analyzer (http://www.rgenome.net/be-analyzer/) (Hwang et al., 2018). Primer sequences and list of off-targets are in Tables 12 and 13.

7. Treatment with Ataluren and Gentamicin

GM-14867 cells and the cells treated with xABE and ABEmax were maintained in EMEM with 15% FBS. When the confluency was 60%–70%, the cells were treated with ataluren (10 μM; cat. no. S6003, Selleck) or gentamicin (1 mg/mL; cat. no. G1397, Sigma) for 48 h.

8. Western Blotting

Cell lysates were homogenized in 1× cell lysis buffer (cat. no. #9803, Cell Signaling Technology), and the supernatants were collected after centrifugation for 10 min at 14,000 × g. An equal amount (35 μg) of the protein was separated by SDS-PAGE in 4%–15% mini-PROTEAN TGX precast protein gels (cat. no. 4561084, Bio-Rad) and transferred to nitrocellulose membranes. The membranes were incubated with primary antibodies overnight at 4°C. The primary antibodies utilized in this study were as follows: anti-XPC antibody (cat. no. MA1-23328, Thermo) and anti-β-actin antibody (catalog no. A2668, Sigma). Then, the membranes were treated with the appropriate species-specific secondary antibodies (cat. no. sc-2357 and sc-516102, Santa Cruz) for 1 h at room temperature. After treatment of the membranes with reagents from the EZ-Western Lumi pico kit (cat. no. DG-WP100, DoGEN), the protein bands were visualized using the ImageQuant LAS4000 system with the accompanying software program (GE).

9. Functional Assessment

To assess the functional recovery of GM14867 cells, which carry a homozygous mutation in the *XPC* gene, after treatment with xABE, ABEmax, ataluren, or gentamicin, these cells, together with BJ-5ta WT cells, were exposed to ultraviolet irradiation at 254 nm at 1 $J/m^2/s$ (cat. no. CL-1000, Analytik Jena) and left to grow for 72 h. Cells treated with ataluren or gentamicin underwent treatment for 48 h before ultraviolet exposure. Cell survival was evaluated with a water-soluble tetrazolium salt assay using an EZ-Cytox kit (cat. no. EZ-1000, DoGEN).

10. Statistics

All statistical analyses were performed using the GraphPad Prism 5 program (GraphPad), and results are indicated in the figure legends. The values of each mean and SEM were visualized as horizontal lines and error bars, respectively, in graphs.

11. Data Availability

Sequencing data has been uploaded to the Sequence Read Archive under Bioproject: PRJNA518883. All data are available from the authors upon reasonable request.

Ⅲ. Results

1. *In Silico* Investigation of Applicable Targets for CRISPR-Pass in the ClinVar Database

In Silico Investigation of Applicable Targets for CRISPR-Pass in the ClinVar Database We first inspected all targetable variations registered in the ClinVar database in silico to investigate how many genetic diseases with nonsense mutations could potentially be treated with CRISPR-pass. Of the 50,376 mutations causing pathological phenotypes in the database, nonsense mutations account for 16.2% (Figure 23B); among these, 41.1% are targetable by conventional ABEs that recognize a canonical protospacer adjacent motif (PAM), 5′-NGG-3′, and 95.5% are covered by xABEs, which recognizes a noncanonical set of PAMs, 5′-NG-3′, and 5′-NAR-3′ (Figure 23C). Only 31.5% of the nonsense mutations in the database can be exactly corrected to amino acids found in the nonmutant protein by xABEs, implying that the set of mutations that can be modified for read through by CRISPR-pass is much larger than the set for which exact gene correction in DNA is possible (Figure 23C).

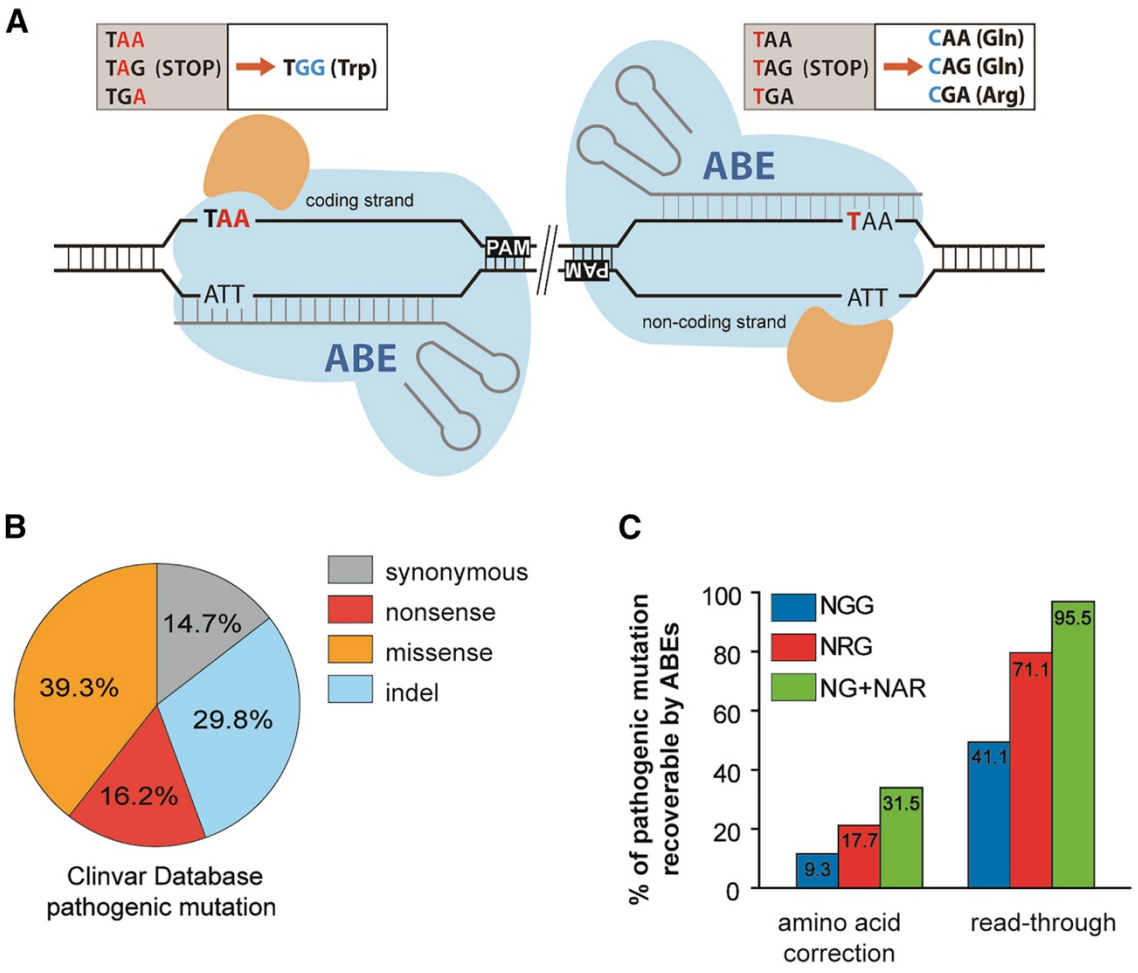

(with Gue-Ho Hwang in Hanyang University)

Figure 23. CRISPR-Pass for Restoring Abbreviated Gene Expression. (A) Schematic of ABE-mediated CRISPR-pass. Targetable adenines are located in the coding or noncoding strand depending on the PAM's orientation. All possible PTCs are shown in the upper boxes (coding strand targeting-TAA, TAG, TGA; noncoding strand targeting-TAA, TAG, TGA). The orange-colored shapes represent adenosine deaminase. (B) The percentages of different types of mutations causing pathological phenotypes in the ClinVar database. (C) The percentages of PTCs that are targetable by CRISPR-pass with various PAMs of variant ABEs and the recoverable rate of intact amino acids and bypassing alternative amino acids are depicted.

2. Construction of Six KI HeLa Cell Lines Carrying Various Types of PTCs in *EGFP* Gene

To demonstrate the efficiency of CRISPR-pass in human cells, as a proof of concept, we tried to construct six KI HeLa cell lines, each carrying a different mutated version of the *EGFP* gene. We first prepared six DNA plasmids having different types of PTCs in the *EGFP* gene. The mutant EGFP genes as a set contain each type of PTC at two locations: the three PTCs in a position that can be converted by targeting the coding strand and the three PTCs in a position that can be converted by targeting the noncoding strand. The first position corresponds to a codon for lysine (Lys53) and the second to a codon for aspartate (Asp217); the encoded residues are located in connecting loop domains of EGFP (Figures 27A and 24). After preparing plasmids containing the six mutated *EGFP* genes, each plasmid was inserted into the genome in an endogenous safe-harbor region, the AAVS1 site, 19 using CRISPR-Cas9 via a nonhomologous end-joining (NHEJ) pathway (Maresca et al., 2013) (Figure 27). The cell lines were named c-TAA, c-TAG, c-TGA, nc-TAA, nc-TAG, and nc-TGA, respectively.

Figure 24. Coding or noncoding targeting depends on the *EGFP* sequence and the PTC position. The sequence of the *EGFP* gene is shown. ABE target sequences are underlined. Depending on the target strand, codons for Lys53 or Asn213 were mutated such that they became STOP codons. The codons that are mutated are shown in blue and the PAM sequences are shown in red.

3. CRISPR-Pass Rescues the Function of the *EGFP* Gene in Six KI HeLa Cell Lines

To test whether ABE treatment would allow bypass of these nonsense mutations, we transfected plasmids expressing sgRNAs designed to target both locations harboring PTCs, together with ABE-encoding plasmids, into the prepared HeLa cell lines. After ABE treatment by lipofection, we found that functional EGFP was expressed, as seen by green fluorescence, in all cell lines. For example, in the case of c-TAA cells, the function of EGFP would be rescued when two adenines are changed to guanines simultaneously for bypassing the PTC. As shown in Figure 27C, the functional EGFPs were observed after various ABEs (ABE7.10, xABE, and ABEmax) were treated. We quantified the ratios of rescued to mutated EGFPs by flow cytometry (Figure 27D). We also confirmed the A-to-G conversion at target DNA regions by targeted deep sequencing in bulk cell populations; the conversion rate of two adenines (A_7A_8) to two guanines (G_7G_8) at once was 11.2% here (Figure 27E).

Similar to the c-TAA cells, we repeatedly carried out CRISPR-pass for all other types of KI cell lines (Figure 25). The quantitative ratios of the functional EGFP expression were also measured by flow cytometry and targeted deep sequencing. As a result, the flow cytometry analysis demonstrated that nonsense mutations were bypassed in 0.7%–17.8% of cells (Figures 27F and 26; Table 8). And targeted deep sequencing analysis confirmed that 0.2%–15.2% of the cells showed A-to-G conversions at target regions with a comparable tendency (Figure 27G; Table 9). It is noteworthy to mention that ABEmax was the most effective one in all cases, resulting in up to 59.6% rescue of the mutant EGFP gene, compared to the ABE7.10 and xABE. And there seems to be some mismatches between EGFP expression levels and substitution rates especially in the case of c-TAG cells, which might be caused by the different expression capacity of each KI cell line due to cell-to-cell variations.

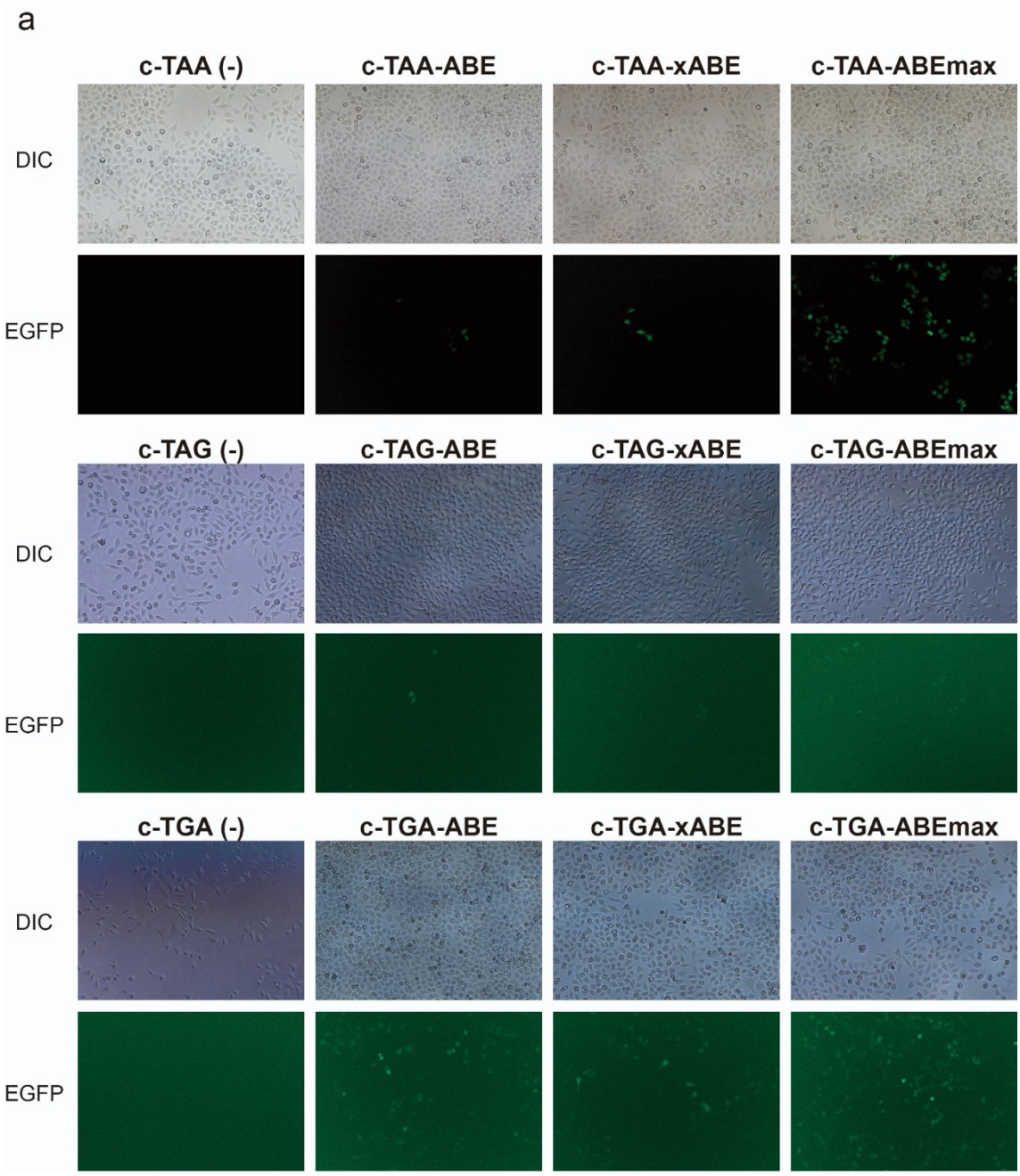
a
c-TAA (-)
c-TAA-ABE
c-TAA-xABE
c-TAA-ABEmax
DIC
EGFP
c-TAG (-)
c-TAG-ABE
c-TAG-xABE
c-TAG-ABEmax
DIC
EGFP
c-TGA (-)
c-TGA-ABE
c-TGA-xABE
c-TGA-ABEmax
DIC
EGFP

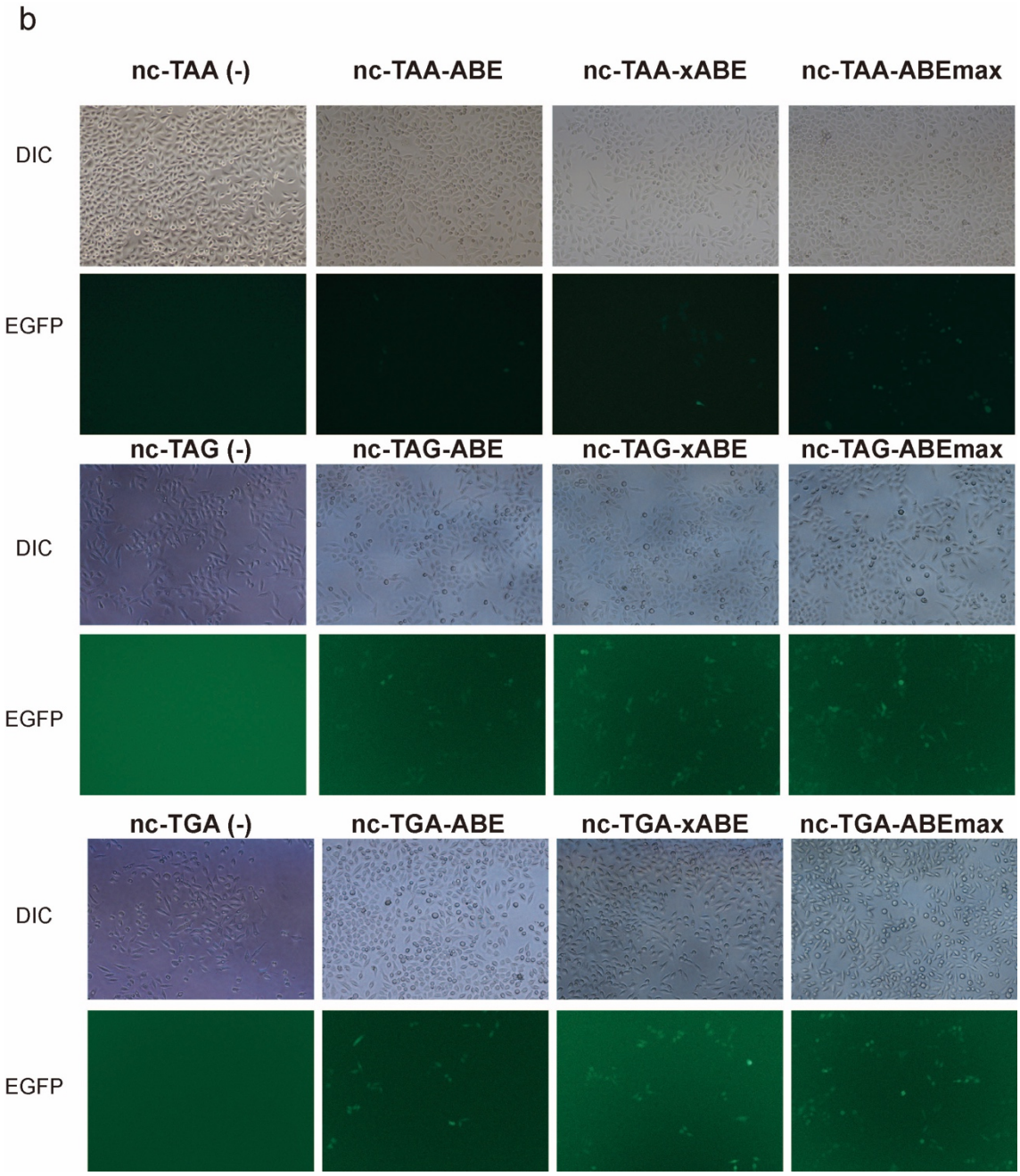

Figure 25. Rescued EGFP expression after treatment with ABEs. Rescued EGFP expression in EGFP-PTC-KI cell lines in which the coding strand (a) or noncoding strand (b) is targeted for PTC bypass.

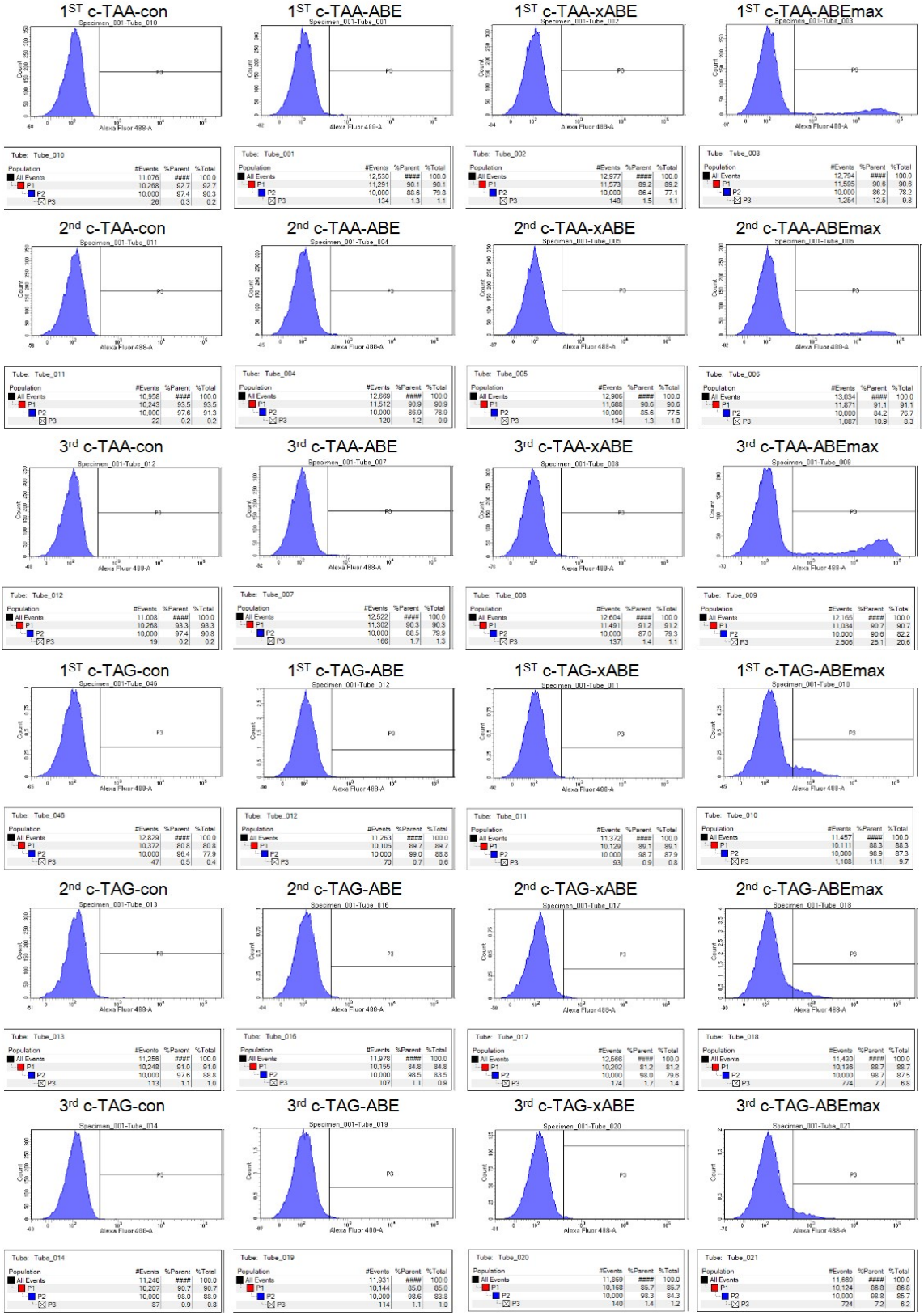
1ST c-TAA-con
1ST c-TAA-ABE
1ST c-TAA-xABE
1ST c-TAA-ABEmax
2nd c-TAA-con
2nd c-TAA-ABE
2nd c-TAA-xABE
2nd c-TAA-ABEmax
3rd c-TAA-con
3rd c-TAA-ABE
3rd c-TAA-xABE
3rd c-TAA-ABEmax
1ST c-TAG-con
1ST c-TAG-ABE
1ST c-TAG-xABE
1ST c-TAG-ABEmax
2nd c-TAG-con
2nd c-TAG-ABE
2nd c-TAG-xABE
2nd c-TAG-ABEmax
3rd c-TAG-con
3rd c-TAG-ABE
3rd c-TAG-xABE
3rd c-TAG-ABEmax

1ST c-TGA-con

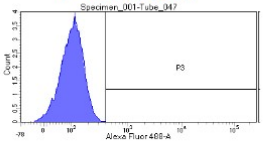

Population	#Events	%Parent	%Total
All Events	12,077	####	100.0
P1	10,212	84.6	84.6
P2	10,000	97.9	82.8
P3	43	0.4	0.4

1ST c-TGA-ABE

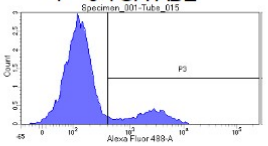

Population	#Events	%Parent	%Total
All Events	11,540	####	100.0
P1	10,131	87.8	87.8
P2	10,000	98.7	86.7
P3	1,784	17.8	15.5

1ST c-TGA-xABE

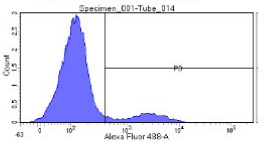

Population	#Events	%Parent	%Total
All Events	11,610	####	100.0
P1	10,176	87.6	87.6
P2	10,032	98.6	86.4
P3	1,315	13.1	11.3

1ST c-TGA-ABEmax

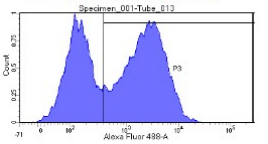

Population	#Events	%Parent	%Total
All Events	11,796	####	100.0
P1	10,153	86.3	86.3
P2	10,000	98.5	85.0
P3	5,962	59.6	50.7

2nd c-TGA-con

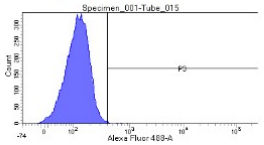

Population	#Events	%Parent	%Total
All Events	11,156	####	100.0
P1	10,185	91.3	91.3
P2	10,000	98.2	89.6
P3	78	0.8	0.7

2nd c-TGA-ABE

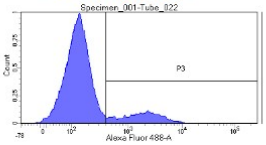

Population	#Events	%Parent	%Total
All Events	11,931	####	100.0
P1	10,169	85.2	85.2
P2	10,000	98.3	83.8
P3	1,622	16.2	13.6

2nd c-TGA-xABE

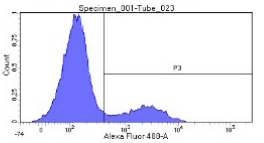

Population	#Events	%Parent	%Total
All Events	11,650	####	100.0
P1	10,190	87.1	87.1
P2	10,000	98.5	85.8
P3	2,035	20.3	17.5

2nd c-TGA-ABEmax

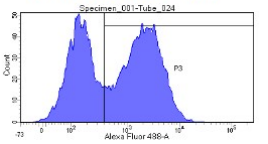

Population	#Events	%Parent	%Total
All Events	11,986	####	100.0
P1	10,242	85.4	85.4
P2	10,000	97.6	83.4
P3	5,771	57.7	48.1

3rd c-TGA-con

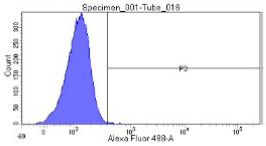

Population	#Events	%Parent	%Total
All Events	11,163	####	100.0
P1	10,209	91.4	91.4
P2	10,000	98.0	89.6
P3	81	0.8	0.7

3rd c-TGA-ABE

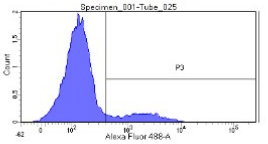

Population	#Events	%Parent	%Total
All Events	11,772	####	100.0
P1	10,156	86.3	86.3
P2	10,000	98.4	84.9
P3	1,418	14.2	12.0

3rd c-TGA-xABE

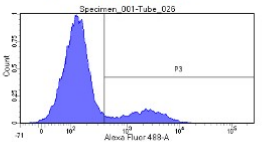

Population	#Events	%Parent	%Total
All Events	11,737	####	100.0
P1	10,161	86.6	86.6
P2	10,000	98.4	85.2
P3	1,823	18.2	15.5

3rd c-TGA-ABEmax

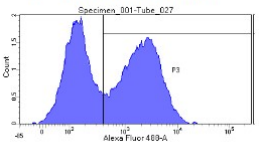

Population	#Events	%Parent	%Total
All Events	11,939	####	100.0
P1	10,209	85.5	85.5
P2	10,000	98.0	83.8
P3	5,502	55.0	46.1

1ST nc-TAA-con

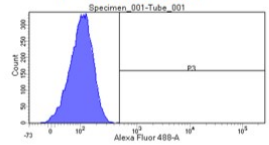

Population	#Events	%Parent	%Total
All Events	11,918	####	100.0
P1	10,578	88.8	88.8
P2	10,025	94.8	84.1
P3	19	0.2	0.2

1ST nc-TAA-ABE

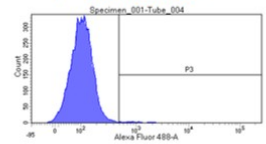

Population	#Events	%Parent	%Total
All Events	11,427	####	100.0
P1	10,267	89.8	89.8
P2	10,000	97.4	87.5
P3	272	2.7	2.4

1ST nc-TAA-xABE

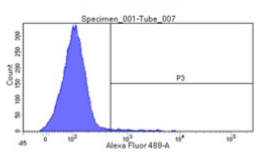

Population	#Events	%Parent	%Total
All Events	11,799	####	100.0
P1	10,282	87.1	87.1
P2	10,000	97.3	84.8
P3	422	4.2	3.6

1ST nc-TAA-ABEmax

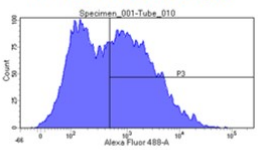

Population	#Events	%Parent	%Total
All Events	11,905	####	100.0
P1	10,437	87.7	87.7
P2	10,000	95.8	84.0
P3	5,218	52.2	43.8

2nd nc-TAA-con

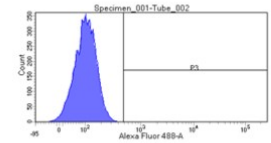

Population	#Events	%Parent	%Total
All Events	12,053	####	100.0
P1	10,691	88.7	88.7
P2	10,040	93.9	83.3
P3	10	0.1	0.1

2nd nc-TAA-ABE

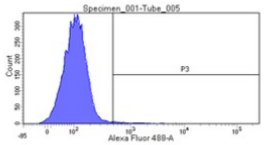

Population	#Events	%Parent	%Total
All Events	11,774	####	100.0
P1	10,332	87.8	87.8
P2	10,000	96.8	84.9
P3	320	3.2	2.7

2nd nc-TAA-xABE

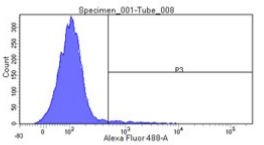

Population	#Events	%Parent	%Total
All Events	12,031	####	100.0
P1	10,472	87.0	87.0
P2	10,000	95.5	83.1
P3	533	5.3	4.4

2nd nc-TAA-ABEmax

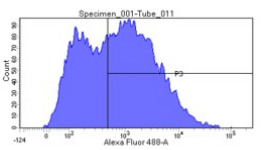

Population	#Events	%Parent	%Total
All Events	11,922	####	100.0
P1	10,307	86.5	86.5
P2	10,000	97.0	83.9
P3	5,895	59.0	49.4

3rd nc-TAA-con

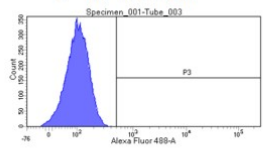

Population	#Events	%Parent	%Total
All Events	11,490	####	100.0
P1	10,369	90.2	90.2
P2	10,000	96.4	87.0
P3	17	0.2	0.1

3rd nc-TAA-ABE

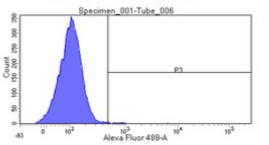

Population	#Events	%Parent	%Total
All Events	12,094	####	100.0
P1	10,401	86.0	86.0
P2	10,000	96.1	82.7
P3	226	2.3	1.9

3rd nc-TAA-xABE

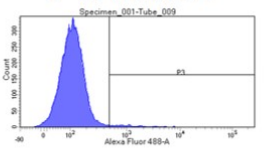

Population	#Events	%Parent	%Total
All Events	12,085	####	100.0
P1	10,352	85.7	85.7
P2	10,000	96.6	82.7
P3	415	4.2	3.4

3rd nc-TAA-ABEmax

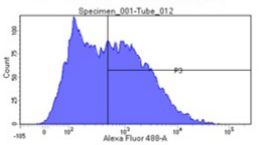

Population	#Events	%Parent	%Total
All Events	11,813	####	100.0
P1	10,312	87.3	87.3
P2	10,000	97.0	84.7
P3	5,064	50.6	42.9

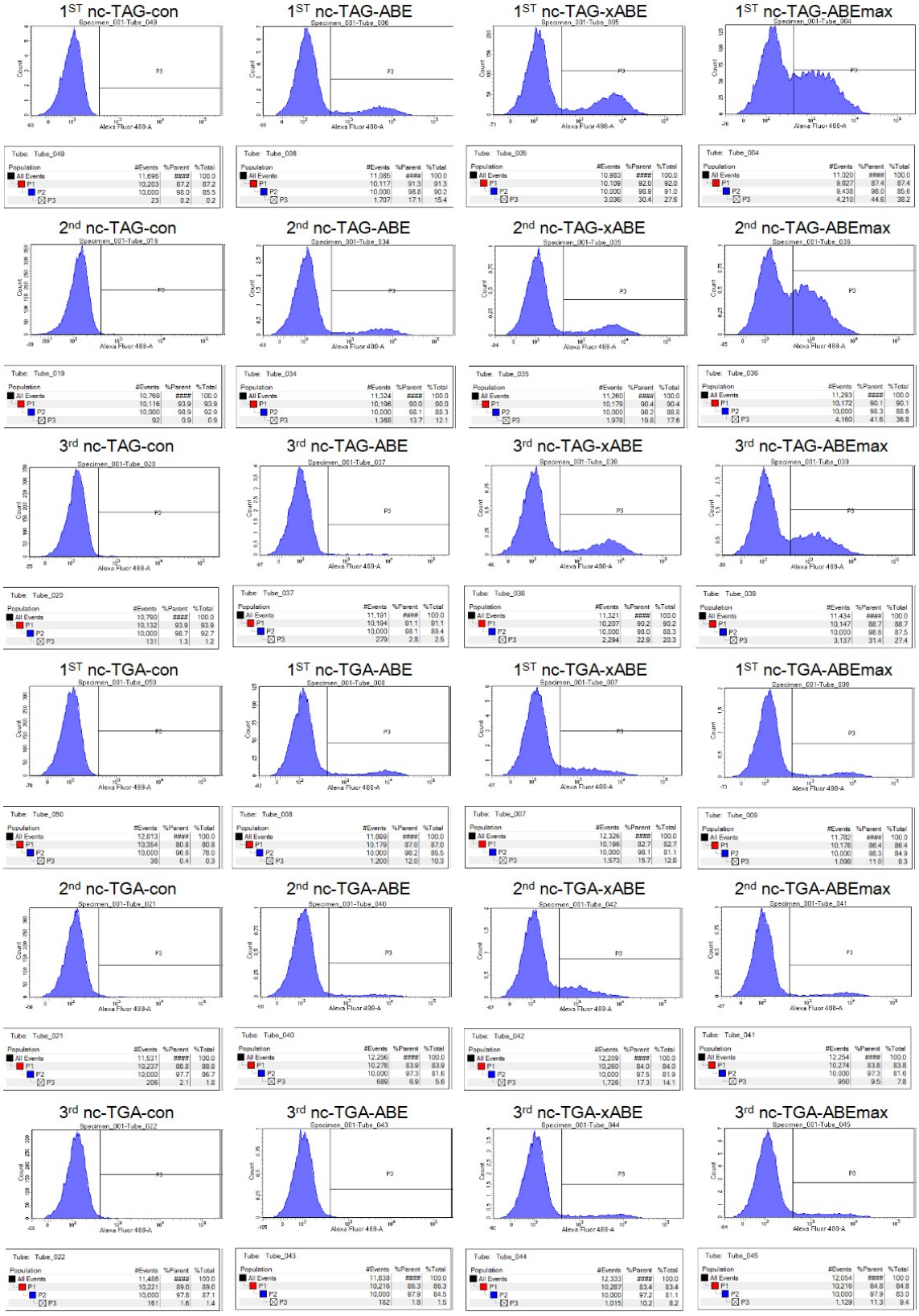

Figure 26. FACS results.

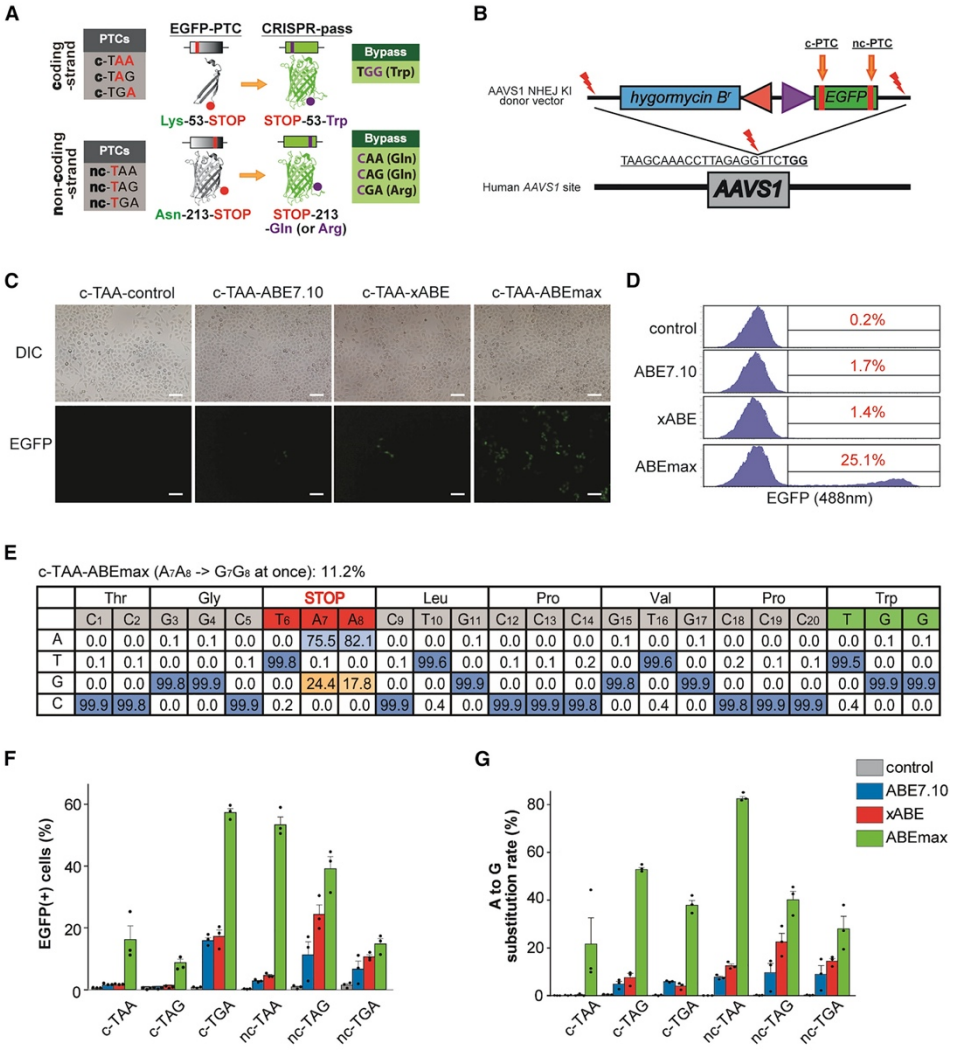

	Thr		Gly			STOP			Leu			Pro			Val			Pro			Trp		
	C1	C2	G3	G4	C5	T6	A7	A8	C9	T10	G11	C12	C13	C14	G15	T16	G17	C18	C19	C20	T	G	G
A	0.0	0.0	0.1	0.1	0.0	0.0	75.5	82.1	0.0	0.0	0.1	0.0	0.0	0.0	0.1	0.0	0.1	0.0	0.0	0.0	0.0	0.1	0.1
T	0.1	0.1	0.0	0.0	0.1	99.8	0.1	0.0	0.1	99.6	0.0	0.1	0.1	0.2	0.0	99.6	0.0	0.2	0.1	0.1	99.5	0.0	0.0
G	0.0	0.0	99.8	99.9	0.0	0.0	24.4	17.8	0.0	0.0	99.9	0.0	0.0	0.0	99.8	0.0	99.9	0.0	0.0	0.0	0.0	99.9	99.9
C	99.9	99.8	0.0	0.0	99.9	0.2	0.0	0.0	99.9	0.4	0.0	99.9	99.9	99.8	0.0	0.4	0.0	99.8	99.9	99.9	0.4	0.0	0.0

Figure 27. Restoring the Function of EGFP Gene Expression in Six KI HeLa Cell Lines Carrying Various Types of PTCs. (A) Scheme for restoration of EGFP expression by CRISPR-pass. The first set of PTCs, which can be converted by targeting the coding strand, affect a residue that is located on a loop between the third and fourth beta strands; the second set of PTCs, which can be converted by targeting the noncoding strand, affect a residue that is located on a loop between the 10th and 11th beta strands. c-PTC, coding strand PTC; nc-PTC, noncoding strand PTC. GFP structures were originated from Wikimedia Commons created by Zephyris. (B) Schematic of NHEJ-mediated KI of the EGFP-PTC constructs into the AAVS1site. Mutated EGFP KI cell lines were established for the three types of PTCs (TAA, TAG, and TGA). EGFP-PTC constructs were inserted into the *AAVS1* site by NHEJ-mediated KI methods. The hygromysin B-resistant gene was also inserted for cell selection. (C) Fluorescence image of rescued EGFP expression in the c-TAA cell line after CRISPR-pass treatment. Three different

versions of ABEs (ABE7.10, xABE, and ABEmax) were used for bypassing the PTCs in the *EGFP* gene. All scale bars are 100 μm. (D) Flow cytometry data after the different versions of ABEs (ABE7.10, xABE, and ABEmax) were treated in the c-TAA cell line. (E) Targeted deep-sequencing data showing the percentages of each of the four nucleotides at each position in the target DNA sequences as a substitution table, which was obtained from the c-TAA cell line after the ABEmax treatment. Bar graphs showing recovered EGFP expression levels as determined by flow cytometry (F) and showing A-to-G substitution rates at PTC sites as determined by targeted deep sequencing (G) for each EGFP-PTC KI cell line, after treatment with ABEs (ABE7.10, xABE, or ABEmax). Each dot represents the three independent experiments. Error bars represent SEM.

Table 8. FACS results. The percentages of EGFP (+) cells in populations of ABE-treated EGFP-PTC-KI cells. Each experiment was repeated 3 times.

	(-)			ABE			xABE			ABEmax		
	1st trial	2nd trial	3rd trial	1st trial	2nd trial	3rd trial	1st trial	2nd trial	3rd trial	1st trial	2nd trial	3rd trial
c-TAA	0.3%	0.2%	0.2%	1.3%	1.2%	1.7%	1.5%	1.3%	1.4%	12.5%	10.9%	25.1%
c-TAG	0.5%	1.1%	0.9%	0.7%	1.1%	1.1%	0.9%	1.7%	1.4%	11.1%	7.7%	7.2%
c-TGA	0.4%	0.8%	0.8%	17.8%	16.2%	14.2%	13.1%	20.3%	18.2%	59.6%	57.7%	55.0%
nc-TAA	0.2%	0.1%	0.2%	2.7%	3.2%	2.3%	4.2%	5.3%	4.2%	52.2%	59.0%	50.6%
nc-TAG	0.2%	0.9%	1.3%	17.1%	13.7%	2.8%	30.4%	19.8%	22.9%	44.6%	41.6%	31.4%
nc-TGA	0.4%	2.1%	1.6%	11.0%	6.9%	1.8%	12.0%	9.5%	10.2%	15.7%	17.3%	11.3%

Table 9. NGS results. The percentages of A to G substitutions in populations of ABE-treated EGFP-PTC-KI cells. Each experiment was repeated 3 times.

	(-)			ABE			xABE			ABEmax		
	1st trial	2nd trial	3rd trial	1st trial	2nd trial	3rd trial	1st trial	2nd trial	3rd trial	1st trial	2nd trial	3rd trial
c-TAA	0.0%	0.1%	0.0%	0.2%	0.2%	0.0%	0.0%	0.0%	0.9%	11.2%	9.7%	43.5%
c-TAG	0.5%	0.6%	0.4%	5.3%	6.5%	2.7%	9.1%	9.5%	4.0%	51.2%	52.2%	54.1%
c-TGA	0.3%	0.3%	0.0%	6.2%	5.9%	5.4%	5.1%	4.4%	2.4%	37.5%	34.0%	41.3%
nc-TAA	0.0%	0.0%	0.0%	6.7%	8.6%	7.2%	11.2%	14.0%	11.8%	80.9%	84.2%	81.6%
nc-TAG	0.3%	0.1%	0.2%	12.7%	1.8%	14.3%	16.3%	22.2%	28.7%	41.9%	33.1%	44.8%
nc-TGA	0.2%	0.3%	0.4%	9.1%	2.3%	15.2%	15.0%	12.1%	16.0%	37.4%	19.2%	26.9%

4. CRISPR-Pass Rescues the Function of the *XPC* Gene in Patient-Derived Fibroblasts

We next applied CRISPR-pass to the rescue of a nonsense mutation in fibroblasts (GM14867) derived from a patient with xeroderma pigmentosum, complementation group C (*XPC*). *XPC*, which affects the skin, is a genetic disorder caused by nonsense mutations in the *XPC* gene. The XPC protein is an initiator of global nucleotide excision repair (Sugasawa et al., 1998). Thus, XPC-deficient cells accumulate DNA damage when they are exposed to chemical or physical stimuli including ultraviolet irradiation(Dupuy et al., 2013). GM14867 cells have a homozygous C > T nonsense mutation at nucleotide 1840 in the *XPC* gene, which creates a 5′-TGA-3′ stop codon that replaces a codon for Arg (Arg579) (1840C > T, Arg-579-UGA stop codon) (Figure 29A). After treating GM14867 cells with ABE7.10-encoding plasmid and sgRNA-encoding plasmid by electroporation, the adenine base in the 5′-TGA-3′ stop codon was converted to guanine to create 5′-TGG-3′ at a rate of 3.4%, as measured by targeted deep sequencing (Figure 28), indicating partial rescue of the *XPC* gene. Similar to the previous experiments, xABE and ABEmax resulted in higher base-editing rates more than 10% (Figures 29B and S4), respectively. Western blot analyses demonstrated that both xABE and ABEmax treatment led to recovery of expression of the full-length XPC protein, with a molecular weight similar to that in wild-type (WT) cells (ARPE-19), at considerably higher levels than induced by ataluren or gentamicin (Figure 29C).

a

*XPC*_wt

	Trp		Val			STOP			Asp			Val			Thr			Gln			Arg		
	G	G	G	T	C	T	G	A	G	A	T	G	T	C	A	C	A	C	A	G	A	G	G
A	0.1	0.1	0.1	0.0	0.0	0.0	0.0	99.7	0.0	99.7	0.0	0.1	0.0	0.0	99.7	0.0	99.8	0.0	99.8	0.0	99.7	0.1	0.1
T	0.0	0.0	0.0	99.6	0.0	99.8	0.0	0.0	0.0	0.0	99.7	0.0	99.6	0.1	0.0	0.1	0.0	0.0	0.0	0.0	0.0	0.0	0.0
G	99.9	99.9	99.9	0.1	0.0	0.0	100	0.2	100	0.2	0.0	99.9	0.0	0.0	0.2	0.0	0.2	0.0	0.2	100	0.3	99.9	99.9
C	0.0	0.0	0.0	0.3	100	0.2	0.0	0.0	0.0	0.0	0.3	0.0	0.4	99.9	0.0	99.9	0.0	100	0.0	0.0	0.0	0.0	0.0

b

*XPC*_ABE

	Trp		Val			STOP			Asp			Val			Thr			Gln			Arg		
	G	G	G	T	C	T	G	A	G	A	T	G	T	C	A	C	A	C	A	G	A	G	G
A	0.1	0.1	0.1	0.0	0.0	0.0	0.1	96.5	0.1	99.3	0.0	0.0	0.0	0.0	99.6	0.0	99.7	0.0	99.8	0.0	99.7	0.1	0.1
T	0.0	0.0	0.0	99.5	0.4	99.8	0.0	0.1	0.0	0.0	99.7	0.0	99.5	0.1	0.0	0.0	0.0	0.1	0.0	0.0	0.0	0.0	0.0
G	99.9	99.9	99.9	0.0	0.0	0.0	99.9	3.4	99.9	0.7	0.0	99.9	0.0	0.0	0.3	0.0	0.3	0.0	0.2	99.9	0.3	99.9	99.9
C	0.0	0.0	0.0	0.4	99.6	0.2	0.0	0.0	0.0	0.0	0.3	0.0	0.4	99.9	0.0	99.9	0.0	99.9	0.0	0.0	0.0	0.0	0.0

c

*XPC*_xABE

	Trp		Val			STOP			Asp			Val			Thr			Gln			Arg		
	G	G	G	T	C	T	G	A	G	A	T	G	T	C	A	C	A	C	A	G	A	G	G
A	0.1	0.1	0.1	0.0	0.0	0.0	0.0	86.2	0.0	99.3	0.0	0.0	0.0	0.0	99.7	0.0	99.7	0.0	99.8	0.0	99.6	0.1	0.1
T	0.0	0.0	0.0	99.5	0.7	99.7	0.0	0.1	0.0	0.0	99.7	0.0	99.5	0.0	0.0	0.1	0.0	0.1	0.0	0.0	0.1	0.0	0.0
G	99.9	99.9	99.9	0.0	0.1	0.0	99.9	13.7	99.9	0.7	0.0	99.9	0.0	0.0	0.3	0.0	0.2	0.0	0.2	100	0.4	99.9	99.9
C	0.0	0.0	0.0	0.4	99.2	0.2	0.0	0.0	0.0	0.0	0.2	0.0	0.5	99.9	0.0	99.9	0.0	99.9	0.0	0.0	0.0	0.0	0.0

d

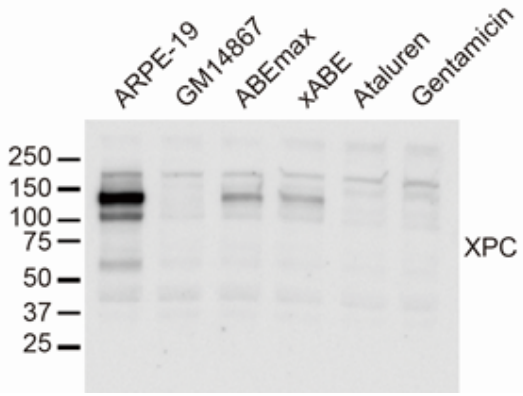

(with Dong Hyun Jo in Seoul National University College of Medicine)

Figure 28. CRISPR-pass for XPC patient-derived fibroblasts. Next generation sequencing (NGS) results from (a) untreated GM14867 fibroblasts, (b) ABE-treated GM143867 fibroblasts, and (c) xABE-treated GM143867 fibroblasts. (d) Image of complete SDS-PAGE gel that is shown in part in Figure 29c.

Next, to determine the functional activity of the recovered XPC protein, we evaluated the viability of GM14867 cells at 72 h after exposure to 254 nm ultraviolet light. To our surprise, both xABE- and ABEmax-treated GM14867 cells had significantly regained resistance to ultraviolet irradiation-induced DNA damage, causing an increase in cellular viability (Student's t test, $p < 0.001$; Figure 29D). More importantly, ABEmax-treated GM14867 cells sustained such XPC protein expression for at least 4 weeks, whereas the cells treated with ataluren or gentamicin gradually lost XPC protein expression (Figures 29E and 30), implying that CRISPR-pass induces persistent expression for the nonsense-mediated disease therapies.

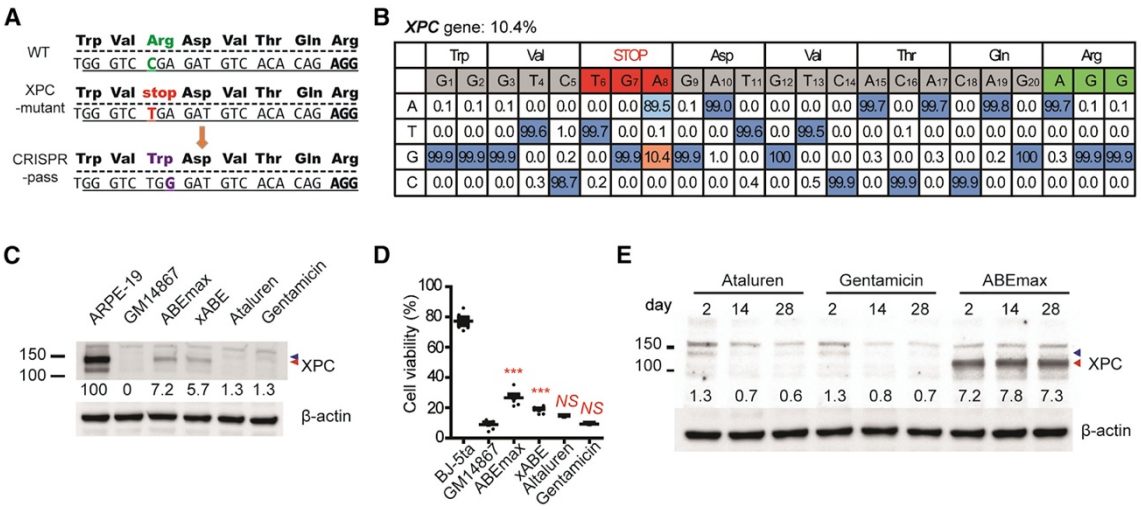

	Trp		Val			STOP			Asp			Val			Thr			Gln			Arg		
	G1	G2	G3	T4	C5	T6	G7	A8	G9	A10	T11	G12	T13	C14	A15	C16	A17	C18	A19	G20	A	G	G
A	0.1	0.1	0.1	0.0	0.0	0.0	0.0	89.5	0.1	99.0	0.0	0.0	0.0	0.0	99.7	0.0	99.7	0.0	99.8	0.0	99.7	0.1	0.1
T	0.0	0.0	0.0	99.6	1.0	99.7	0.0	0.1	0.0	0.0	99.6	0.0	99.5	0.0	0.0	0.1	0.0	0.0	0.0	0.0	0.0	0.0	0.0
G	99.9	99.9	99.9	0.0	0.2	0.0	99.9	10.4	99.9	1.0	0.0	100	0.0	0.0	0.3	0.0	0.3	0.0	0.2	100	0.3	99.9	99.9
C	0.0	0.0	0.0	0.3	98.7	0.2	0.0	0.0	0.0	0.0	0.4	0.0	0.5	99.9	0.0	99.9	0.0	99.9	0.0	0.0	0.0	0.0	0.0

(with Dong Hyun Jo in Seoul National University College of Medicine)

Figure 29. Restoring Abbreviated *XPC* Gene Expression in Patient-Derived Fibroblasts. (A) Scheme for ABE-induced read through of an *XPC*-associated PTC. (B) Targeted deep-sequencing data showing the A-to-G substitution rate induced by ABEmax treatment at the PTC site in the *XPC* gene. (C) Expression level of the XPC protein in *XPC* mutant cells rescued by treatment with ABEs (ABEmax or xABE), compared with the expression level in untreated cells and cells treated with ataluren or gentamicin for 48 h. (D) Cell viability of WT skin fibroblasts (BJ-5ta), *XPC* mutant cells (GM14867), and *XPC* mutant cells treated with ABEs (ABEmax or xABE), ataluren, or gentamicin at 3 days after exposure to 254 nm ultraviolet radiation at a dose of 25 J/m^2. p values were calculated by one-way ANOVA with post-hoc Bonferroni's multiple comparison tests (n = 6). p value indicators from a comparison with GM14867 cell viability are shown above each treatment group. *NS*, not significant ($p > 0.05$); *$p < 0.05$; ***$p < 0.001$. (E) Prolonged expression of the XPC protein after CRISPR-pass treatment. Significant and stable XPC protein expression was observed until at least 4 weeks after ABEmax treatment. However, XPC protein expression declined after removal of ataluren and gentamycin. Proteins were also prepared from ABEmax-treated *XPC* mutant cells at 2 and 4 weeks (subculturing twice per week) for comparison. Blue and red arrowheads indicate the positions of XPC protein.

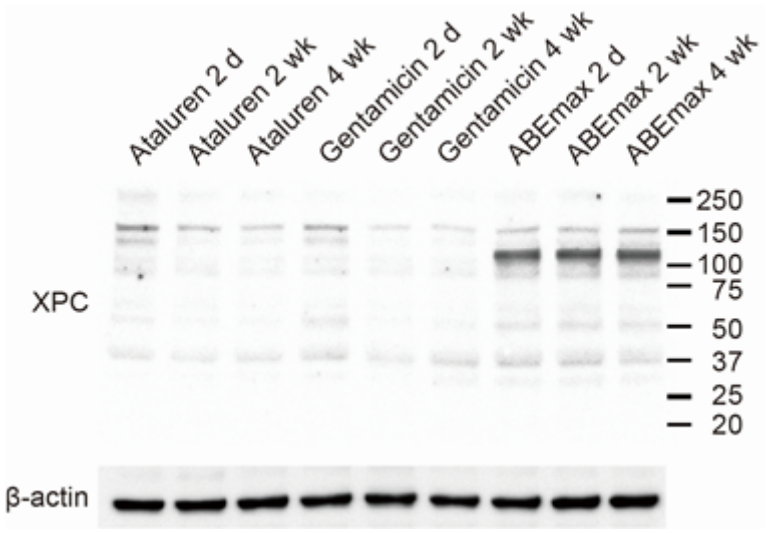

(by Dong Hyun Jo in Seoul National University College of Medicine)

Figure 30. Prolonged expression of the XPC protein after ABE treatment. Image of complete SDS-PAGE gel that is shown in part in Figure 29e.

Finally, to examine the off-target effects of CRISPR-pass in GM14867 fibroblasts, we searched for potential off-target sites using Cas-OFFinder (Bae et al., 2014) and carried out targeted deep sequencing for 12 candidate target sites (Figure 31; Table 10). As a result, we found no noticeable off-target sites likewise to the previous ABE-based gene-editing studies, (Lee et al., 2018; Liang et al., 2019; Liu et al., 2018) suggesting potential clinical utility.

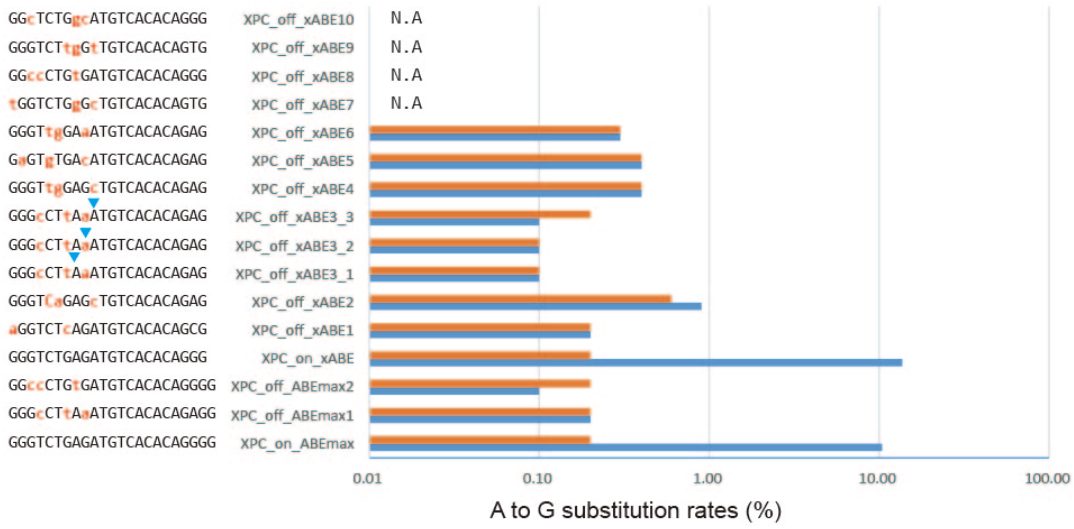

Figure 31. Off-target analysis for CRISPR-pass targeting *XPC*. A to G substitution rates at off-target sites are displayed. The percentages of substitutions at each site are summarized in Table 10. The red bars depict A to G substitution rates in untreated samples, whereas the blue bars depict A to G substitution rates in ABE-treated samples. Blue arrowhead indicates a target "A" which shows the A to G substitution rates (%).

Table 10. A-to-G substitution rates (%) in potential ABE off-target sites. N.A., not available; these sites are a Cas9 or xCas9 off-target site but do not contain an A targetable by ABEs. Blue colored letter means a target "A" which shows the A to G substitution rates (%)**.**

Name	Target sequences	ABE treated	wt
XPC_ABEmax_on	GGGTCTGAGATGTCACACAGNGG	10.40%	0.20%
XPC__ABEmax off_1	GGGcCTtAaATGTCACACAGAGG	0.20%	0.20%
XPC__ABEmax off_2	GGccCTGtGATGTCACACAGGGG	0.10%	0.20%
XPC_ xABE_on	GGGTCTGAGATGTCACACAGNG	13.70%	0.20%
XPC_ xABE_off_1	aGGTCTcAGATGTCACACAGCG	0.20%	0.20%
XPC_ xABE_off_2	GGGTCaGAGcTGTCACACAGAG	0.90%	0.60%
XPC_ xABE_off_3_1	GGGcCTtAaATGTCACACAGAG	0.10%	0.10%
XPC_ xABE_off_3_2	GGGcCTtAaATGTCACACAGAG	0.10%	0.10%
XPC_ xABE_off_3_3	GGGcCTtAaATGTCACACAGAG	0.10%	0.20%
XPC_ xABE_off_4	GGGTtgGAGcTGTCACACAGAG	0.40%	0.40%
XPC_ xABE_off_5	GaGTgTGAcATGTCACACAGAG	0.40%	0.40%
XPC_ xABE_off_6	GGGTtgGAaATGTCACACAGAG	0.30%	0.30%
XPC_ xABE_off_7	tGGTCTGgGcTGTCACACAGTG	N.A	N.A
XPC_ xABE_off_8	GGccCTGtGATGTCACACAGGG	N.A	N.A
XPC_ xABE_off_9	GGGTCTtgGtTGTCACACAGTG	N.A	N.A
XPC_ xABE_off_10	GGcTCTGgcATGTCACACAGGG	N.A	N.A

Table 11. List of oligomers encoding sgRNAs.

Name	sequences
psg-nc-TAA-up	CACCGTCTCTTAGGGGTCTTTGCTC
psg-nc-TAG-up	CACCGTCTCCTAGGGGTCTTTGCTC
psg-nc-TGA-up	CACCGTCTCTCAGGGGTCTTTGCTC
psg-nc-TAA-bo	AAACGAGCAAAGACCCCTAAGAGAC
psg-nc-TAG-bo	AAACGAGCAAAGACCCCTAGGAGAC
psg-nc-TGA-bo	AAACGAGCAAAGACCCCTGAGAGAC
psg-c-TAG_1up	CACCGCCGGCTAGCTGCCCGTGCCC
psg-c-TAA_2up	CACCGCCGGCTAACTGCCCGTGCCC
psg-c-TGA_3up	CACCGCCGGCTGACTGCCCGTGCCC
psg-c-TAG_1bo	AAACGGGCACGGGCAGCTAGCCGGC
psg-c-TAA_2bo	AAACGGGCACGGGCAGTTAGCCGGC
psg-c-TGA_3bo	AAACGGGCACGGGCAGTCAGCCGGC
psg-XPC-up	CACCGGGGTCTGAGATGTCACACAG
psg-XPC-bo	AAACGACACACTGTAGAGACTGGGC
psg-AAVS1-up	CACCGTAAGCAAACCTTAGAGGTTC
psg-AAVS1-bo	AAACCTTGGAGATTCCAAACGAATC

Table 12. PCR primers used in this study.

Name	Sequences
EGFP-1stF	gacatatccacgccctccta
EGFP-1stR	ctgacaattccgtggtgttg
EGFP_c_PTC_Deep_F	ACACTCTTTCCCTACACGAC GCTCTTCCGATCT acgtaaacggccacaagttc
EGFP_c_PTC_Deep_R	GTGACTGGAGTTCAGACGTGT GCTCTTCCGATCT tcgtccttgaagaagatggtg
EGFP_nc_PTC_Deep_F	ACACTCTTTCCCTACACGAC GCTCTTCCGATCT gaacggcatcaaggtgaact
EGFP_nc_PTC_Deep_R	GTGACTGGAGTTCAGACGTGT GCTCTTCCGATCT cttgtacagctcgtccatgc
inf_sacI_Cgo_add_F	GGTCTATATAAGCAGAGCTC TCGTCGACGAGCTCGTTTAGTG
inf_sacI_Cgo_add_R	CTCACCATGGCGGCGAGCTC GGTACCCTGGACACCTGTGG
inf_ccn_n2_TAA_2F	CTGAGCAAAGACCCCtgagagaagcgcgatcacatgg
inf_ccn_n2_TAA_1R	tcaGGGGTCTTTGCTCAGGGCG
inf_ccn_n2_TAG_2F	CTGAGCAAAGACCCCcaagagaagcgcgatcacatgg
inf_ccn_n2_TAG_1R	ttgGGGGTCTTTGCTCAGGGCG
inf_ccn_n2_TGA_2F	CTGAGCAAAGACCCCcgagagaagcgcgatcacatgg
inf_ccn_n2_TGA_1R	tcgGGGGTCTTTGCTCAGGGCG
inf_go_F1-1	TGGGAGGTCTATATAAGCAGAGCTCATGGTGAGCAAGGGCGAGG
inf_go_R1-TAG	CCATGTGCTAGCGCTTCTCGTTGGGGTC
inf_go_R1-TAA	CCATGTGTTAGCGCTTCTCGTTGGGGTC
inf_go_R1-TGA	CCATGTGTCAGCGCTTCTCGTTGGGGTC
inf_go_F1-2TAG	CGAGAAGCGCTAGcacatggtcctgctggagtt
inf_go_F1-2TAA	CGAGAAGCGCTAAcacatggtcctgctggagtt
inf_go_F1-2TGA	CGAGAAGCGCTGAcacatggtcctgctggagtt
inf_go_R1-2	TGAGATGTCTCTGTGCGGCTCACTTGTACAGCTCGTCCATGC
inf_go_R2-1TAG	CGGGCAGCTAGCCGGTGGTGCAGATGAAC
inf_go_R2-1TAA	CGGGCAGTTAGCCGGTGGTGCAGATGAAC
inf_go_R2-1TGA	CGGGCAGTCAGCCGGTGGTGCAGATGAAC
inf_go_F2-2TAG	CACCACCGGCTAGCTGCCCGTGCCCTGGCCC
inf_go_F2-2TAA	CACCACCGGCTAACTGCCCGTGCCCTGGCCC
inf_go_F2-2TGA	CACCACCGGCTGACTGCCCGTGCCCTGGCCC

(Continued)

Name	Sequences
XPC_1stF	ccaggagacaagcaggagaa
XPC_1stR	cgcggcagttcatctttcaa
XPC_deepF	ACACTCTTTCCCTACACGAC GCTCTTCCGATCT gtgagcaggaggaaaagtgg
XPC_deepR	GTGACTGGAGTTCAGACGTGT GCTCTTCCGATCT gtatggtctcaaggtctcggc
XPC_off_2nd_F1	ACACTCTTTCCCTACACGAC GCTCTTCCGATCT CACATGCTCCTGGAAGGGAA
XPC_off_2nd_R1	GTGACTGGAGTTCAGACGTGT GCTCTTCCGATCT AGGAGTGCCTACAGATGGGT
XPC_off_2nd_F2	ACACTCTTTCCCTACACGAC GCTCTTCCGATCT TTCACAGGCTGGCATTGAGT
XPC_off_2nd_R2	GTGACTGGAGTTCAGACGTGT GCTCTTCCGATCT TGCCCAGACAGAAGTTTGCT
XPC_off_2nd_F3_NGG_F1	ACACTCTTTCCCTACACGAC GCTCTTCCGATCT TGGAAGTGTAAAGGGGTTGTCT
XPC_off_2nd_R3_NGG_R1	GTGACTGGAGTTCAGACGTGT GCTCTTCCGATCT TCCATCTTTCACAGAGCTTCCA
XPC_off_2nd_F4	ACACTCTTTCCCTACACGAC GCTCTTCCGATCT GCATTTCCAGGCACACAGTG
XPC_off_2nd_R4	GTGACTGGAGTTCAGACGTGT GCTCTTCCGATCT CAGAGGATGCAAGGAAACACC
XPC_off_2nd_F5	ACACTCTTTCCCTACACGAC GCTCTTCCGATCT TCCATTTAGCTCGGGATGGC
XPC_off_2nd_R5	GTGACTGGAGTTCAGACGTGT GCTCTTCCGATCT TGCCTCATTGTTCATTAGTGTCT
XPC_off_2nd_F6	ACACTCTTTCCCTACACGAC GCTCTTCCGATCT AGTCATAATATTTCAAGGCAGAAAAGA
XPC_off_2nd_R6	GTGACTGGAGTTCAGACGTGT GCTCTTCCGATCT ACGCTCTTTTCAGACATTCTTGT
XPC_off_2nd_F7	ACACTCTTTCCCTACACGAC GCTCTTCCGATCT TGGCAGCAAGAGAAAGGAGG
XPC_off_2nd_R7	GTGACTGGAGTTCAGACGTGT GCTCTTCCGATCT GTGACCTTCCTCCTTCCGTG
XPC_off_2nd_F8_NGG_F1	ACACTCTTTCCCTACACGAC GCTCTTCCGATCT GACCTGTACTATGGGCTGCC
XPC_off_2nd_R8_NGG R1	GTGACTGGAGTTCAGACGTGT GCTCTTCCGATCT TCATCATCCCCTCCCTGTGT
XPC_off_2nd_F9	ACACTCTTTCCCTACACGAC GCTCTTCCGATCT ACCTCCCTCCTGAAGAAGTGA
XPC_off_2nd_R9	GTGACTGGAGTTCAGACGTGT GCTCTTCCGATCT TGGGCAGGACTGATATCCCT
XPC_off_2nd_F10	ACACTCTTTCCCTACACGAC GCTCTTCCGATCT CCTCCTAAGGAACAACATGGTGT
XPC_off_2nd_R10	GTGACTGGAGTTCAGACGTGT GCTCTTCCGATCT TGCAATTTCTTCTTTGTCCTGAGT
XPC_off_1st_F1	TGCAAACCCCTTCTGTCTGT
XPC_off_1st_R1	TGCAGTGAGCTGAGATTGGG
XPC_off_1st_F2	AATGGGGGTACAGGCATTGG
XPC_off_1st_R2	AGCTGGCTGCAGAAATTTGC
XPC_off_1st_F3_NGG_F1	GAGGTTGCAGTGAGCCAAGA
XPC_off_1st_R3_NGG_R1	GGAGGGAGAGAGGAGTGGAG
XPC_off_1st_F4	GCCTTCTCAACAATCCCCCA
XPC_off_1st_R4	CCACTGTTTTGTGCAGCCTC
XPC_off_1st_F5	TGAGGCGTGGAAGTGTGTAC
XPC_off_1st_R5	TCAGCTCACTGCAACCTCTG
XPC_off_1st_F6	CTTACCAGCGGCTCTTGGAA
XPC_off_1st_R6	CATCTGCTAAAGGGCTGGCT
XPC_off_1st_F7	CCTCACAGCCAATCCCATGT
XPC_off_1st_R7	AGGAGTGGCTCATCAAAGGC
XPC_off_1st_F8_NGG_F1	ATGTGGACCCAGGCATTCTG
XPC_off_1st_R8_NGG_R1	CAGAGGGAGCACCAAGGAAG

(Continued)

XPC_off_1st_F9	GCAAGGGAGAAAGGAGGGTC
XPC_off_1st_R9	CTCCTTCTTGTCGTGGGGAC
XPC_off_1st_F10	TTCCAAACCCCCAGGAACTT
XPC_off_1st_R10	TCAGCCATACCACACCAAGA

Table 13. List of off-target sites.

Name	On-target sequences	Off-target sequences	chr no.	position	direction	no. of mismatches	sequence ID	features
XPC_ABEmax_off_1	GGGTCTGAGATGTCACACAGNGG	GGccCTGtGATGTCACACAGGGG	chr1	55008670	-	3	NC_000001.11	intergenic region
XPC_ABEmax_off_2	GGGTCTGAGATGTCACACAGNGG	GGGcCTtAaATGTCACACAGAGG	chr1	199005822	+	3	NC_000001.11	intergenic region
XPC_xABE_off_1	GGGTCTGAGATGTCACACAGNG	aGGTCTcAGATGTCACACAGCG	chr7	24217661	-	2	NC_000007.14	intragenic region; intron
XPC_xABE_off_2	GGGTCTGAGATGTCACACAGNG	GGGTCaGAGcTGTCACACAGAG	chr13	47873206	-	2	NC_000013.11	intergenic region
XPC_xABE_off_3	GGGTCTGAGATGTCACACAGNG	GGGcCTtAaATGTCACACAGAG	chr1	199005822	+	3	NC_000001.11	intergenic region
XPC_xABE_off_4	GGGTCTGAGATGTCACACAGNG	GGGTtgGAGcTGTCACACAGAG	chr2	102917030	-	3	NC_000002.12	intergenic region
XPC_xABE_off_5	GGGTCTGAGATGTCACACAGNG	GaGTgTGAcATGTCACACAGAG	chr17	48043863	+	3	NC_000017.11	intergenic region
XPC_xABE_off_6	GGGTCTGAGATGTCACACAGNG	GGGTtgGAaATGTCACACAGAG	chr6	148983560	+	3	NC_000006.12	intragenic region; intron
XPC_xABE_off_7	GGGTCTGAGATGTCACACAGNG	tGGTCTGgGcTGTCACACAGTG	chr16	66513305	-	3	NC_000016.10	intragenic region; intron
XPC_xABE_off_8	GGGTCTGAGATGTCACACAGNG	GGccCTGtGATGTCACACAGGG	chr1	55008671	-	3	NC_000001.11	intergenic region
XPC_xABE_off_9	GGGTCTGAGATGTCACACAGNG	GGGTCTtgGtTGTCACACAGTG	chr21	35580798	+	3	NC_000021.9	intergenic region
XPC_xABE_off_10	GGGTCTGAGATGTCACACAGNG	GGcTCTGgcATGTCACACAGGG	chr10	9927098	+	3	NC_000010.11	intergenic region

Ⅳ. Discussion

Previously, Kuscu et al. (Kuscu et al., 2017) and Billon et al. (Billon et al., 2017) demonstrated gene-silencing methods, named CRISPR-STOP and iSTOP, respectively, through CBE-induced nonsense mutations. In this study, we analogously demonstrated that CRISPR-pass is a straightforward method for inducing read through of PTCs by ABEs, covering most (95%) nonsense mutations in the ClinVar database that cause pathological phenotypes. We first demonstrated the CRISPR-pass activities in six types of EGPF-PTCs-KI human cells, as a proof of concept. In these experiments, CRISPR-pass efficiently rescued functional EGFP expression by bypassing all PTCs. Then we successfully confirmed the activity of CRISPR-pass in a patient-derived fibroblast, GM14867, which contains a nonsense mutation at the *XPC* gene.

Until now, researchers have tried to correct the PTC in the *XPC* coding gene by various approaches. One suggested a viral delivery method of intact *XPC*-coding plasmids, (Warrick et al., 2012) but it has potential problems such as a random integration of the transgene in viral delivery (Hacein-Bey-Abina et al., 2003) and overexpression effects of the exogenous *XPC* gene. Alternatively, another approach to correct the endogenous *XPC* gene was demonstrated by using meganucleases and TALENs (Dupuy et al., 2013). In this study, the authors tried to correct the *XPC* gene via a HDR pathway after producing double-strand breaks (DSBs) of DNA, which might induce DSB-mediated cell apoptosis (Roos and Kaina, 2006), whereas the CRISPR-pass does not generate DSBs of DNA. Furthermore, we showed that the A-to-G conversions at a rate of about 10% can rescue the expression of functional XPC protein (Figures 29B–D) without detectable off-target effects, strongly indicating that the CRISPR-pass is a relevant approach for rescuing the nonsense-associated diseases with higher editing efficiencies than using HDR (Hess et al., 2017) and without the loss of large portion of protein via the exon removal (Nelson et al., 2016) or skipping strategies(Benchaouir et al., 2007). More importantly, CRISPR-pass induced prolonged XPC protein expression, unlike ataluren and gentamycin that are known as current nonsense mutation disease therapies (Roy et al., 2016), (Kuschal et al., 2013). Recently, it is reported that DNA cleavages at on-target sites frequently cause undesired large deletions or

complex genomic rearrangements (Kosicki et al., 2018). In this aspect, CRISPR-pass has important safety advantages relative to approaches that do rely on DNA cleavage. Furthermore, recent off-target profiling experiments on ABEs supported the high specificity of ABEs (Liu et al., 2018), (Liang et al., 2019), (Lee et al., 2018) increasing the potential clinical utility of it. These characteristics suggest that CRISPR-pass might be useful for gene rescue in a clinical setting, as an alternative to existing drugs.

Reference

Aartsma-Rus, A., and van Ommen, G.J. (2007). Antisense-mediated exon skipping: a versatile tool with therapeutic and research applications. RNA *13*, 1609-1624.

Aida, T., Chiyo, K., Usami, T., Ishikubo, H., Imahashi, R., Wada, Y., Tanaka, K.F., Sakuma, T., Yamamoto, T., and Tanaka, K. (2015). Cloning-free CRISPR/Cas system facilitates functional cassette knock-in in mice. Genome Biol *16*, 87.

Aigner, B., Renner, S., Kessler, B., Klymiuk, N., Kurome, M., Wunsch, A., and Wolf, E. (2010). Transgenic pigs as models for translational biomedical research. J Mol Med (Berl) *88*, 653-664.

Alter, J., Lou, F., Rabinowitz, A., Yin, H., Rosenfeld, J., Wilton, S.D., Partridge, T.A., and Lu, Q.L. (2006). Systemic delivery of morpholino oligonucleotide restores dystrophin expression bodywide and improves dystrophic pathology. Nat Med *12*, 175-177.

Anzalone, A.V., Randolph, P.B., Davis, J.R., Sousa, A.A., Koblan, L.W., Levy, J.M., Chen, P.J., Wilson, C., Newby, G.A., Raguram, A.*, et al.* (2019). Search-and-replace genome editing without double-strand breaks or donor DNA. Nature.

Backliwal, G., Hildinger, M., Chenuet, S., Wulhfard, S., De Jesus, M., and Wurm, F.M. (2008). Rational vector design and multi-pathway modulation of HEK 293E cells yield recombinant antibody titers exceeding 1 g/l by transient transfection under serum-free conditions. Nucleic Acids Research *36*.

Bae, S., Park, J., and Kim, J.S. (2014). Cas-OFFinder: a fast and versatile algorithm that searches for potential off-target sites of Cas9 RNA-guided endonucleases. Bioinformatics *30*, 1473-1475.

Beerli, R.R., and Barbas, C.F., 3rd (2002). Engineering polydactyl zinc-finger transcription factors. Nat Biotechnol *20*, 135-141.

Benchaouir, R., Meregalli, M., Farini, A., D'Antona, G., Belicchi, M., Goyenvalle, A., Battistelli, M., Bresolin, N., Bottinelli, R., Garcia, L.*, et al.* (2007). Restoration of human dystrophin following transplantation of exon-skipping-engineered DMD patient stem cells into dystrophic mice. Cell Stem Cell *1*, 646-657.

Bibikova, M., Beumer, K., Trautman, J.K., and Carroll, D. (2003). Enhancing gene targeting with designed zinc finger nucleases. Science *300*, 764.

Billon, P., Bryant, E.E., Joseph, S.A., Nambiar, T.S., Hayward, S.B., Rothstein, R., and Ciccia, A. (2017). CRISPR-Mediated Base Editing Enables Efficient Disruption of Eukaryotic Genes through Induction of STOP Codons. Mol Cell *67*, 1068-1079.

Bitinaite, J., Wah, D.A., Aggarwal, A.K., and Schildkraut, I. (1998). FokI dimerization is required for DNA cleavage. Proc Natl Acad Sci U S A *95*, 10570-10575.

Boch, J., Scholze, H., Schornack, S., Landgraf, A., Hahn, S., Kay, S., Lahaye, T., Nickstadt, A., and Bonas, U. (2009). Breaking the code of DNA binding specificity of TAL-type III effectors. Science *326*, 1509-1512.

Buja, L.M., Eigenbrodt, M.L., and Eigenbrodt, E.H. (1993). Apoptosis and necrosis. Basic types and mechanisms of cell death. Arch Pathol Lab Med *117*, 1208-1214.

Carbery, I.D., Ji, D., Harrington, A., Brown, V., Weinstein, E.J., Liaw, L., and Cui, X. (2010). Targeted genome modification in mice using zinc-finger nucleases. Genetics *186*, 451-459.

Carlson, D.F., Tan, W., Lillico, S.G., Stverakova, D., Proudfoot, C., Christian, M., Voytas, D.F., Long, C.R., Whitelaw, C.B., and Fahrenkrug, S.C. (2012). Efficient TALEN-mediated gene knockout in livestock. Proc Natl Acad Sci U S A *109*, 17382-17387.

Cermak, T., Doyle, E.L., Christian, M., Wang, L., Zhang, Y., Schmidt, C., Baller, J.A., Somia, N.V., Bogdanove, A.J., and Voytas, D.F. (2011). Efficient design and assembly of custom TALEN and other TAL effector-based constructs for DNA targeting. Nucleic Acids Res *39*, e82.

Chan, F.K., Moriwaki, K., and De Rosa, M.J. (2013). Detection of necrosis by release of lactate dehydrogenase activity. Methods Mol Biol *979*, 65-70.

Chen, K., and Gao, C. (2013). TALENs: customizable molecular DNA scissors for genome engineering of plants. J Genet Genomics *40*, 271-279.

Cho, S.W., Kim, S., Kim, J.M., and Kim, J.S. (2013). Targeted genome engineering in human cells with the Cas9 RNA-guided endonuclease. Nat Biotechnol *31*, 230-232.

Cho, S.W., Kim, S., Kim, Y., Kweon, J., Kim, H.S., Bae, S., and Kim, J.S. (2014). Analysis of off-target effects of CRISPR/Cas-derived RNA-guided endonucleases and nickases. Genome Res *24*, 132-141.

Cocking EC, P.J. (1974). The use protoplasts from fungi and higher plants as genetic systems—a practical handbook. Department of Botany, University of Nottingham, Nottingham.

Cong, L., Ran, F.A., Cox, D., Lin, S., Barretto, R., Habib, N., Hsu, P.D., Wu, X., Jiang, W., Marraffini, L.A.*, et al.* (2013). Multiplex genome engineering using CRISPR/Cas systems. Science *339*, 819-823.

Conner AJ, Albert NW, and Deroles, S. (2009). Transfection and regeneration of Petunia. In: Gerats T, Strommer J (eds) Petunia: evolutionary, developmental and physiological genetics, 2nd edn. Springer *New York, pp 395-416*.

Cui, W., Wylie, D., Aslam, S., Dinnyes, A., King, T., Wilmut, I., and Clark, A.J. (2003). Telomerase-immortalized sheep fibroblasts can be reprogrammed by nuclear transfer to undergo early development. Biol Reprod *69*, 15-21.

DiCarlo, J.E., Norville, J.E., Mali, P., Rios, X., Aach, J., and Church, G.M. (2013). Genome engineering in Saccharomyces cerevisiae using CRISPR-Cas systems. Nucleic Acids Res *41*, 4336-4343.

Ding, Q., Lee, Y.K., Schaefer, E.A., Peters, D.T., Veres, A., Kim, K., Kuperwasser, N., Motola, D.L., Meissner, T.B., Hendriks, W.T.*, et al.* (2013). A TALEN genome-editing system for generating human stem cell-based disease models. Cell Stem Cell *12*, 238-251.

Doyon, Y., McCammon, J.M., Miller, J.C., Faraji, F., Ngo, C., Katibah, G.E., Amora, R., Hocking, T.D., Zhang, L., Rebar, E.J.*, et al.* (2008). Heritable targeted gene disruption in zebrafish using designed zinc-finger nucleases. Nat Biotechnol *26*, 702-708.

Dubois, V., Botton, E., Meyer, C., Rieu, A., Bedu, M., Maisonneuve, B., and Mazier, M. (2005). Systematic silencing of a tobacco nitrate reductase transgene in lettuce (Lactuca sativa L.). J Exp Bot *56*, 2379-2388.

Dupuy, A., Valton, J., Leduc, S., Armier, J., Galetto, R., Gouble, A., Lebuhotel, C., Stary, A., Paques, F., Duchateau, P.*, et al.* (2013). Targeted gene therapy of xeroderma pigmentosum cells using meganuclease and TALEN. PLoS One *8*, e78678.

Feng, Z., Zhang, B., Ding, W., Liu, X., Yang, D.L., Wei, P., Cao, F., Zhu, S., Zhang, F., Mao, Y.*, et al.* (2013). Efficient genome editing in plants using a CRISPR/Cas system. Cell Res *23*, 1229-1232.

Flisikowska, T., Thorey, I.S., Offner, S., Ros, F., Lifke, V., Zeitler, B., Rottmann, O., Vincent, A., Zhang, L., Jenkins, S.*, et al.* (2011). Efficient immunoglobulin gene disruption and targeted replacement in rabbit using zinc finger nucleases. PLoS One *6*, e21045.

Gaj, T., Gersbach, C.A., and Barbas, C.F., 3rd (2013). ZFN, TALEN, and CRISPR/Cas-based methods for genome engineering. Trends Biotechnol *31*, 397-405.

Gao, J., Wang, G., Ma, S., Xie, X., Wu, X., Zhang, X., Wu, Y., Zhao, P., and Xia, Q. (2015). CRISPR/Cas9-mediated targeted mutagenesis in Nicotiana tabacum. Plant Mol Biol *87*, 99-110.

Garcia-Escudero, V., Garcia-Gomez, A., Gargini, R., Martin-Bermejo, M.J., Langa, E., de Yebenes, J.G., Delicado, A., Avila, J., Moreno-Flores, M.T., and Lim, F. (2010). Prevention of senescence progression in reversibly immortalized human ensheathing glia permits their survival after deimmortalization. Mol Ther *18*, 394-403.

Gaudelli, N.M., Komor, A.C., Rees, H.A., Packer, M.S., Badran, A.H., Bryson, D.I., and Liu, D.R. (2017). Programmable base editing of A*T to G*C in genomic DNA without DNA cleavage. Nature *551*, 464-471.

Gerats, T., and Vandenbussche, M. (2005). A model system for comparative research: Petunia. Trends Plant Sci *10*, 251-256.

Geurts, A.M., Cost, G.J., Freyvert, Y., Zeitler, B., Miller, J.C., Choi, V.M., Jenkins, S.S., Wood, A., Cui, X., Meng, X.*, et al.* (2009). Knockout rats via embryo microinjection of zinc-finger nucleases. Science *325*, 433.

Gil, M.A., Cuello, C., Parrilla, I., Vazquez, J.M., Roca, J., and Martinez, E.A. (2010). Advances in swine in vitro embryo production technologies. Reprod Domest Anim *45 Suppl 2*, 40-48.

Graham, F.L., Smiley, J., Russell, W.C., and Nairn, R. (1977). Characteristics of a human cell line transformed by DNA from human adenovirus type 5. J Gen Virol *36*, 59-74.

Gübitz, T., Hoballah, M.E., Dell'Olivo, A., and Kuhlemeier, C. (2009). Petunia as a Model System for the Genetics and Evolution of Pollination Syndromes. In Petunia: Evolutionary, Developmental and Physiological Genetics, T. Gerats, and J. Strommer, eds. (New York, NY: Springer New York), pp. 29-49.

Hacein-Bey-Abina, S., Von Kalle, C., Schmidt, M., McCcormack, M.P., Wulffraat, N., Leboulch, P., Lim, A., Osborne, C.S., Pawliuk, R., Morillon, E.*, et al.* (2003). LMO2-associated clonal T cell proliferation in two patients after gene therapy for SCID-X1. Science *302*, 415-419.

Hauschild, J., Petersen, B., Santiago, Y., Queisser, A.L., Carnwath, J.W., Lucas-Hahn, A., Zhang, L., Meng, X., Gregory, P.D., Schwinzer, R.*, et al.* (2011). Efficient generation of a biallelic knockout in pigs using zinc-finger nucleases. Proc Natl Acad Sci U S A *108*, 12013-12017.

Hess, G.T., Tycko, J., Yao, D., and Bassik, M.C. (2017). Methods and Applications of CRISPR-Mediated Base Editing in Eukaryotic Genomes. Mol Cell *68*, 26-43.

Hsu, P.D., Lander, E.S., and Zhang, F. (2014). Development and applications of CRISPR-Cas9 for genome engineering. Cell *157*, 1262-1278.

Hu, J.H., Miller, S.M., Geurts, M.H., Tang, W.X., Chen, L.W., Sun, N., Zeina, C.M., Gao, X., Rees, H.A., Lin, Z.*, et al.* (2018). Evolved Cas9 variants with broad PAM compatibility and high DNA specificity. Nature *556*, 57-63.

Hwang, G.H., Park, J., Lim, K., Kim, S., Yu, J., Yu, E., Kim, S.T., Eils, R., Kim, J.S., and Bae, S. (2018). Web-based design and analysis tools for CRISPR base editing. Bmc Bioinformatics *19*.

Hwang, H.S., Moon, J.G., Kim, C.H., Oh, S.M., Song, J.H., and Jeong, J.H. (2013a). The comparative morphometric study of the posterior cranial fossa : what is effective approaches to the treatment of Chiari malformation type 1? J Korean Neurosurg Soc *54*, 405-410.

Hwang, W.Y., Fu, Y., Reyon, D., Maeder, M.L., Tsai, S.Q., Sander, J.D., Peterson, R.T., Yeh, J.R., and Joung, J.K. (2013b). Efficient genome editing in zebrafish using a CRISPR-Cas system. Nat Biotechnol *31*, 227-229.

Hyun, Y., Kim, J., Cho, S.W., Choi, Y., Kim, J.S., and Coupland, G. (2015). Site-directed mutagenesis in Arabidopsis thaliana using dividing tissue-targeted RGEN of the CRISPR/Cas system to generate heritable null alleles. Planta *241*, 271-284.

Jiang, W., Bikard, D., Cox, D., Zhang, F., and Marraffini, L.A. (2013a). RNA-guided editing of bacterial genomes using CRISPR-Cas systems. Nat Biotechnol *31*, 233-239.

Jiang, W., Yang, B., and Weeks, D.P. (2014). Efficient CRISPR/Cas9-mediated gene editing in Arabidopsis thaliana and inheritance of modified genes in the T2 and T3 generations. PLoS One *9*, e99225.

Jiang, W., Zhou, H., Bi, H., Fromm, M., Yang, B., and Weeks, D.P. (2013b). Demonstration of CRISPR/Cas9/sgRNA-mediated targeted gene modification in Arabidopsis, tobacco, sorghum and rice. Nucleic Acids Res *41*, e188.

Jinek, M., Chylinski, K., Fonfara, I., Hauer, M., Doudna, J.A., and Charpentier, E. (2012). A programmable dual-RNA-guided DNA endonuclease in adaptive bacterial immunity. Science *337*, 816-821.

Kanchiswamy, C.N., Malnoy, M., Velasco, R., Kim, J.S., and Viola, R. (2015). Non-GMO genetically edited crop plants. Trends Biotechnol *33*, 489-491.

Kim, H., Farris, J., Christman, S.A., Kong, B.W., Foster, L.K., O'Grady, S.M., and Foster, D.N. (2002). Events in the immortalizing process of primary human mammary epithelial cells by the catalytic subunit of human telomerase. Biochem J *365*, 765-772.

Kim, H., and Kim, J.S. (2014). A guide to genome engineering with programmable nucleases. Nat Rev Genet *15*, 321-334.

Kim, H., Kim, M.S., Wee, G., Lee, C.I., Kim, H., and Kim, J.S. (2013a). Magnetic separation and antibiotics selection enable enrichment of cells with ZFN/TALEN-induced mutations. PloS one *8*, e56476.

Kim, H., Um, E., Cho, S.R., Jung, C., Kim, H., and Kim, J.S. (2011a). Surrogate reporters for enrichment of cells with nuclease-induced mutations. Nat Methods *8*, 941-943.

Kim, H.J., Lee, H.J., Kim, H., Cho, S.W., and Kim, J.S. (2009). Targeted genome editing in human cells with zinc finger nucleases constructed via modular assembly. Genome Res *19*, 1279-1288.

Kim, J.S. (2018). Precision genome engineering through adenine and cytosine base editing. Nat Plants *4*, 148-151.

Kim, S., Kim, D., Cho, S.W., Kim, J., and Kim, J.S. (2014). Highly efficient RNA-guided genome editing in human cells via delivery of purified Cas9 ribonucleoproteins. Genome Res *24*, 1012-1019.

Kim, S., Lee, M.J., Kim, H., Kang, M., and Kim, J.S. (2011b). Preassembled zinc-finger arrays for rapid construction of ZFNs. Nat Methods *8*, 7.

Kim, Y., Kweon, J., Kim, A., Chon, J.K., Yoo, J.Y., Kim, H.J., Kim, S., Lee, C., Jeong, E., Chung, E.*, et al.* (2013b). A library of TAL effector nucleases spanning the human genome. Nat Biotechnol *31*, 251-258.

Kim, Y., Kweon, J., and Kim, J.S. (2013c). TALENs and ZFNs are associated with different mutation signatures. Nat Methods *10*, 185.

Koblan, L.W., Doman, J.L., Wilson, C.A.-O.h.o.o., Levy, J.M.A.-O.h.o.o., Tay, T., Newby, G.A.A.-O.h.o.o., Maianti, J.P., Raguram, A.,

and Liu, D.R. (2018). Improving cytidine and adenine base editors by expression optimization and ancestral reconstruction. Nature biotechnol *36(9)*, 843-846.
Komor, A.C., Badran, A.H., and Liu, D.R. (2018). Editing the Genome Without Double-Stranded DNA Breaks. ACS Chem Biol *13*, 383-388.
Komor, A.C., Kim, Y.B., Packer, M.S., Zuris, J.A., and Liu, D.R. (2016). Programmable editing of a target base in genomic DNA without double-stranded DNA cleavage. Nature *533*, 420-424.
Koo, O.J., ;, G. Jang, and Lee., a.B.C. (2012). Minipig as laboratory animals: Facility management and husbandry. Reprod Dev Biol *36:79-85.*
Koo, O.J., Park, H.J., Kwon, D.K., Kang, J.T., Jang, G., and Lee, B.C. (2009). Effect of recipient breed on delivery rate of cloned miniature pig. Zygote *17*, 203-207.
Kosicki, M., Tomberg, K., and Bradley, A. (2018). Repair of double-strand breaks induced by CRISPR-Cas9 leads to large deletions and complex rearrangements. Nature Biotechnology *36*, 765-771.
Kuschal, C., DiGiovanna, J.J., Khan, S.G., Gatti, R.A., and Kraemer, K.H. (2013). Repair of UV photolesions in xeroderma pigmentosum group C cells induced by translational readthrough of premature termination codons. P Natl Acad Sci USA *110*, 19483-19488.
Kuscu, C., Parlak, M., Tufan, T., Yang, J., Szlachta, K., Wei, X., Mammadov, R., and Adli, M. (2017). CRISPR-STOP: gene silencing through base-editing-induced nonsense mutations. Nat Methods *14*, 710-712.
Kwon, D.N., Lee, K., Kang, M.J., Choi, Y.J., Park, C., Whyte, J.J., Brown, A.N., Kim, J.H., Samuel, M., Mao, J.*, et al.* (2013). Production of biallelic CMP-Neu5Ac hydroxylase knock-out pigs. Sci Rep *3*, 1981.
Lai, L., Kolber-Simonds, D., Park, K.W., Cheong, H.T., Greenstein, J.L., Im, G.S., Samuel, M., Bonk, A., Rieke, A., Day, B.N.*, et al.* (2002). Production of alpha-1,3-galactosyltransferase knockout pigs by nuclear transfer cloning. Science *295*, 1089-1092.
Lee, H.K., Willi, M., Miller, S.M., Kim, S., Liu, C.Y., Liu, D.R., and Hennighausen, L. (2018). Targeting fidelity of adenine and cytosine base editors in mouse embryos. Nat Commun *9*.
Li, C., Zong, Y., Wang, Y.P., Jin, S., Zhang, D.B., Song, Q.N., Zhang, R., and Gao, C.X. (2018). Expanded base editing in rice and wheat using a Cas9-adenosine deaminase fusion. Genome Biology *19(1):59*.
Li, J.F., Norville, J.E., Aach, J., McCormack, M., Zhang, D., Bush, J., Church, G.M., and Sheen, J. (2013a). Multiplex and homologous recombination-mediated genome editing in Arabidopsis and Nicotiana benthamiana using guide RNA and Cas9. Nat Biotechnol *31*, 688-691.
Li, P., Estrada, J.L., Burlak, C., and Tector, A.J. (2013b). Biallelic knockout of the alpha-1,3 galactosyltransferase gene in porcine liver-derived cells using zinc finger nucleases. J Surg Res *181*, e39-45.

Li, T., Liu, B., Spalding, M.H., Weeks, D.P., and Yang, B. (2012). High-efficiency TALEN-based gene editing produces disease-resistant rice. Nat Biotechnol *30*, 390-392.

Liang, P., Xie, X., Zhi, S., Sun, H., Zhang, X., Chen, Y., Chen, Y., Xiong, Y., Ma, W., Liu, D.*, et al.* (2019). Genome-wide profiling of adenine base editor specificity by EndoV-seq. Nat Commun *10*, 67.

Liang, Z., Zhang, K., Chen, K., and Gao, C. (2014). Targeted mutagenesis in Zea mays using TALENs and the CRISPR/Cas system. J Genet Genomics *41*, 63-68.

Liu, Y., Yang, J.Y., Lu, Y., Yu, P., Dove, C.R., Hutcheson, J.M., Mumaw, J.L., Stice, S.L., and West, F.D. (2013). alpha-1,3-Galactosyltransferase knockout pig induced pluripotent stem cells: a cell source for the production of xenotransplant pigs. Cell Reprogram *15*, 107-116.

Liu, Z., Lu, Z.Y., Yang, G., Huang, S.S., Li, G.L., Feng, S.J., Liu, Y.J., Li, J.N., Yu, W.X., Zhang, Y.*, et al.* (2018). Efficient generation of mouse models of human diseases via ABE- and BE-mediated base editing. Nat Commun *9*.

Luo, S., Li, J., Stoddard, T.J., Baltes, N.J., Demorest, Z.L., Clasen, B.M., Coffman, A., Retterath, A., Mathis, L., Voytas, D.F.*, et al.* (2015). Non-transgenic Plant Genome Editing Using Purified Sequence-Specific Nucleases. Mol Plant *8*, 1425-1427.

Lutz, A.J., Li, P., Estrada, J.L., Sidner, R.A., Chihara, R.K., Downey, S.M., Burlak, C., Wang, Z.Y., Reyes, L.M., Ivary, B.*, et al.* (2013). Double knockout pigs deficient in N-glycolylneuraminic acid and galactose alpha-1,3-galactose reduce the humoral barrier to xenotransplantation. Xenotransplantation *20*, 27-35.

Macheda, M.L., Rogers, S., and Best, J.D. (2005). Molecular and cellular regulation of glucose transporter (GLUT) proteins in cancer. J Cell Physiol *202*, 654-662.

Maeder, M.L., Thibodeau-Beganny, S., Osiak, A., Wright, D.A., Anthony, R.M., Eichtinger, M., Jiang, T., Foley, J.E., Winfrey, R.J., Townsend, J.A.*, et al.* (2008). Rapid "open-source" engineering of customized zinc-finger nucleases for highly efficient gene modification. Mol Cell *31*, 294-301.

Mali, P., Yang, L., Esvelt, K.M., Aach, J., Guell, M., DiCarlo, J.E., Norville, J.E., and Church, G.M. (2013). RNA-guided human genome engineering via Cas9. Science *339*, 823-826.

Maresca, M., Lin, V.G., Guo, N., and Yang, Y. (2013). Obligate Ligation-Gated Recombination (ObLiGaRe): Custom-designed nuclease-mediated targeted integration through nonhomologous end joining. Genome Research *23*, 539-546.

Matsunari, H., and Nagashima, H. (2009). Application of genetically modified and cloned pigs in translational research. J Reprod Dev *55*, 225-230.

Meng, F.Y., Chen, Z.S., Han, M., Hu, X.P., He, X.X., Liu, Y., He, W.T., Huang, W., Guo, H., and Zhou, P. (2010). Porcine hepatocyte isolation and reversible immortalization mediated by retroviral transfer and site-specific recombination. World J Gastroenterol *16*, 1660-1664.

Meyer, P. (2001). Chromatin remodelling. Curr Opin Plant Biol *4*, 457-462.

Meyer. L, Serek. M, and T, W. (2009). Protoplast isolation and plant regeneration of different genotypes of Petunia and Calibrachoa. Plant Cell Tissue Organ Cult *99:27-34*.

Miao, J., Guo, D., Zhang, J., Huang, Q., Qin, G., Zhang, X., Wan, J., Gu, H., and Qu, L.J. (2013). Targeted mutagenesis in rice using CRISPR-Cas system. Cell Res *23*, 1233-1236.

Miller, J.C., Holmes, M.C., Wang, J., Guschin, D.Y., Lee, Y.L., Rupniewski, I., Beausejour, C.M., Waite, A.J., Wang, N.S., Kim, K.A., *et al.* (2007). An improved zinc-finger nuclease architecture for highly specific genome editing. Nat Biotechnol *25*, 778-785.

Miller, J.C., Tan, S., Qiao, G., Barlow, K.A., Wang, J., Xia, D.F., Meng, X., Paschon, D.E., Leung, E., Hinkley, S.J., *et al.* (2011). A TALE nuclease architecture for efficient genome editing. Nat Biotechnol *29*, 143-148.

Morton, J., Davis, M.W., Jorgensen, E.M., and Carroll, D. (2006). Induction and repair of zinc-finger nuclease-targeted double-strand breaks in Caenorhabditis elegans somatic cells. Proc Natl Acad Sci U S A *103*, 16370-16375.

Moscou, M.J., and Bogdanove, A.J. (2009). A simple cipher governs DNA recognition by TAL effectors. Science *326*, 1501.

Nami, F., Basiri, M., Satarian, L., Curtiss, C., Baharvand, H., and Verfaillie, C. (2018). Strategies for In Vivo Genome Editing in Nondividing Cells. Trends in Biotechnology *36*, 770-786.

Negrutiu, I., Shillito, R., Potrykus, I., Biasini, G., and Sala, F. (1987). Hybrid genes in the analysis of transformation conditions : I. Setting up a simple method for direct gene transfer in plant protoplasts. Plant Mol Biol *8*, 363-373.

Nekrasov, V., Staskawicz, B., Weigel, D., Jones, J.D., and Kamoun, S. (2013). Targeted mutagenesis in the model plant Nicotiana benthamiana using Cas9 RNA-guided endonuclease. Nat Biotechnol *31*, 691-693.

Nelson, C.E., Hakim, C.H., Ousterout, D.G., Thakore, P.I., Moreb, E.A., Castellanos Rivera, R.M., Madhavan, S., Pan, X., Ran, F.A., Yan, W.X., *et al.* (2016). In vivo genome editing improves muscle function in a mouse model of Duchenne muscular dystrophy. Science *351*, 403-407.

Nguyen, T.A., Jo, M.H., Choi, Y.G., Park, J., Kwon, S.C., Hohng, S., Kim, V.N., and Woo, J.S. (2015). Functional Anatomy of the Human Microprocessor. Cell *161*, 1374-1387.

Nishida, K., Arazoe, T., Yachie, N., Banno, S., Kakimoto, M., Tabata, M., Mochizuki, M., Miyabe, A., Araki, M., Hara, K.Y., *et al.* (2016). Targeted nucleotide editing using hybrid prokaryotic and vertebrate adaptive immune systems. Science *353*, aaf8729.

Nishimasu, H., Shi, X., Ishiguro, S., Gao, L.Y., Hirano, S., Okazaki, S., Noda, T., Abudayyeh, O.O., Gootenberg, J.S., Mori, H., *et al.* (2018). Engineered CRISPR-Cas9 nuclease with expanded targeting space. Science *361*, 1259-1262.

Oh, H.Y., Jin, X., Kim, J.G., Oh, M.J., Pian, X., Kim, J.M., Yoon, M.S., Son, C.I., Lee, Y.S., Hong, K.C., *et al.* (2007). Characteristics of primary and immortalized fibroblast cells derived from the miniature and domestic pigs. BMC Cell Biol *8*, 20.

Oh. MH, K.S. (1994). Plant regeneration from petal protoplast culture of Petunia hybrida. Plant Cell Tissue Organ Cult *36:275-283*.

Panda, S.K., Wefers, B., Ortiz, O., Floss, T., Schmid, B., Haass, C., Wurst, W., and Kuhn, R. (2013). Highly efficient targeted mutagenesis in mice using TALENs. Genetics *195*, 703-713.

Park, J., Bae, S., and Kim, J.S. (2015). Cas-Designer: a web-based tool for choice of CRISPR-Cas9 target sites. Bioinformatics *31*, 4014-4016.

Park, S.J., Park, H.J., Koo, O.J., Choi, W.J., Moon, J.H., Kwon, D.K., Kang, J.T., Kim, S., Choi, J.Y., Jang, G., *et al.* (2012). Oxamflatin improves developmental competence of porcine somatic cell nuclear transfer embryos. Cell Reprogram *14*, 398-406.

Pichavant, C., Aartsma-Rus, A., Clemens, P.R., Davies, K.E., Dickson, G., Takeda, S., Wilton, S.D., Wolff, J.A., Wooddell, C.I., Xiao, X., *et al.* (2011). Current status of pharmaceutical and genetic therapeutic approaches to treat DMD. Mol Ther *19*, 830-840.

Ray, F.A., Peabody, D.S., Cooper, J.L., Cram, L.S., and Kraemer, P.M. (1990). SV40 T antigen alone drives karyotype instability that precedes neoplastic transformation of human diploid fibroblasts. J Cell Biochem *42*, 13-31.

Rodriguez-Martinez, H., and Wallgren, M. (2010). Advances in boar semen cryopreservation. Vet Med Int *2010*.

Rogers, C.S., Hao, Y., Rokhlina, T., Samuel, M., Stoltz, D.A., Li, Y., Petroff, E., Vermeer, D.W., Kabel, A.C., Yan, Z., *et al.* (2008a). Production of CFTR-null and CFTR-DeltaF508 heterozygous pigs by adeno-associated virus-mediated gene targeting and somatic cell nuclear transfer. J Clin Invest *118*, 1571-1577.

Rogers, C.S., Stoltz, D.A., Meyerholz, D.K., Ostedgaard, L.S., Rokhlina, T., Taft, P.J., Rogan, M.P., Pezzulo, A.A., Karp, P.H., Itani, O.A., *et al.* (2008b). Disruption of the CFTR gene produces a model of cystic fibrosis in newborn pigs. Science *321*, 1837-1841.

Roos, W.P., and Kaina, B. (2006). DNA damage-induced cell death by apoptosis. Trends Mol Med *12*, 440-450.

Roy, B., Friesen, W.J., Tomizawa, Y., Leszyk, J.D., Zhuo, J., Johnson, B., Dakka, J., Trotta, C.R., Xue, X., Mutyam, V., *et al.* (2016). Ataluren stimulates ribosomal selection of near-cognate tRNAs to promote nonsense suppression. Proc Natl Acad Sci U S A *113*, 12508-12513.

Ryu, S.M., Koo, T., Kim, K., Lim, K., Baek, G., Kim, S.T., Kim, H.S., Kim, D.E., Lee, H., Chung, E., *et al.* (2018). Adenine base editing in mouse embryos and an adult mouse model of Duchenne muscular dystrophy. Nature Biotechnology *36*, 536-539.

Sagong, M., Park, C.K., Kim, S.H., Lee, K.K., Lee, O.S., Lee du, S., Cha, S.Y., and Lee, C. (2012). Human telomerase reverse transcriptase-immortalized porcine monomyeloid cell lines for the production of porcine reproductive and respiratory syndrome virus. J Virol Methods *179*, 26-32.

Saito, M., Handa, K., Kiyono, T., Hattori, S., Yokoi, T., Tsubakimoto, T., Harada, H., Noguchi, T., Toyoda, M., Sato, S., *et al.* (2005). Immortalization of cementoblast progenitor cells with Bmi-1 and TERT. J Bone Miner Res *20*, 50-57.

Salanoubat, M., and Bui Dang Ha, D. (1993). Analysis of the petunia nitrate reductase apoenzyme-encoding gene: a first step for sequence modification analysis. Gene *128*, 147-154.

Sander, J.D., and Joung, J.K. (2014). CRISPR-Cas systems for editing, regulating and targeting genomes. Nat Biotechnol *32*, 347-355.

Scherer, W.F., Syverton, J.T., and Gey, G.O. (1953). Studies on the propagation in vitro of poliomyelitis viruses. IV. Viral multiplication in a stable strain of human malignant epithelial cells (strain HeLa) derived from an epidermoid carcinoma of the cervix. J Exp Med *97*, 695-710.

Shan, Q., Wang, Y., Li, J., Zhang, Y., Chen, K., Liang, Z., Zhang, K., Liu, J., Xi, J.J., Qiu, J.L., *et al.* (2013). Targeted genome modification of crop plants using a CRISPR-Cas system. Nat Biotechnol *31*, 686-688.

Siddiqui, N., and Sonenberg, N. (2016). Proposing a mechanism of action for ataluren. Proc Natl Acad Sci U S A *113*, 12353-12355.

Singh, A., Ursic, D., and Davies, J. (1979). Phenotypic suppression and misreading Saccharomyces cerevisiae. Nature *277*, 146-148.

Smith, A.C., and Swindle, M.M. (2006). Preparation of swine for the laboratory. ILAR J *47*, 358-363.

Sugasawa, K., Ng, J.M.Y., Masutani, C., Iwai, S., van der Spek, P.J., Eker, A.P.M., Hanaoka, F., Bootsma, D., and Hoeijmakers, J.H.J. (1998). Xeroderma Pigmentosum Group C Protein Complex Is the Initiator of Global Genome Nucleotide Excision Repair. Mol Cell *2*, 223-232.

Sung, Y.H., Baek, I.J., Kim, D.H., Jeon, J., Lee, J., Lee, K., Jeong, D., Kim, J.S., and Lee, H.W. (2013). Knockout mice created by TALEN-mediated gene targeting. Nat Biotechnol *31*, 23-24.

Svitashev, S., Young, J.K., Schwartz, C., Gao, H., Falco, S.C., and Cigan, A.M. (2015). Targeted Mutagenesis, Precise Gene Editing, and Site-Specific Gene Insertion in Maize Using Cas9 and Guide RNA. Plant Physiol *169*, 931-945.

Todaro, G.J., and Green, H. (1963). Quantitative studies of the growth of mouse embryo cells in culture and their development into established lines. J Cell Biol *17*, 299-313.

Tong, C., Huang, G., Ashton, C., Wu, H., Yan, H., and Ying, Q.L. (2012). Rapid and cost-effective gene targeting in rat embryonic stem cells by TALENs. J Genet Genomics *39*, 275-280.

Urnov, F.D., Miller, J.C., Lee, Y.L., Beausejour, C.M., Rock, J.M., Augustus, S., Jamieson, A.C., Porteus, M.H., Gregory, P.D., and Holmes, M.C. (2005). Highly efficient endogenous human gene correction using designed zinc-finger nucleases. Nature *435*, 646-651.

Van Cruchten, S., and Van Den Broeck, W. (2002). Morphological and biochemical aspects of apoptosis, oncosis and necrosis. Anat Histol Embryol *31*, 214-223.

van Houwelingen, A., Souer, E., Mol, J., and Koes, R. (1999). Epigenetic interactions among three dTph1 transposons in two homologous chromosomes activate a new excision-repair mechanism in petunia. Plant Cell *11*, 1319-1336.

Vandenbussche, M., Zethof, J., Royaert, S., Weterings, K., and Gerats, T. (2004). The duplicated B-class heterodimer model: whorl-specific effects and complex genetic interactions in Petunia hybrida flower development. Plant Cell *16*, 741-754.

Vaucheret. H, Palauqui. JC, Mourrain. P, and T, E. (1997). Nitrate reductase and nitrite reductase as targets to study gene silencing phenomena in transgenic plants. Euphytica *00:195-200*.

Wang, E., Zhang, C., Polavaram, N., Liu, F., Wu, G., Schroeder, M.A., Lau, J.S., Mukhopadhyay, D., Jiang, S.W., O'Neill, B.P.*, et al.* (2014a). The role of factor inhibiting HIF (FIH-1) in inhibiting HIF-1 transcriptional activity in glioblastoma multiforme. PLoS One *9*, e86102.

Wang, Y., Cheng, X., Shan, Q., Zhang, Y., Liu, J., Gao, C., and Qiu, J.L. (2014b). Simultaneous editing of three homoeoalleles in hexaploid bread wheat confers heritable resistance to powdery mildew. Nat Biotechnol *32*, 947-951.

Warrick, E., Garcia, M., Chagnoleau, C., Chevallier, O., Bergoglio, V., Sartori, D., Mavilio, F., Angulo, J.F., Avril, M.F., Sarasin, A.*, et al.* (2012). Preclinical Corrective Gene Transfer in Xeroderma Pigmentosum Human Skin Stem Cells. Molecular Therapy *20*, 798-807.

Watanabe, M., Umeyama, K., Matsunari, H., Takayanagi, S., Haruyama, E., Nakano, K., Fujiwara, T., Ikezawa, Y., Nakauchi, H., and Nagashima, H. (2010). Knockout of exogenous EGFP gene in porcine

somatic cells using zinc-finger nucleases. Biochem Biophys Res Commun *402*, 14-18.
Whyte, J.J., and Prather, R.S. (2011). Genetic modifications of pigs for medicine and agriculture. Mol Reprod Dev *78*, 879-891.
Whyte, J.J., Zhao, J., Wells, K.D., Samuel, M.S., Whitworth, K.M., Walters, E.M., Laughlin, M.H., and Prather, R.S. (2011). Gene targeting with zinc finger nucleases to produce cloned eGFP knockout pigs. Mol Reprod Dev *78*, 2.
Wilkinson, J.Q., and Crawford, N.M. (1993). Identification and characterization of a chlorate-resistant mutant of Arabidopsis thaliana with mutations in both nitrate reductase structural genes NIA1 and NIA2. Mol Gen Genet *239*, 289-297.
Wolf, D.P., Mitalipov, S., and Norgren, R.B., Jr. (2001). Nuclear transfer technology in mammalian cloning. Arch Med Res *32*, 609-613.
Wolff, A., Perch-Nielsen, I.R., Larsen, U.D., Friis, P., Goranovic, G., Poulsen, C.R., Kutter, J.P., and Telleman, P. (2003). Integrating advanced functionality in a microfabricated high-throughput fluorescent-activated cell sorter. Lab Chip *3*, 22-27.
Woo, J.W., Kim, J., Kwon, S.I., Corvalan, C., Cho, S.W., Kim, H., Kim, S.G., Kim, S.T., Choe, S., and Kim, J.S. (2015). DNA-free genome editing in plants with preassembled CRISPR-Cas9 ribonucleoproteins. Nat Biotechnol *33*, 1162-1164.
Wyman, C., and Kanaar, R. (2006). DNA double-strand break repair: all's well that ends well. Annu Rev Genet *40*, 363-383.
Xie, K., and Yang, Y. (2013). RNA-guided genome editing in plants using a CRISPR-Cas system. Mol Plant *6*, 1975-1983.
Yang, D., Yang, H., Li, W., Zhao, B., Ouyang, Z., Liu, Z., Zhao, Y., Fan, N., Song, J., Tian, J.*, et al.* (2011). Generation of PPARgamma mono-allelic knockout pigs via zinc-finger nucleases and nuclear transfer cloning. Cell Res *21*, 979-982.
Young, J.I., Sedivy, J.M., and Smith, J.R. (2003). Telomerase expression in normal human fibroblasts stabilizes DNA 5-methylcytosine transferase I. J Biol Chem *278*, 19904-19908.
Zakhartchenko, V., Alberio, R., Stojkovic, M., Prelle, K., Schernthaner, W., Stojkovic, P., Wenigerkind, H., Wanke, R., Duchler, M., Steinborn, R.*, et al.* (1999). Adult cloning in cattle: potential of nuclei from a permanent cell line and from primary cultures. Mol Reprod Dev *54*, 264-272.
Zhao, X.Q., Nie, X.L., and Xiao, X.G. (2013). Over-expression of a tobacco nitrate reductase gene in wheat (Triticum aestivum L.) increases seed protein content and weight without augmenting nitrogen supplying. PloS one *8*, e74678.
Zhu, H., Lau, C.H., Goh, S.L., Liang, Q., Chen, C., Du, S., Phang, R.Z., Tay, F.C., Tan, W.K., Li, Z.*, et al.* (2013). Baculoviral transduction facilitates TALEN-mediated targeted transgene integration and

Cre/LoxP cassette exchange in human-induced pluripotent stem cells. Nucleic Acids Res *41*, e180.

국문초록

생명과학의 발달이 새로운 산업 동력과 미래의 대체의학으로 떠오름에 따라서 유전자 가위를 통한 생명과학 발달 가능성이 더더욱 명확해 지고 있으며, 또한 유전체에 대한 이해를 바탕으로, 이를 활용하기 위한 방법으로써 유전자 가위의 올바른 활용과 이해가 절실해지고 있다. 이에 따라 다양한 유전자 가위를 다양한 생물체의 유전체 교정에 활용함으로써, 동·식물자원의 유전형질개량을 통한 식량 및 생물자원의 증진과 나아가서는 인간 및 생물자원의 질병치료를 통한 건강한 삶을 만들어 갈 수 있을 것이다.

이러한 목표를 추구하기 위하여 ZFN, TALEN, CRISPR 과 같은 유전자 가위를 다양한 생물체에서 활용해보고자 하였다. 첫번째 연구로써는 ZFN 과 돼지 귀의 피부세포를 이용하여 유전자 교정을 통해 *CMAH* 유전자가 녹아웃(Knockout)된 세포를 얻어 돼지의 난자에 체세포 핵 치환 (SCNT)을 통해 *CMAH* 유전자가 녹아웃 된 돼지를 생산하고자 시도하였다. *CMAH* 유전자는 이종장기이식에 있어서 면역거부반응을 일으키는 유전자로써 녹아웃을 통해 이종장기이식 시에 면역거부반응을 제거하고자 목표하였다. 녹아웃 세포의 확보 효율을 높이기 위해 FACS 리포터와 MACS 리포터 시스템을 활용하였으며, 이를 통해 *CMAH* 유전자가 녹아웃된 배아를 확인할 수 있었다. 두번째 연구에서는 TALEN을 이용하여 돼지의 *CMAH*와 *GGTA1*유전자를 녹아웃하고자 시도하였으며, 이때에는 돼지의 유전자 교정을 용이하게 하기 위해 돼지 귀의 피부세포를 불멸화(immortalization)하여 다양한 녹아웃 세포주를 확보하고, 이를 통해 SCNT 후 배아로의 발달 과정을 확인해 볼 수 있었다. 세번째 연구에서는 CRISPR-Cas9 단백질을 페투니아의 원형질체에 전달함으로써 *NR* gene 이 녹아웃되는 효율을 확인하고자 목표하였으며, Cas9 RNP 전달을 통해 효율적으로 *NR* gene 이 녹아웃되는 것을 확인하고, 이를 통해 페투니아의 다른 유전자를 녹아웃할 수 있는 가능성을 확인하였다. 마지막으로는 CRISPR-Cas9 에 아데닌 탈아미노효소

(adenine deaminase)를 연결한 ABE 를 이용하여 미성숙 종결코돈(premature termination codon)으로 인한 질병을 치료할 수 있는 방법을 제시하고자 하였다. ClinVar 전산망에 있는 유전질환 중 미성숙 종결코돈으로 인한 비율을 확인 후, 이를 극복하기 위해서 CRISPR-pass 방법을 제시하였고, 그 치료 가능성을 *XPC* gene 에 돌연변이가 생긴 환자의 세포에서 확인할 수 있었다.

이와 같이 ZFN, TALEN, CRISPR 뿐만 아니라 ABE 와 같은 다양한 유전자 가위를 활용하여 동물과 식물 그리고 인간의 유전자 교정을 시도하여, 유전자 가위의 활용과 그 활용방안에 대한 이해를 돕고자 하였다.

학 번: 2012-20286